Title
The Regulation of Chromatin Dynamics by Histone Chaperones and Variants

Author
Zunder, Rachel Miriam

Publication Date
2011

Peer reviewed|Thesis/dissertation

The Regulation of Chromatin Dynamics by Histone Chaperones and Variants

By

Rachel Miriam Zunder

A dissertation submitted in partial satisfaction of the

requirements for the degree of

Doctor of Philosophy

in

Molecular and Cell Biology

in the

Graduate Division

of the

University of California, Berkeley

Committee in charge:

Professor Jasper Rine, Chair
Professor Barbara Meyer
Professor Robert Tjian
Professor Robert Fischer

Spring 2011

Abstract

The Regulation of Chromatin Dynamics by Histone Chaperones and Variants

by

Rachel Miriam Zunder

Doctor of Philosophy in Molecular and Cell Biology

University of California, Berkeley

Professor Jasper Rine, Chair

In all eukaryotic organisms, DNA is packaged into chromatin, which controls gene expression and genomic stability. The chromatin landscape is dynamic and responds to environmental signals to direct different cellular programs. Chromatin architecture is regulated by a network of structural and enzymatic proteins that interact with histones to alter nucleosome composition. In my dissertation, I examined 1) the interaction between histone chaperones and newly synthesized histones during nucleosome assembly and 2) the interplay between canonical histone isotypes, histone variants, and histone modifications. My work established how the unusual domain architecture of a newly discovered histone chaperone, Rtt106, provides specificity for acetylated histone cargo. Additionally, I discovered several new histone modifications and examined the relationship between the histone variant H2A.Z and two canonical histone H2B isotypes (Htb1 and Htb2). My dissertation establishes a framework for understanding the additional levels of genomic regulation achieved by histone chaperones, variants, isotypes, and modifications.

In chapter 2, I examine the structural basis for the specificity of the histone chaperone Rtt106 for H3 molecules modified by an acetylation at lysine 56 (H3K56ac). The X ray crystal structure, determined by our collaborators Andy Antczak and James Berger, revealed that Rtt106 contains a double pleckstrin homology (PH) motif. A targeted mutational screen identified two regions on Rtt106 that, when mutated individually, each disrupted Rtt106-H3 binding. One region was a basic surface on the N-terminal PH domain and the other was a loop within the C-terminal PH domain. Although binding experiments did not directly identify an H3K56ac binding pocket on Rtt106, a comparative analysis with the chromatin remodeling protein Pob3 implicated the C-terminal loop as the source of H3K56ac-specificity in the Rtt106-H3 interaction. This work establishes new domain architecture for acetyl-lysine recognition and expands our understanding of how chaperone-histone binding is regulated.

Armed with Rtt106 mutants that reduced H3 binding activity, in chapter 3 I examine the role of Rtt106-mediated nucleosome assembly during replication, transcription, and silencing. Although Rtt106 mutant proteins localized to origins of replication and silent chromatin, without the ability to bind H3, these mutants could not

deliver H3K56ac into chromatin. Reduced H3K56ac occupancy was detrimental to replication whereas excess unincorporated H3K56ac was antagonistic to silencing. In contrast, H3K56ac binding was required to recruit Rtt106 to histone gene promoters. Without recruitment of Rtt106 to these loci, we observed defects in H3K56ac incorporation and histone gene repression. Our work demonstrates that Rtt106-H3 binding is necessary for all known branches Rtt106-mediated nucleosome assembly, however these different branches rely on distinct genomic localization cues to target Rtt106 to chromatin.

To analyze the relationships between canonical histones, modifications, and variants, in chapter 4 I explore the unique functions of two histone H2B isotypes, Htb1 and Htb2. In collaboration with the Freitas lab at the Ohio State University, we discovered three new modifications on H2B, one of which was isotype-specific. Although the dimeric association of H2A.Z with H2B did not reveal an isotype-specific interaction, the interplay between canonical histone isotypes and variants remains an intriguing paradigm for chromatin regulation. In collaboration with the Giaever lab at the University of Toronto, we used chemical genomic profiling to define unique functions associated with the Htb1 and Htb2 isotypes. However, all chemical sensitivities identified resulted from changes in histone expression rather than Htb1 and Htb2 protein activity. Although we are still searching for a functional distinction between the two H2B isotypes, mass spectrometry analyses coupled with chemical-genomic profiling represents a promising strategy for discovering these relationships and defining their functional impact.

Table of Contents

List of Tables

Chapter 2

Chapter 3

Chapter 4

List of Figures

Chapter 2

Chapter 3

Chapter 4

Acknowledgements

This thesis would not have been possible without the guidance and encouragement that I received from my mentor, Jasper Rine. Jasper, you taught me to savor all the small victories that come along in day-to-day work. Your excitement for scientific discovery is completely refreshing. Everyone who knows you respects both your passion for research and the compassion you show to all of your students and peers. It was a true honor to work in your lab and I will take the lessons I've learned with me for the rest of my career.

The Rine lab was a place where I learned how to conduct high-quality research, but more than that, it was a place I enjoyed being everyday. Thank you to Josh Babiarz for catalyzing the H2B experiments, and for teaching me how to work with chromatin. Josh, thank you especially for your generosity with both your time and your reagents. I was lucky to have Laura Lombardi as a classmate. Thank you, Laura, for making the Rine lab a place full of excitement for both science and life. Erin Osborne and Oliver Zill, thank you for inspiring me (to attempt) to perform beautiful, elegant genetic experiments. Thank you to Nick, Dago, Jake, Qiaoning, Meru, Dave, Debbie, Meara, and Kripa for advice, friendship, and kindness over the years.

I chose Berkeley for graduate school not only for its excellent science, but also because it seemed like a place that valued teaching. Now, having gone through the program, I can attest that this is absolutely true. Thank you to my thesis committee, Barbara Meyer, Tij, and Bob Fischer for support and for thinking critically about my project and my future.

My project was greatly aided by the highly collaborative atmosphere in the Berkeley community. Thank you to Andy Antczak and James Berger for sharing the Rtt106 structure with us and for inspiring our investigation into this fascinating chaperone. Thank you to Scott Gradia and Abbey Hartland in the Macrolab for performing site-directed mutagenesis on Rtt106. Thank you to Jeff Woodruff for performing the phos-tag analysis on Rtt106. And thank you to Caitlin Schartner, who worked we me as a rotation student and helped with the Rtt106 mutational analysis.

My project was also aided by collaborations with labs outside of Berkeley. Thank you to Xiaodan Su, Bei Zhao, Lanhao Yang, and Michael Freitas at the Ohio State University for histone purification protocols and mass spectrometry analysis of H2B. Thank you to Marinella Gebbia and Guri Giaever at the University of Toronto for chemical-genomic profiling of our integrated *htb1*- and *htb2*- strains. Thank you to Tim Formosa at the University of Utah for strains, plasmids, and advice on our Pob3 comparative analysis.

I first learned to love science working as an undergraduate in the labs of Victoria Meller and Catherine Freudenreich at Tufts University. Thank you both for allowing me to work independently and for giving me a strong foundation in genetic research. And

thank you to Priya Sundararajan, a graduate student in the Freudenreich lab, for sharing her project with me and for teaching me how to perform molecular biology experiments

Julie, since graduating from Tufts I've learned that friends like you do not come along often. Even though we live in different cities, I know we will always be close. Our "catch-up" phone calls and visits are so special to me. Thank you for continuing to be my best friend though all of this. I am so lucky to have you in my life.

Although I grew up in Vermont, I was fortunate to have family close by in San Francisco. Thank you Barb, Eli, Noah, and now Logan for providing an escape from Berkeley and a second home during holidays and celebrations. I wasn't scared to move to California because I knew that you guys would be there for me. I'm so happy we now live in the same city and that our time spent together is no longer dictated by bridge traffic. Barb, thank you for being such a fantastic person; our family is beyond lucky to have you. Eli, now that we no longer have to share a bathroom, I'm so glad that we have finally become good friends. Thank you for sharing your new family with me.

Thank you to Jaime's family, Debbie, Jim, Becky, and Pepe for welcoming me into their home and for treating me with such kindness. I've loved spending time in Toronto and getting to know their extended family. Don't worry Debbie; even though he lives with me now, you will always be Jaime's number one.

Mom and Dad, you are both the biggest inspirations in my life. I am so proud to have both of you as parents. Thank you for always encouraging my education and for being understanding when that meant long hours and long distance. Mom, you are the strongest person I know. I am the person I am today because of you. Dad, I learn so much from you. The breadth of your knowledge is astounding and your ability to solve problems is something that I could not live without. You both always come to my rescue whenever I need you. Thank you both for providing such a strong example of the person I one day hope to become.

Jaime, I am so thankful that you followed me to Berkeley. You were here at the beginning, through the trenches, and now at the end as we celebrate the conclusion of this chapter and the beginning of the rest of our lives. I will always remember graduate school as the best of times, because it was the time when we fell in love. You are my everything, and I simply could not have done this without you.

Chapter 1

An introduction to chromatin dynamics in *S. cerevisiae*

1.1 The packaging unit of DNA is the nucleosome

Nucleosome structure

A universal problem facing all organisms is how to pack DNA such that it will fit inside a tiny cell. For example, the haploid human genome contains over three billion base pairs totaling approximately two meters of linear DNA. The average human cell is 10 micrometers. Therefore, to fit inside the nucleus, the genome must undergo ~40,000-fold compaction. Genome compaction is achieved by DNA-protein complexes, referred to collectively as chromatin. To allow DNA to be accessed during DNA-dependent processes, the chromatin compaction must be reversible and highly dynamic. Global unpacking is required during DNA replication and localized unpacking is necessary for transcription and DNA repair. Hundreds of distinct proteins are required to orchestrate the transitions between compacted and unpacked DNA as cells grow and divide. This thesis focuses on the interplay between chromatin structure and genomic regulation.

The principle packaging unit of chromatin is the nucleosome, consisting of an octamer of the four canonical histones (H2A, H2B, H3, and H4) wrapped in 146-bp of DNA (*1*). Histones are small, highly positively charged proteins that maintain strong ionic interactions with the negatively charged nucleic acid of DNA. The nucleosome structure contains two H2A/H2B dimers and one H3/H4 tetramer that form a complex using a “handshake motif” (*2*). Each histone contains an unstructured N-terminal tail that extends out from the globular core. These N-terminal tails are decorated with a plethora of post-translational modifications of chemically distinct types that influence chromatin architecture and genomic processes. Repeating nucleosome units form a 10 nm “beads on a string” fiber. Nucleosomal arrays are further condensed into 30 nm fibers, which are then folded into metaphase chromosomes (*3*). The regulation of these transitions between each level of packaging and the structural organization of the fiber at each step is a major focus in the field of chromatin biology.

The role of histones extends beyond simple DNA compaction. Chromatin architecture is dynamic and responds to environmental signals to direct different cellular programs. Therefore, the formation of higher-order chromatin structures must be regulated in such a way that some regions of the genome are more accessible than others. During replication and transcription, the passage of highly processive DNA and RNA polymerases requires localized unwrapping of the DNA, removal of histones upstream of the polymerase and histone replacement downstream of the polymerase (*4, 5*). The location and timing of each unwinding event is highly regulated and requires the coordinated action of a large hierarchy of enzymes and chaperones. These changes in DNA accessibility are necessary for genome replication and highly specific patterns of gene expression, which dictate cellular identity.

Canonical histones in *S. cerevisiae* are highly conserved

Histones are highly conserved at the level of both sequence and structure in all eukaryotes, suggesting that they evolved under great functional constraint. *S. cerevisiae*

H3 and H4 proteins are 90% and 92% identical, respectively, to their human orthologs (*6*). H2A and H2B are slightly more diverged: *S. cerevisiae* and human H2A orthologs are 76% identical and H2B orthologs are 71% identical (*6*). However, much of the divergence resides within the N-terminal tails; the core globular domains of H2A and H2B are 90% and 80% identical between human and *S. cerevisiae*, respectively. Mammalian genomes encode canonical histone genes as organized tandem arrays of histone gene repeats, each repeat containing one copy of each canonical histone gene. In contrast, the yeast genome contains only two copies of each canonical histone gene (*7*). Each gene copy is expressed off a divergent promoter region as an H2A-H2B or an H3-H4 pair (*8, 9*). The two copies of H3 (*HHT1* and *HHT2*) and H4 (*HHF1* and *HHF2*) each encode identical proteins (*10*). However, the two copies of H2A (*HTA1* and *HTA2*) differ at 2 residues, and the two copies of H2B (*HTB1* and *HTB2*) differ at 4 residues (*11, 12*). The functional consequences of these 4 amino acid changes on Htb1 and Htb2 are explored in Chapter 4. The high degree of sequence conservation and the limited copy number makes yeast an ideal organism for studying chromatin biology. This work takes advantage of the yeast genetic toolbox to study the impact of histone mutants on chromatin function.

1.2 Histone modifications and histone variants define the chromatin landscape

Histone modifications

Post-translational modifications to the canonical histone proteins add an additional layer of complexity to chromatin regulation. There are several distinct classes of modifications including acetylation, methylation, phosphorylation, and mono-ubiquitination, as well as several other modifications that are less well characterized (*13*). These modifications influence chromatin architecture by modulating interactions between neighboring histones, histones and DNA, and histones and chromatin-associated proteins. The majority of modified sites are located on the histone N-terminal tails, which are unstructured and extend away from the nucleosome core. More recently, several modifications have been characterized within histone globular domains that are essential for a variety of chromatin-related processes. “Cross-talk” has been used to refer to one modification controlling the presence or absence of a different modification either on the same histone or a neighboring histone (*14*). One of the first examples of histone modification cross-talk came from the discovery of a ubiquitin modification within the globular domain of H2B. In this case, ubiquitination of H2B at lysine 123 (H2BK123ub) is required for methylation of H3 at lysines 4 and 79 (H3K4,79me) (*15, 16*), which in turn each regulate transcription via distinct mechanisms (*5*). Novel histone modifications are reported frequently; therefore, our current profile is likely an under-representation of the full complexity of the chromatin landscape.

Regulators of chromatin structure: histone-modifying enzymes and chromatin remodelers

To regulate the rapid winding and un-winding of DNA, chromatin modifications must be highly dynamic. The addition and removal of histone modifications is catalyzed by several multi-subunit enzyme complexes. Histone-modifying enzymes that put on modifications, such as histone acetyl-transferases (HATs) and histone methyl-transferases (HMTs), are often referred to as "writers", and enzymes that remove modifications, such as histone deacetylases (HDACs) and histone demetylases (HDMs) are referred to as "erasers" (*13*). Histone modifying enzymes have different degrees of specificity. In yeast, HMTs and HDMs target only a single lysine residue whereas in larger eukaryotes HMTs can methylate multiple sites (*17*). In contrast, HATs and HDACs often but not always target several lysine residues on multiple histone types. The major HAT complexes in yeast, SAGA and NuA4, target multiple lysines on H3 and H2B, and on H4, H2A and H2A.Z, respectively (*18, 19*). Conversely, the major target of the SAS HAT complex is H4K16 (*20*). Precise addition and removal of chromatin marks creates unique chromatin signatures that are essential for the regulation of DNA-dependent processes.

Throughout the cell cycle, replication, transcription, and DNA repair proteins require continual access to DNA. Additionally, each DNA-dependent process results in nucleosome turnover in which old histones are either recycled or replaced with newly synthesized histones. Chromatin remodelers are multi-subunit molecular machines that regulate access to nucleosomal DNA by altering nucleosome structure (*21*). Remodeling complexes are defined by a catalytic ATPase subunit that enables DNA translocation and subsequent changes in histone-DNA contacts. Specific remodeling activity can achieve nucleosome incorporation, eviction, sliding, or histone variant replacement. For example, elegant *in vitro* studies show that although SWI/SNF and ISWI (known as ACF in other species) remodeling complexes both catalyze nucleosome sliding, the end products of their remodeling activity are quite distinct. SWI/SNF remodeling of a phased nucleosome template leads to disordered, irregular spacing whereas the ISWI remodeling complex can change a randomly distributed nucleosome array into an ordered template with equally spaced nucleosomes (*22, 23*). Changes in nucleosome arrangements are necessary for DNA binding proteins to gain access through the repressive chromatin complex. Remodelers often associate with modifying enzymes and distinct modification "readers" (described below) to regulate changes in nucleosome structure. Additionally, non-coding RNAs, such as HOTAIR, represent an exciting new paradigm for targeting chromatin enzymes to distinct genomic regions (*24*).

Histone modification readers

In addition to changing the biochemical properties of the nucleosome, histone modifications serve as integrative platforms that are recognized by "reader" effector proteins and translated into a cellular response. Readers contain one or many conserved domains that bind histone modifications in a manner that is dependent upon the status of the modification and the sequence flanking the modified site (*25*). Although acetyl-lysine is the most abundant histone modification, until recently, the bromodomain was the only domain known to bind this mark (*26*). A recent structural analysis identifies

the plant homeodomain finger, which has previously been shown to recognize methyl-lysine, as an acetyl-lysine recognition motif during chromatin remodeling in human cells (*27*). Methylated lysine, on the other hand, is recognized by a variety of domains including chromodomains, plant homedomains, tudor domains, and WD40-repeats, to name a few (*28*). Reader proteins are often members of histone-modifying and chromatin-remodeling complexes and target their enzymatic activity to a specific region of the genome.

Bromodomain-containing effector proteins can couple histone acetylation to transcriptional activation by recruiting chromatin remodelers (*29*), HATs (*30*), transcription factors (*31*), and components of the transcriptional machinery (*32*). The chromodomain was first identified in the heterochromatin-associated proteins HP1 and Polycomb in Drosophila (*33*). In yeast, histone-methyl readers facilitate transcriptional activation and DNA repair by recognizing specific methyl marks and recruiting HATs and DNA repair enzymes respectively (*34, 35*). The HAT complex SAGA is a beautiful example of how the coordinated activity of multiple histone modification readers can integrate a specific pattern of modifications to direct a highly regulated transcriptional response. SAGA utilizes the bromodomains of Gcn5 and Spt7 and the chromodomain of Chd1 to target the complex to regions containing a specific combination of H3K4-methylation and several acetyl marks on the H3 and H4 tails (*36, 37*). Following recruitment, SAGA catalyzes further acetylation of the region to establish a transcriptionally competent chromatin environment (*38*). Chapters 2 and 3 of this thesis describe a new acetyl-lysine binding motif, the pleckstrin homology (PH) domain.

Histone variants

In addition to modifications of canonical histones, biochemical changes to the nucleosome are also achieved by the incorporation of non-canonical histone variants. Histone variants may differ from their canonical histone paralogs at only a few residues (H3.3), or they may contain significant structural changes (macroH2A, CENP-A) (*39*). Unlike canonical histones, which are organized in gene arrays and are expressed exclusively during S-phase, histone variants are expressed from a single gene pair in diploids in a cell cycle-independent manner (*39*). As with modifications, histone variants have specialized roles in a variety of DNA-dependent processes such as repair, segregation, transcription initiation and elongation, sex determination, etc. Although many variants have been characterized in larger eukaryotes, the *S. cerevisiae* genome contains only two: the H2A variant H2A.Z (encoded by the *HTZ1* gene) that affects gene-specific expression and the maintenance of chromatin boundaries (*40*), and the H3 variant CENP-A (encoded by the *CSE4* gene) that controls chromatin segregation (*41*). It should be noted that some authors describe yeast H3 as H3.3 because the single species of H3 in yeast is more similar to the H3.3 variant than to the canonical H3 of other species. Likewise, yeast H2A is sometimes referred to as H2A.X for a similar reason (*6*). In this thesis, I follow the convention, which refers to these two proteins simply as H2A and H3.

Like canonical histones, histone variants are regulated by distinct modification patterns. Studies performed by the Rine lab and others showed that all four lysines within the N-terminal tail of H2A.Z are acetylated by the NuA4 HAT complex (*42, 43*). These acetylations are required for maintaining chromatin boundaries and for primary induction of the *GAL* gene cluster (*42, 44*). Modifications on canonical histones can regulate histone variant incorporation. For example, H4 lysine 16 acetylation (H4K16ac) is required for H2A.Z incorporation at telomeres, and incorporation of H2A.Z subsequently affects the modification profile of neighboring canonical histones (*45*). Histone variants, histone modifications, and the interplay between the two are a primary determinant for chromatin structure. Modifications and variant functions are largely conserved from yeast to humans, making *S. cerevisiae* an ideal organism to study histone variants and novel marks. Chapter 4 of this thesis identifies several new modifications on the canonical histone H2B subtypes Htb1 and Htb2 and explores the role of each H2B subtype in H2A.Z function.

1.3 Functional consequences of histone modifications and variants

A histone code?

Histone modifications and histone variants serve two primary functions: to establish and maintain distinct global chromatin environments and to orchestrate DNA-dependent processes. Some have proposed that the pattern of modifications make up a histone code. The histone code hypothesis states that, “multiple histone modifications, acting in a combinatorial or sequential fashion on one or multiple tails, specify unique downstream functions” (*46*). Whether or not histone modifications specify a true code is subject to debate and depends on precise details of definition (*47*). For example, lysine acetylation on the tail of H4 has an additive rather than combinatorial affect on transcription (*48*). Additionally, the role of certain modifications appears to be context dependent. In flies, H3K9me is required for heterochromatin formation. However, at actively transcribed genes, H3K9me is necessary for the maintenance of transcription-associated modifications (*49*). Although the original histone code hypothesis has undergone some fine-tuning, it is clear that effector proteins recognize some histone modifications individually and others in combination to elicit specific biological programs.

Chromatin domains: euchromatin, heterochromatin, and silencing

The eukaryotic genome comes in two flavors: euchromatin and heterochromatin. Although first characterized by distinct cytological staining (*50*), extensive genome-wide analyses have revealed that each region is demarcated by a highly specific pattern of histone modifications and histone variants (*51*). Euchromatin contains the vast majority of protein coding genes. Although these genes may be transcriptionally active or repressed, euchromatic nucleosomes must maintain a more open conformation that is readily accessible to the transcriptional machinery. The *S. cerevisiae* genome is primarily euchromatic. Actively transcribed genes are characterized by a plethora of “active” transcription marks such as H3K4, 36, and 79 methylation and hyper-acetylation of H3 and H4 tails (*51*). Gene-specific repression within euchromatin is

defined by hypoacetylated and hypomethylated open reading frames (ORFs), however the intergenic regions between repressed ORFs remain hyperacetylated (*51*).

In contrast to euchromatin, heterochromatin is highly condensed, gene poor, and refractive to transcription. Budding yeast heterochromatin, referred to as silent chromatin, is found within the cryptic *HML* and *HMR* mating type loci and telomeres (*52*). These repressive chromatin domains are formed by localization of the SIR (Silent Information Regulator) complex (*53, 54*). At the silent *HM* loci, Sir1 nucleates the spreading of the Sir2, 3, 4 complex throughout the region (*54*). Sir2 is an NAD-dependent HDAC that removes H4K16ac from adjacent nucleosomes to create high affinity binding sites for Sir3 and Sir4, which preferentially bind unacetyllated tails of H3 and H4 (*55, 56*). Although the sequential spreading model for silencing is currently being re-evaluated using high-resolution ChIP-seq analysis (O. Zill and D. Thurtle, Rine Lab unpublished data), the enrichment of the SIR complex throughout regions of silent chromatin is necessary to maintain the silent state. Silent chromatin is hypoacetylated and hypomethylated (*57*). The boundary between euchromatin and heterochromatin is maintained by both sequence-specific elements and the histone variant H2A.Z (*42, 58*). Silent chromatin in budding yeast is distinct from heterochromatin in other eukaryotes, which is characterized by histone methyl modifications that are not found in *S. cerevisiae*. In mammals, heterochromatic regions are enriched with H3K9,27me and H4K20me, which recruit polycomb proteins that spread to create a repressive chromatin structure (*59*). Although distinct players are involved, *S. cerevisiae* silent chromatin provides an ideal opportunity to study how chromatin modifications, histone variants, and chromatin-associated enzymes regulate gene expression by establishing a specific chromatin landscape.

1.4 Histone chaperones mediate nucleosome traffic

Defining a histone chaperone

During every DNA-dependent process, chromatin must disassemble to grant the cellular machinery access to specific regions of DNA, and then reassemble in a way that preserves and propagates the local chromatin architecture. Histone proteins are highly basic, which makes them prone to aggregation and to inappropriate interactions when not associated with DNA. Therefore, chaperones are required to prevent these adverse effects and guide newly synthesized histones from the cytosol into chromatin (*60-63*). Histone chaperones were originally defined as proteins that bind histones and stimulate histone transfer without being a part of the assembled nucleosome. Histone chaperones are unique from other chromatin remodelers because they regulate chromatin structure without the use of ATP hydrolysis. Chaperone-mediated histone transfer was first visualized with *in vitro* nucleosome assembly reactions using purified chaperone, histones, and DNA. Further *in vivo* analyses revealed that different histone chaperones stimulate different types of histone movement, such as histone transfer from one chaperone to another, presenting histones to an enzyme, histone loading onto DNA, and eviction off DNA. Histone chaperones interact with H2A/H2B dimers, H3/H4

dimers or tetramers, or histone variants, and these interactions may be regulated by specific histone modifications.

Although it is known that chaperones have unique histone specificities, the general principles of chaperone-histone recognition are poorly defined. Studying the specificity of chaperones for distinct flavors of histones will provide a mechanistic understanding of how histone chaperones create distinct chromatin landscapes. A single chaperone can play multiples roles in creating these landscapes. Additional regulatory complexity is achieved by the interactions of chaperone-histone complexes with other chromatin factors, greatly expanding the potential for novel combinations of factors to mediate nucleosome turnover during distinct DNA-dependent processes. Below, I review the roles of histone chaperones in yeast replication, transcription, and silencing. Chapters 2 and 3 focus on a newly discovered histone chaperone, Rtt106, and its role in nucleosome turnover.

Chaperoning histones into the nucleus

During yeast nucleosome assembly, newly synthesized histones are acetylated in the cytosol at H4 K5 and K12 by the Hat1-Hat2 HAT complex (*64*). Interactions with the histone chaperone Asf1, Hat1-Hat2, and the karyopherin Kap123 promote H3/H4 transport into the nucleus (*65*). Similarly, H2A/H2B associates with the Nap1 histone chaperone and Kap114 for proper nuclear import (*66*). Nap1 shuttles H2A/H2B from the cytosol into the nucleus and then directly into chromatin, whereas histones H3/H4 receive additional modifications and are handed off between a series of chaperones. The path of H3/H4 deposition is regulated based on the targeted genomic region and the associated DNA-dependent process.

In addition to modifications within their N-terminal tails, upon nuclear import, H3/H4 histones are acetylated within each globular domain at H3K56 and H4K91 prior to their incorporation into chromatin (*67, 68*). The location of each residue within the nucleosome structure provides a tantalizing clue that these modifications likely play a role in nucleosome formation. H4K91 is located at the interface of H2A/H2B dimers and the H3/H4 tetramer. Acetylation of H4K91 may affect octamer formation by changing charged histone-histone interactions. Indeed, mutating H4K91 to an unacetylatable residue destabilizes nucleosomes and causes sensitivity to S-phase-specific genotoxic agents suggesting that H4K91ac regulates replication-dependent nucleosome turnover (*68*). H3K56 is located at the DNA entry and exit points of the nucleosome and therefore is proposed to affect nucleosome formation via altering histone-DNA binding (*69, 70*). H3K56ac also increases the affinity of several H3/H4 histone chaperones for H3 and promotes the incorporation of newly synthesized histones into chromatin (*71*). Following nuclear import, newly synthesized histones are handed off to a series of replication-dependent and replication-independent histone chaperones to mediate nucleosome assembly.

Histone chaperones in replication

Duplication of the genome requires chromatin unpacking and then repacking on a global scale. The regulation of nucleosome turnover is critical to maintain the chromatin landscape of the cell (*63*). During replication, duplex DNA is unwound by the MCM2-7 (minichromosome maintenance) helicase complex and single-stranded DNA is processed into double-stranded DNA by multiple polymerase complexes. Replication processivity is regulated by PCNA (proliferating cell nuclear antigen), a homotrimeric ring-shaped complex that binds DNA polymerase while encircling DNA to prevent polymerase dissociation. Electron micrographs of replicating SV40 mini-chromosomes estimate that the replication bubble exposes approximately 300 bp and 250 bp of naked DNA ahead of and behind the fork, respectively (*72, 73*). Replication-coupled nucleosome turnover is achieved by two primary mechanisms. 1) Ahead of the fork, parental nucleosomes are disrupted and randomly segregated onto the nascent DNA. 2) Newly synthesized histones are assembled *de novo* on the replicated daughter strands. Histone chaperones are integral in the coordination both types of nucleosome transfer during this elaborate process.

It is challenging to distinguish histone chaperones that are involved in nucleosome disassembly ahead of the fork from those that deposit newly synthesized histones behind the fork. Disrupting either process often results in an identical phenotype: stalled replication. The histone chaperones Asf1 and the FACT complex both promote MCM helicase activity *in vitro*, suggesting that they act ahead of the fork (*74, 75*). H3/H4 histones that co-purify with the Asf1-MCM complex have modifications characteristic of histones that have been incorporated into chromatin rather than the marks of newly synthesized histones (*74*). Asf1 may transfer these “old” histones onto replicated DNA behind the polymerase via direct interactions with PCNA and RFC (*76*). Therefore, in addition to its known role upstream in the *de novo* chromatin assembly pathway, Asf1 may also be required for nucleosome disassembly ahead of replicating polymerases. FACT’s chromatin reorganizing activity results in both displacement and incorporation of H2A/H2B dimers from chromatin (*77*). In *S. cerevisiae*, FACT co-purifies with the GINS complex, which loads DNA polymerase at origins (*78*), and with several components of the MCM helicase complex (*79*) suggesting that is it involved in replication-coupled nucleosome disassembly.

Nucleosome re-assembly after replication fork passage is mediated primarily by the CAF-1 (chromatin assembly factor) histone chaperone complex (*63*). CAF-1 localizes to replication forks via a direct interaction with PCNA (*80*). Mass spectrometry analysis of post-translational modifications shows that CAF-1 co-purifies with newly synthesized histones (*81*) and CAF-1-H3/H4 binding requires H3K56ac, a modification specific to newly synthesized histones (*67, 71*). In other eukaryotes, CAF-1 binds the replication-specific variant H3.1 and not the transcription-specific variant H3.3 (*82*).

Histone chaperones in transcription

As is the case for DNA replication, the passage of RNA polymerases requires coordinated nucleosome disassembly and assembly. Unlike replication, transcription occurs throughout the cell cycle and is regulated by a distinct set of histone chaperones,

modifications, and variants. The RNA polymerase II (Pol II) transcription program begins with transcription activators binding upstream DNA regulatory elements such as the TATA box and the transcription start site (TSS). Activators recruit adaptor complexes such as Mediator and SAGA, which in turn recruit general transcription factors (*83*). TFIID, TFIIA, and TFIIB position Pol II on the core promoter to form the closed pre-initiation complex (PIC). The helicase activity of TFIIH unwinds 11-15 bp of DNA, which generates a single-stranded template within the Pol II active cleft, forming the open PIC. Initiation of RNA synthesis triggers phosphorylation the Pol II carboxy-terminal domain (CTD) by TFIIH, which releases the associated general transcription factors. The transcribing Pol II utilizes CTD phosphorylation to recruit additional elongation components and mRNA processing factors (*84*).

During transcription initiation, Nap1 stimulates chromatin remodeler-mediated nucleosome eviction to expose the upstream regulatory DNA elements (*85, 86*). The FACT complex enhances subsequent TBP binding to TATA sequences (*87*). FACT mutants show reduced recruitment of transcription initiation factors and Pol II at gene promoters (*87, 88*) and a decreased stringency of promoter recognition (*89*).

During transcription elongation, FACT, Spt6, and Nap1 all are thought to facilitate the nucleosome disassembly in front of the Pol II and nucleosome reassembly onto transcribed DNA (*5*). The FACT complex associates with the PAF elongation complex (*90*) and co-localizes with Pol II throughout transcribed genes (*91*). Nap1 exhibits nucleosome removal during elongation on chromatin templates *in vitro* (*92*). Newly synthesized histones are deposited behind the transcribing Pol II by Asf1 and the HIR histone chaperone complex (*60*). In other eukaryotes, the HIR complex (HIRA) specifically binds the transcription-associated H3 variant H3.3 (*93*). Asf1 binds either the replication variant H3.1 or H3.3 and deposits both types into newly transcribed ORFs (*82*). *hir-* and *asf1-* mutants show delayed re-assembly of nucleosomes at certain genes following transcription (*94*). In addition to its role in active transcription, the HIR complex directs gene-specific repression of the histone genes outside of S-phase (*95*). These opposing functions suggest that histone chaperone activity is differentially regulated by unique protein interactions in different chromatin processes.

In addition to nucleosome turnover, histone chaperones modulate transcription-associated chromatin modifications by presenting histone targets to their specific modifying enzyme, directly stimulating enzyme activity, or recruiting modifying enzymes to chromatin. Asf1 presents H3 to the Rtt109/Vps75 HAT complex for the acetylation of K56 (*96*). H3K56ac is subsequently incorporated at the promoters of highly transcribed genes and is required for rapid nucleosome turnover (*97, 98*). Following the passage of Pol II, Spt6 recruits the Set2 HMT to methylate H3K36 on reassembled nucleosomes (*99, 100*). H3K36 methylation is then recognized by readers within the Rpd3S HDAC complex, which removes acetyl marks to prevent cryptic initiation within the coding region (*101*). Although it has been shown that histone chaperones can stimulate changes to histone modifications, less is known about how modifications can alter the affinity of chaperone-histone interactions. Given that chaperones bind histones during

all stages of turnover, the specificity of histone chaperones for certain modifications likely plays an underappreciated role in subsequent chromatin incorporation.

Histone chaperones in silencing

Both replication-dependent and replication-independent histone chaperones are important for the establishment and maintenance of silent chromatin. Asf1, HIR, and CAF-1 single mutants each show mild silencing defects. However *asf1Δ cac1Δ* and *hir1Δ cac1Δ* double mutants have synergistic silencing defects suggesting over-lapping roles for chaperones in silencing (*102*). *hir1Δ asf1Δ* double mutants, on the other hand, have mild silencing phenotypes similar to the single mutants (*102*). These data suggest that silencing is maintained by two partially redundant histone chaperone pathways in yeast, one involving CAF-1 and the other involving Asf1 and HIR. The role of CAF-1 in silencing is dependent upon its interaction with PCNA, suggesting that CAF-1 maintains silent chromatin during replication (*103*). *ASF1* was identified in two independent genetic screens for high-dosage disrupters of position-dependent gene silencing in yeast (*104, 105*). In *S. pombe*, Asf1 and HIRA spread across heterochromatic regions and interact with the Clr6 HDAC to promote histone deacetylation and further heterochromatin spreading (*106*).

Compared to replication and transcription, fewer studies have focused on the role of histone chaperones in silencing. Chaperone mutants lead to silencing defects, however, it is unclear at which stage of the silencing process they exert their effect. Additionally, it is unclear whether these defects arise because chaperones are required for positioning nucleosomes at silent loci or for depositing histones with modifications that are compatible with silencing. Studies of how chaperones function during this process will advance our understanding of the silent chromatin landscape.

Histone chaperones, where do we go from here

While the breadth and depth of the chromatin field continues to grow rapidly, much is still unknown about how histone chaperones coordinate nucleosome assembly and disassembly. Although originally thought to be blind histone carriers, it is now clear that chaperones have preferences for distinct histone compositions and that their activities are regulated by specific interactions with non-histone proteins. Here, we examine how chaperones regulate the delivery of specific histones to precise genomic sites and during distinct chromatin processes.

This dissertation focuses on the newest histone chaperone to enter the scene, Rtt106, which binds specifically to H3K56ac and coordinates nucleosome turnover during replication, transcription, and silencing (*71, 107-110*). Because Rtt106 does not contain a bromodomain, the mechanism used to distinguish H3K56ac from unmodified H3 is currently unclear. Studying how structural motifs on histone chaperones regulate interactions with specific marks will expand our knowledge of modification-recognition domains and the regulation of chaperone-histone binding. In Chapter 2, I address these questions through a structure-function analysis of Rtt106. Additionally, I gained insight

into the specificity of Rtt106 for H3K56ac through a comparative analysis of the histone reorganizer Pob3, which has similar domain architecture, but different binding specificity.

After examining Rtt106 binding specificity, I addressed the function of Rtt106 during three DNA-dependent processes: replication, transcription, and silencing. How histone chaperones target specifically modified histones to appropriate chromatin locations is not well understood. In Chapter 3, I show that the localization of Rtt106 to chromatin was process dependent, suggesting that in some cases the H3 was responsible for localizing the chaperone, whereas in others, Rtt106 was responsible for localizing the histone protein. Reduced binding of Rtt106 to H3 caused a reduction of H3K56ac in chromatin and disruption of several DNA-dependent processes. My results further establish the importance of H3K56ac in transcription, replication, and silencing and show that Rtt106 plays a key role in its deposition during each process.

Histone chaperones comprise a sophisticated network to guide histones through all stages of the cell cycle. Challenging questions remain about when and where specific chaperone-histone interactions function during distinct biological processes. A molecular understanding of how histone hand-off between chaperones is regulated will advance our knowledge of chromatin dynamics.

1.5 References

1. Luger, K., Mader, A. W., Richmond, R. K., Sargent, D. F., and Richmond, T. J. (1997) Crystal structure of the nucleosome core particle at 2.8 A resolution, *Nature 389*, 251-260.
2. Arents, G., Burlingame, R. W., Wang, B. C., Love, W. E., and Moudrianakis, E. N. (1991) The nucleosomal core histone octamer at 3.1 A resolution: a tripartite protein assembly and a left-handed superhelix, *Proceedings of the National Academy of Sciences of the United States of America 88*, 10148-10152.
3. Tremethick, D. J. (2007) Higher-order structures of chromatin: the elusive 30 nm fiber, *Cell 128*, 651-654.
4. Groth, A., Rocha, W., Verreault, A., and Almouzni, G. (2007) Chromatin challenges during DNA replication and repair, *Cell 128*, 721-733.
5. Li, B., Carey, M., and Workman, J. L. (2007) The role of chromatin during transcription, *Cell 128*, 707-719.
6. Malik, H. S., and Henikoff, S. (2003) Phylogenomics of the nucleosome, *Nature structural biology 10*, 882-891.
7. Albig, W., and Doenecke, D. (1997) The human histone gene cluster at the D6S105 locus, *Human genetics 101*, 284-294.
8. Hereford, L., Fahrner, K., Woolford, J., Jr., Rosbash, M., and Kaback, D. B. (1979) Isolation of yeast histone genes H2A and H2B, *Cell 18*, 1261-1271.
9. Smith, M. M., and Murray, K. (1983) Yeast H3 and H4 histone messenger RNAs are transcribed from two non-allelic gene sets, *Journal of molecular biology 169*, 641-661.

10. Smith, M. M., and Andresson, O. S. (1983) DNA sequences of yeast H3 and H4 histone genes from two non-allelic gene sets encode identical H3 and H4 proteins, *Journal of molecular biology 169*, 663-690.
11. Choe, J., Kolodrubetz, D., and Grunstein, M. (1982) The two yeast histone H2A genes encode similar protein subtypes, *Proceedings of the National Academy of Sciences of the United States of America 79*, 1484-1487.
12. Wallis, J. W., Hereford, L., and Grunstein, M. (1980) Histone H2B genes of yeast encode two different proteins, *Cell 22*, 799-805.
13. Kouzarides, T. (2007) Chromatin modifications and their function, *Cell 128*, 693-705.
14. Fischle, W., Wang, Y., and Allis, C. D. (2003) Histone and chromatin cross-talk, *Current opinion in cell biology 15*, 172-183.
15. Briggs, S. D., Xiao, T., Sun, Z. W., Caldwell, J. A., Shabanowitz, J., Hunt, D. F., Allis, C. D., and Strahl, B. D. (2002) Gene silencing: trans-histone regulatory pathway in chromatin, *Nature 418*, 498.
16. Sun, Z. W., and Allis, C. D. (2002) Ubiquitination of histone H2B regulates H3 methylation and gene silencing in yeast, *Nature 418*, 104-108.
17. Rayasam, G. V., Wendling, O., Angrand, P. O., Mark, M., Niederreither, K., Song, L., Lerouge, T., Hager, G. L., Chambon, P., and Losson, R. (2003) NSD1 is essential for early post-implantation development and has a catalytically active SET domain, *The EMBO journal 22*, 3153-3163.
18. Daniel, J. A., and Grant, P. A. (2007) Multi-tasking on chromatin with the SAGA coactivator complexes, *Mutation research 618*, 135-148.
19. Lu, P. Y., Levesque, N., and Kobor, M. S. (2009) NuA4 and SWR1-C: two chromatin-modifying complexes with overlapping functions and components, *Biochemistry and cell biology = Biochimie et biologie cellulaire 87*, 799-815.
20. Shia, W. J., Osada, S., Florens, L., Swanson, S. K., Washburn, M. P., and Workman, J. L. (2005) Characterization of the yeast trimeric-SAS acetyltransferase complex, *The Journal of biological chemistry 280*, 11987-11994.
21. Saha, A., Wittmeyer, J., and Cairns, B. R. (2006) Chromatin remodelling: the industrial revolution of DNA around histones, *Nature reviews 7*, 437-447.
22. Owen-Hughes, T., Utley, R. T., Cote, J., Peterson, C. L., and Workman, J. L. (1996) Persistent site-specific remodeling of a nucleosome array by transient action of the SWI/SNF complex, *Science (New York, N.Y 273*, 513-516.
23. Varga-Weisz, P. D., Wilm, M., Bonte, E., Dumas, K., Mann, M., and Becker, P. B. (1997) Chromatin-remodelling factor CHRAC contains the ATPases ISWI and topoisomerase II, *Nature 388*, 598-602.
24. Woo, C. J., and Kingston, R. E. (2007) HOTAIR lifts noncoding RNAs to new levels, *Cell 129*, 1257-1259.
25. Taverna, S. D., Li, H., Ruthenburg, A. J., Allis, C. D., and Patel, D. J. (2007) How chromatin-binding modules interpret histone modifications: lessons from professional pocket pickers, *Nature structural & molecular biology 14*, 1025-1040.
26. Kouzarides, T. (2000) Acetylation: a regulatory modification to rival phosphorylation?, *The EMBO journal 19*, 1176-1179.

27. Zeng, L., Zhang, Q., Li, S., Plotnikov, A. N., Walsh, M. J., and Zhou, M. M. (2010) Mechanism and regulation of acetylated histone binding by the tandem PHD finger of DPF3b, *Nature 466*, 258-262.
28. Yun, M., Wu, J., Workman, J. L., and Li, B. (2011) Readers of histone modifications, *Cell research 21*, 564-578.
29. Kasten, M., Szerlong, H., Erdjument-Bromage, H., Tempst, P., Werner, M., and Cairns, B. R. (2004) Tandem bromodomains in the chromatin remodeler RSC recognize acetylated histone H3 Lys14, *The EMBO journal 23*, 1348-1359.
30. Hassan, A. H., Prochasson, P., Neely, K. E., Galasinski, S. C., Chandy, M., Carrozza, M. J., and Workman, J. L. (2002) Function and selectivity of bromodomains in anchoring chromatin-modifying complexes to promoter nucleosomes, *Cell 111*, 369-379.
31. Ladurner, A. G., Inouye, C., Jain, R., and Tjian, R. (2003) Bromodomains mediate an acetyl-histone encoded antisilencing function at heterochromatin boundaries, *Molecular cell 11*, 365-376.
32. Jacobson, R. H., Ladurner, A. G., King, D. S., and Tjian, R. (2000) Structure and function of a human TAFII250 double bromodomain module, *Science (New York, N.Y 288*, 1422-1425.
33. Paro, R., and Hogness, D. S. (1991) The Polycomb protein shares a homologous domain with a heterochromatin-associated protein of Drosophila, *Proceedings of the National Academy of Sciences of the United States of America 88*, 263-267.
34. Huyen, Y., Zgheib, O., Ditullio, R. A., Jr., Gorgoulis, V. G., Zacharatos, P., Petty, T. J., Sheston, E. A., Mellert, H. S., Stavridi, E. S., and Halazonetis, T. D. (2004) Methylated lysine 79 of histone H3 targets 53BP1 to DNA double-strand breaks, *Nature 432*, 406-411.
35. Taverna, S. D., Ilin, S., Rogers, R. S., Tanny, J. C., Lavender, H., Li, H., Baker, L., Boyle, J., Blair, L. P., Chait, B. T., Patel, D. J., Aitchison, J. D., Tackett, A. J., and Allis, C. D. (2006) Yng1 PHD finger binding to H3 trimethylated at K4 promotes NuA3 HAT activity at K14 of H3 and transcription at a subset of targeted ORFs, *Molecular cell 24*, 785-796.
36. Hassan, A. H., Awad, S., Al-Natour, Z., Othman, S., Mustafa, F., and Rizvi, T. A. (2007) Selective recognition of acetylated histones by bromodomains in transcriptional co-activators, *The Biochemical journal 402*, 125-133.
37. Pray-Grant, M. G., Daniel, J. A., Schieltz, D., Yates, J. R., 3rd, and Grant, P. A. (2005) Chd1 chromodomain links histone H3 methylation with SAGA- and SLIK-dependent acetylation, *Nature 433*, 434-438.
38. Li, S., and Shogren-Knaak, M. A. (2009) The Gcn5 bromodomain of the SAGA complex facilitates cooperative and cross-tail acetylation of nucleosomes, *The Journal of biological chemistry 284*, 9411-9417.
39. Kamakaka, R. T., and Biggins, S. (2005) Histone variants: deviants?, *Genes & development 19*, 295-310.
40. Guillemette, B., and Gaudreau, L. (2006) Reuniting the contrasting functions of H2A.Z, *Biochemistry and cell biology = Biochimie et biologie cellulaire 84*, 528-535.
41. Yeh, E., and Bloom, K. (2006) Hitching a ride, *EMBO reports 7*, 985-987.

42. Babiarz, J. E., Halley, J. E., and Rine, J. (2006) Telomeric heterochromatin boundaries require NuA4-dependent acetylation of histone variant H2A.Z in Saccharomyces cerevisiae, *Genes & development 20*, 700-710.
43. Keogh, M. C., Mennella, T. A., Sawa, C., Berthelet, S., Krogan, N. J., Wolek, A., Podolny, V., Carpenter, L. R., Greenblatt, J. F., Baetz, K., and Buratowski, S. (2006) The Saccharomyces cerevisiae histone H2A variant Htz1 is acetylated by NuA4, *Genes & development 20*, 660-665.
44. Halley, J. E., Kaplan, T., Wang, A. Y., Kobor, M. S., and Rine, J. (2010) Roles for H2A.Z and its acetylation in GAL1 transcription and gene induction, but not GAL1-transcriptional memory, *PLoS biology 8*, e1000401.
45. Shia, W. J., Li, B., and Workman, J. L. (2006) SAS-mediated acetylation of histone H4 Lys 16 is required for H2A.Z incorporation at subtelomeric regions in Saccharomyces cerevisiae, *Genes & development 20*, 2507-2512.
46. Strahl, B. D., and Allis, C. D. (2000) The language of covalent histone modifications, *Nature 403*, 41-45.
47. Kurdistani, S. K., and Grunstein, M. (2003) Histone acetylation and deacetylation in yeast, *Nature reviews 4*, 276-284.
48. Dion, M. F., Altschuler, S. J., Wu, L. F., and Rando, O. J. (2005) Genomic characterization reveals a simple histone H4 acetylation code, *Proceedings of the National Academy of Sciences of the United States of America 102*, 5501-5506.
49. Beisel, C., Imhof, A., Greene, J., Kremmer, E., and Sauer, F. (2002) Histone methylation by the Drosophila epigenetic transcriptional regulator Ash1, *Nature 419*, 857-862.
50. Schultz, J. (1936) Variegation in Drosophila and the Inert Chromosome Regions, *Proceedings of the National Academy of Sciences of the United States of America 22*, 27-33.
51. Millar, C. B., and Grunstein, M. (2006) Genome-wide patterns of histone modifications in yeast, *Nature reviews 7*, 657-666.
52. Rusche, L. N., Kirchmaier, A. L., and Rine, J. (2003) The establishment, inheritance, and function of silenced chromatin in Saccharomyces cerevisiae, *Annual review of biochemistry 72*, 481-516.
53. Rine, J., and Herskowitz, I. (1987) Four genes responsible for a position effect on expression from HML and HMR in Saccharomyces cerevisiae, *Genetics 116*, 9-22.
54. Rusche, L. N., Kirchmaier, A. L., and Rine, J. (2002) Ordered nucleation and spreading of silenced chromatin in Saccharomyces cerevisiae, *Molecular biology of the cell 13*, 2207-2222.
55. Hoppe, G. J., Tanny, J. C., Rudner, A. D., Gerber, S. A., Danaie, S., Gygi, S. P., and Moazed, D. (2002) Steps in assembly of silent chromatin in yeast: Sir3-independent binding of a Sir2/Sir4 complex to silencers and role for Sir2-dependent deacetylation, *Molecular and cellular biology 22*, 4167-4180.
56. Carmen, A. A., Milne, L., and Grunstein, M. (2002) Acetylation of the yeast histone H4 N terminus regulates its binding to heterochromatin protein SIR3, *The Journal of biological chemistry 277*, 4778-4781.

57. Braunstein, M., Rose, A. B., Holmes, S. G., Allis, C. D., and Broach, J. R. (1993) Transcriptional silencing in yeast is associated with reduced nucleosome acetylation, *Genes & development 7*, 592-604.
58. Donze, D., Adams, C. R., Rine, J., and Kamakaka, R. T. (1999) The boundaries of the silenced HMR domain in Saccharomyces cerevisiae, *Genes & development 13*, 698-708.
59. Schuettengruber, B., Chourrout, D., Vervoort, M., Leblanc, B., and Cavalli, G. (2007) Genome regulation by polycomb and trithorax proteins, *Cell 128*, 735-745.
60. Avvakumov, N., Nourani, A., and Cote, J. (2011) Histone chaperones: modulators of chromatin marks, *Molecular cell 41*, 502-514.
61. Das, C., Tyler, J. K., and Churchill, M. E. (2010) The histone shuffle: histone chaperones in an energetic dance, *Trends in biochemical sciences 35*, 476-489.
62. De Koning, L., Corpet, A., Haber, J. E., and Almouzni, G. (2007) Histone chaperones: an escort network regulating histone traffic, *Nature structural & molecular biology 14*, 997-1007.
63. Ransom, M., Dennehey, B. K., and Tyler, J. K. (2010) Chaperoning histones during DNA replication and repair, *Cell 140*, 183-195.
64. Kleff, S., Andrulis, E. D., Anderson, C. W., and Sternglanz, R. (1995) Identification of a gene encoding a yeast histone H4 acetyltransferase, *The Journal of biological chemistry 270*, 24674-24677.
65. Mosammaparast, N., Guo, Y., Shabanowitz, J., Hunt, D. F., and Pemberton, L. F. (2002) Pathways mediating the nuclear import of histones H3 and H4 in yeast, *The Journal of biological chemistry 277*, 862-868.
66. Mosammaparast, N., Ewart, C. S., and Pemberton, L. F. (2002) A role for nucleosome assembly protein 1 in the nuclear transport of histones H2A and H2B, *The EMBO journal 21*, 6527-6538.
67. Masumoto, H., Hawke, D., Kobayashi, R., and Verreault, A. (2005) A role for cell-cycle-regulated histone H3 lysine 56 acetylation in the DNA damage response, *Nature 436*, 294-298.
68. Ye, J., Ai, X., Eugeni, E. E., Zhang, L., Carpenter, L. R., Jelinek, M. A., Freitas, M. A., and Parthun, M. R. (2005) Histone H4 lysine 91 acetylation a core domain modification associated with chromatin assembly, *Molecular cell 18*, 123-130.
69. Xu, F., Zhang, K., and Grunstein, M. (2005) Acetylation in histone H3 globular domain regulates gene expression in yeast, *Cell 121*, 375-385.
70. Neumann, H., Hancock, S. M., Buning, R., Routh, A., Chapman, L., Somers, J., Owen-Hughes, T., van Noort, J., Rhodes, D., and Chin, J. W. (2009) A method for genetically installing site-specific acetylation in recombinant histones defines the effects of H3 K56 acetylation, *Molecular cell 36*, 153-163.
71. Li, Q., Zhou, H., Wurtele, H., Davies, B., Horazdovsky, B., Verreault, A., and Zhang, Z. (2008) Acetylation of histone H3 lysine 56 regulates replication-coupled nucleosome assembly, *Cell 134*, 244-255.
72. Gasser, R., Koller, T., and Sogo, J. M. (1996) The stability of nucleosomes at the replication fork, *Journal of molecular biology 258*, 224-239.
73. Sogo, J. M., Stahl, H., Koller, T., and Knippers, R. (1986) Structure of replicating simian virus 40 minichromosomes. The replication fork, core histone segregation and terminal structures, *Journal of molecular biology 189*, 189-204.

74. Groth, A., Corpet, A., Cook, A. J., Roche, D., Bartek, J., Lukas, J., and Almouzni, G. (2007) Regulation of replication fork progression through histone supply and demand, *Science (New York, N.Y 318*, 1928-1931.
75. Tan, B. C., Chien, C. T., Hirose, S., and Lee, S. C. (2006) Functional cooperation between FACT and MCM helicase facilitates initiation of chromatin DNA replication, *The EMBO journal 25*, 3975-3985.
76. Franco, A. A., Lam, W. M., Burgers, P. M., and Kaufman, P. D. (2005) Histone deposition protein Asf1 maintains DNA replisome integrity and interacts with replication factor C, *Genes & development 19*, 1365-1375.
77. Belotserkovskaya, R., Oh, S., Bondarenko, V. A., Orphanides, G., Studitsky, V. M., and Reinberg, D. (2003) FACT facilitates transcription-dependent nucleosome alteration, *Science (New York, N.Y 301*, 1090-1093.
78. Gambus, A., Jones, R. C., Sanchez-Diaz, A., Kanemaki, M., van Deursen, F., Edmondson, R. D., and Labib, K. (2006) GINS maintains association of Cdc45 with MCM in replisome progression complexes at eukaryotic DNA replication forks, *Nature cell biology 8*, 358-366.
79. Labib, K., and Gambus, A. (2007) A key role for the GINS complex at DNA replication forks, *Trends in cell biology 17*, 271-278.
80. Shibahara, K., and Stillman, B. (1999) Replication-dependent marking of DNA by PCNA facilitates CAF-1-coupled inheritance of chromatin, *Cell 96*, 575-585.
81. Verreault, A., Kaufman, P. D., Kobayashi, R., and Stillman, B. (1996) Nucleosome assembly by a complex of CAF-1 and acetylated histones H3/H4, *Cell 87*, 95-104.
82. Tagami, H., Ray-Gallet, D., Almouzni, G., and Nakatani, Y. (2004) Histone H3.1 and H3.3 complexes mediate nucleosome assembly pathways dependent or independent of DNA synthesis, *Cell 116*, 51-61.
83. Thomas, M. C., and Chiang, C. M. (2006) The general transcription machinery and general cofactors, *Critical reviews in biochemistry and molecular biology 41*, 105-178.
84. Buratowski, S. (2003) The CTD code, *Nature structural biology 10*, 679-680.
85. Sharma, N., and Nyborg, J. K. (2008) The coactivators CBP/p300 and the histone chaperone NAP1 promote transcription-independent nucleosome eviction at the HTLV-1 promoter, *Proceedings of the National Academy of Sciences of the United States of America 105*, 7959-7963.
86. Walfridsson, J., Khorosjutina, O., Matikainen, P., Gustafsson, C. M., and Ekwall, K. (2007) A genome-wide role for CHD remodelling factors and Nap1 in nucleosome disassembly, *The EMBO journal 26*, 2868-2879.
87. Biswas, D., Dutta-Biswas, R., Mitra, D., Shibata, Y., Strahl, B. D., Formosa, T., and Stillman, D. J. (2006) Opposing roles for Set2 and yFACT in regulating TBP binding at promoters, *The EMBO journal 25*, 4479-4489.
88. Schwabish, M. A., and Struhl, K. (2004) Evidence for eviction and rapid deposition of histones upon transcriptional elongation by RNA polymerase II, *Molecular and cellular biology 24*, 10111-10117.
89. Formosa, T., Eriksson, P., Wittmeyer, J., Ginn, J., Yu, Y., and Stillman, D. J. (2001) Spt16-Pob3 and the HMG protein Nhp6 combine to form the nucleosome-binding factor SPN, *The EMBO journal 20*, 3506-3517.

90. Reinberg, D., and Sims, R. J., 3rd. (2006) de FACTo nucleosome dynamics, *The Journal of biological chemistry 281*, 23297-23301.
91. Saunders, A., Werner, J., Andrulis, E. D., Nakayama, T., Hirose, S., Reinberg, D., and Lis, J. T. (2003) Tracking FACT and the RNA polymerase II elongation complex through chromatin in vivo, *Science (New York, N.Y 301*, 1094-1096.
92. Owen-Hughes, T., and Workman, J. L. (1996) Remodeling the chromatin structure of a nucleosome array by transcription factor-targeted trans-displacement of histones, *The EMBO journal 15*, 4702-4712.
93. Henikoff, S., and Ahmad, K. (2005) Assembly of variant histones into chromatin, *Annual review of cell and developmental biology 21*, 133-153.
94. Adkins, M. W., Carson, J. J., English, C. M., Ramey, C. J., and Tyler, J. K. (2007) The histone chaperone anti-silencing function 1 stimulates the acetylation of newly synthesized histone H3 in S-phase, *The Journal of biological chemistry 282*, 1334-1340.
95. Spector, M. S., Raff, A., DeSilva, H., Lee, K., and Osley, M. A. (1997) Hir1p and Hir2p function as transcriptional corepressors to regulate histone gene transcription in the Saccharomyces cerevisiae cell cycle, *Molecular and cellular biology 17*, 545-552.
96. Tsubota, T., Berndsen, C. E., Erkmann, J. A., Smith, C. L., Yang, L., Freitas, M. A., Denu, J. M., and Kaufman, P. D. (2007) Histone H3-K56 acetylation is catalyzed by histone chaperone-dependent complexes, *Molecular cell 25*, 703-712.
97. Kaplan, T., Liu, C. L., Erkmann, J. A., Holik, J., Grunstein, M., Kaufman, P. D., Friedman, N., and Rando, O. J. (2008) Cell cycle- and chaperone-mediated regulation of H3K56ac incorporation in yeast, *PLoS genetics 4*, e1000270.
98. Williams, S. K., Truong, D., and Tyler, J. K. (2008) Acetylation in the globular core of histone H3 on lysine-56 promotes chromatin disassembly during transcriptional activation, *Proceedings of the National Academy of Sciences of the United States of America 105*, 9000-9005.
99. Yoh, S. M., Lucas, J. S., and Jones, K. A. (2008) The Iws1:Spt6:CTD complex controls cotranscriptional mRNA biosynthesis and HYPB/Setd2-mediated histone H3K36 methylation, *Genes & development 22*, 3422-3434.
100. Youdell, M. L., Kizer, K. O., Kisseleva-Romanova, E., Fuchs, S. M., Duro, E., Strahl, B. D., and Mellor, J. (2008) Roles for Ctk1 and Spt6 in regulating the different methylation states of histone H3 lysine 36, *Molecular and cellular biology 28*, 4915-4926.
101. Carrozza, M. J., Li, B., Florens, L., Suganuma, T., Swanson, S. K., Lee, K. K., Shia, W. J., Anderson, S., Yates, J., Washburn, M. P., and Workman, J. L. (2005) Histone H3 methylation by Set2 directs deacetylation of coding regions by Rpd3S to suppress spurious intragenic transcription, *Cell 123*, 581-592.
102. Kaufman, P. D., Cohen, J. L., and Osley, M. A. (1998) Hir proteins are required for position-dependent gene silencing in Saccharomyces cerevisiae in the absence of chromatin assembly factor I, *Molecular and cellular biology 18*, 4793-4806.

103. Krawitz, D. C., Kama, T., and Kaufman, P. D. (2002) Chromatin assembly factor I mutants defective for PCNA binding require Asf1/Hir proteins for silencing, *Molecular and cellular biology 22*, 614-625.
104. Le, S., Davis, C., Konopka, J. B., and Sternglanz, R. (1997) Two new S-phase-specific genes from Saccharomyces cerevisiae, *Yeast (Chichester, England) 13*, 1029-1042.
105. Singer, M. S., Kahana, A., Wolf, A. J., Meisinger, L. L., Peterson, S. E., Goggin, C., Mahowald, M., and Gottschling, D. E. (1998) Identification of high-copy disruptors of telomeric silencing in Saccharomyces cerevisiae, *Genetics 150*, 613-632.
106. Yamane, K., Mizuguchi, T., Cui, B., Zofall, M., Noma, K., and Grewal, S. I. (2011) Asf1/HIRA facilitate global histone deacetylation and associate with HP1 to promote nucleosome occupancy at heterochromatic loci, *Molecular cell 41*, 56-66.
107. Fillingham, J., Kainth, P., Lambert, J. P., van Bakel, H., Tsui, K., Pena-Castillo, L., Nislow, C., Figeys, D., Hughes, T. R., Greenblatt, J., and Andrews, B. J. (2009) Two-color cell array screen reveals interdependent roles for histone chaperones and a chromatin boundary regulator in histone gene repression, *Molecular cell 35*, 340-351.
108. Huang, S., Zhou, H., Katzmann, D., Hochstrasser, M., Atanasova, E., and Zhang, Z. (2005) Rtt106p is a histone chaperone involved in heterochromatin-mediated silencing, *Proceedings of the National Academy of Sciences of the United States of America 102*, 13410-13415.
109. Huang, S., Zhou, H., Tarara, J., and Zhang, Z. (2007) A novel role for histone chaperones CAF-1 and Rtt106p in heterochromatin silencing, *The EMBO journal 26*, 2274-2283.
110. Imbeault, D., Gamar, L., Rufiange, A., Paquet, E., and Nourani, A. (2008) The Rtt106 histone chaperone is functionally linked to transcription elongation and is involved in the regulation of spurious transcription from cryptic promoters in yeast, *The Journal of biological chemistry 283*, 27350-27354.

Chapter 2

The structural basis for Rtt106 histone chaperone activity

2.1 Introduction

Histone chaperones regulate histone turnover

Histone chaperones are molecular escorts that facilitate nucleosome assembly and disassembly during replication, transcription, and DNA repair (*1-4*). By virtue of their highly basic nature, histones are prone to aggregation and promiscuous interactions when not associated with DNA. To prevent these deleterious effects, a network of histone chaperones regulates each step of the assembly pathway. Histone chaperones are defined as proteins that bind histones and stimulate their transfer, either to another chromatin-associated protein, or directly onto DNA, without using the energy of ATP hydrolysis (*2*). Chaperone-histone binding is regulated by histone type, oligomeric status, and post-translational modifications. Although the structures of several divergent histone chaperones have been solved, a mechanistic understanding of how different domain architectures recognize specific histones and modifications is necessary for a complete picture of the chromatin choreography during molecular transactions on chromosomes. Here, we have examined how Rtt106 recognizes an acetylated form of histone H3 through a tandem pleckstrin homology (PH) domain architecture.

Rtt106 chaperones H3K56ac during replication-dependent and replication-independent nucleosome turnover

Rtt106 is a fungal-specific histone chaperone that was first discovered in a genetic screen as a regulator of Ty1 transposition (*5*). Subsequent studies revealed that during nucleosome assembly, Rtt106 likely receives newly synthesized H3K56ac molecules from the histone chaperone Asf1 and binds H3 in a K56ac-dependent manner (*6*). Rtt106 then delivers H3/H4 into chromatin during replication-coupled and replication-independent nucleosome assembly (figure 2.1) (*6-9*). H3K56 is located on the first alpha helix of H3 and contacts DNA at the entry and exit sites of the nucleosome. Acetylation of H3K56 disrupts the histone-DNA contact, which decreases nucleosome stability (*10*). Mass spectrometry analysis shows that essentially all H3 molecules (98%) are acetylated on K56 by the Rtt109-Vps75 acetyl transferase prior to incorporation into chromatin (*11*). The importance of H3K56ac in nucleosome assembly is reinforced by strong chemical-sensitivity phenotypes observed in strains with altered levels of H3K56ac (*asf1Δ* and *rtt109Δ*, for example) (*12, 13*).

During replication-coupled nucleosome assembly, Rtt106 is thought to deliver H3K56ac to sites of DNA synthesis through a direct, physical interaction with the CAF-1 complex (Cac1, Cac2, Msi1) (*8*). CAF-1 is targeted to replication forks by PCNA and, like Rtt106, binds H3 in a K56ac-dependent manner (*6, 14*). Synergistic sensitivities to S-phase-specific DNA damaging agents in *rtt106*Δ *cac1*Δ double mutants suggest that Rtt106 and CAF-1 perform overlapping functions during replication (*8*). Rtt106 interacts physically with Sir4, and *rtt106*Δ *cac1*Δ mutants have synergistic silencing phenotypes, suggesting the chaperoning H3K56ac at *HMR* and the telomeres is necessary for silent chromatin formation (*8, 15*). Throughout the cell cycle, Rtt106 is also recruited to core histone gene promoters by the HIR complex (Hir1, Hir2, Hir3, Hcp2) and represses

histone transcription outside of S-phase (*7*). Cellular phenotypes associated with Rtt106-H3K56ac binding are analyzed in depth in Chapter 3. In this chapter, we performed a structure-function analysis the Rtt106-H3K56ac binding interaction.

The structure of Rtt106

Structures of several histone-binding proteins provide examples of how histone binding specificity and regulation is achieved. The co-crystal structure of the complex between yeast Asf1 and histones H3 and H4 revealed that Asf1 binds H3/H4 dimers along the H3/H4 tetramerization surface (*16, 17*). By physically occluding H3/H4 tetramerization, this structural analysis provided strong evidence that Asf1 regulates the H3/H4 dimer-to-tetramer transition during nucleosome assembly. Additionally, the Rtt109-AcCoA/Vps75 crystal structure suggests that the histone chaperone Vps75 stimulates Rtt109 acetyl transferase activity by positioning the H3 tail within the holoenzyme's central cavity (*18*). To determine how Rtt106-H3K56ac binding is regulated, our collaborators Andy Antczak and James Berger determined the crystal structure of a truncated form of Rtt106 (residues 69-300 out of a total length of 455) at a resolution of 2.6Å.

The structure of Rtt106 revealed two pleckstrin homology (PH) domains in tandem (figure 2.2). PH domains were first defined in pleckstrin, the major substrate of protein kinase C in platelet cells (*19, 20*). Human PH domains are best known for their ability to target proteins to the cellular membrane by binding phosphoinositides (*21*). However, studies in yeast reveal that only a small fraction of PH domain-containing proteins are capable of inositol lipid binding (*22*). Additional binding targets include phosphotyrosine, polyproline, and other peptide species (*23, 24*). Therefore, a PH domain indicates a possible binding function, but does not reveal the ligand.

The PH domain structure consists of a seven-stranded β-barrel, which is formed by two perpendicular anti-parallel β-sheets, with a C-terminal amphipathic α-helix (*20*). PH domain-like structures are classified into seven distinct subgroups that are prevalent in all species ranging from prokaryotes to mammals (*25*). Each subgroup adopts the same PH fold, but the size and composition of the loops connecting the individual β-strands vary. The loops enable binding promiscuity, but render PH domains difficult to detect based on primary sequence (*26*). Indeed, initial sequence analysis of Rtt106 predicted only a single PH domain (PFAM). Furthermore, because binding sites have been characterized on many different regions of the PH domain, examination of structural properties alone cannot reveal the ligand-binding surface.

Until the discovery of the PH-domain-encoding Rtt106, bromodomains (*27*) and plant homeodomains (*28*) were the only motifs known to specifically bind acetyl-lysine. Both domains are characterized by a hydrophobic binding pocket and are found on numerous chromatin-associated proteins (*27*). For example, Bdf1 is an effector protein that utilizes its double bromodomain motif to recruit the transcriptional machinery to acetylated promoters of active genes (*29*). Because Rtt106-H3 binding is H3K56ac-

dependent (*6*), the PH domain could represent a novel structural motif for acetyl-lysine recognition.

The two PH domains of Rtt106 and their relative orientations are analogous to the organization of two PH domains in Pob3, a member of the chromatin-reorganizing complex, yFACT (facilitates chromatin transactions: Spt16, Pob3, Nhp6). (*30*). The FACT complex destabilizes nucleosomes and is thought to promote the recycling of parental histones during replication and transcription (*31*). However, the role of H3K56ac in Pob3-mediated nucleosome assembly remains unknown. Unlike chromatin remodelers, which use ATP hydrolysis to catalyze nucleosome translocation or exchange, yFACT uses binding energy to alter nucleosome structures and therefore is classified as a "reorganizer" (*32, 33*). Although yFACT was originally shown to mediate H2A-H2B binding through the Spt16 subunit, recent work suggests that yFACT also binds H3/H4 via Pob3 (*6*). The structural similarity between Rtt106 and Pob3 provides an opportunity to pinpoint residues on the PH domain(s) that are necessary for H3/H4 binding, and potentially identify the H3K56ac binding pocket.

Summary of findings

In this chapter, we performed a targeted mutational screen that identified two functionally important clusters of residues on Rtt106 that were required for replication-coupled nucleosome assembly and silencing. One cluster lies within a basic patch on the surface of the N-terminal PH domain and the other critical site is a loop that connects a pair of β-sheets in the C-terminal PH domain. Within each region, *rtt106 S80E, R86A*, and *T265E* single mutants each produced silencing defects and chemical sensitivities that were similar to the *rtt106*Δ phenotype. *In vitro* and *in vivo* affinity purification experiments showed that both regions on Rtt106 were necessary for the direct interaction with histone H3. Therefore, a reduction in Rtt106-H3 binding likely underlies the silencing and replication defects. Although the exact location of the H3K56ac binding pocket remains elusive, a comparative analysis with Pob3 suggested that the C-terminal loop was the source of H3K56ac-specificity in the Rtt106-H3 interaction.

2.2 Materials and Methods

Yeast strains, plasmids, and culture

Yeast:

All yeast strains were generated in the *S. cerevisiae* W303 background unless otherwise indicated (table 2.1). Gene deletions were generated by one-step integration of knock-out cassettes (*34, 35*). PCR analysis of the 5' and 3' end of each targeted gene verified complete knock-outs. The *HMR-a1Δ::K.l.URA3* reporter strain used to screen *RTT106* mutants for silencing defects was previously described (*36*). The *lys2-128∂* reporter strain used to screen *POB3* mutants for transcription initiation (Spt^-) phenotypes was previously described (*30*). *RTT106* plasmids were introduced into each mutant strain using the standard plasmid transformation protocol (*37*). *HHT2-HHF2* and *POB3* plasmids harboring mutations of interest were introduced into strains containing

wild type versions of the relevant gene by plasmid swap using FOA counter selection. Plasmids are described in table 2.2.

Plasmids:

RTT106 was cloned into pRS313 using gap repair to generate pRZ050. *RTT106* was amplified from wild-type genomic DNA (JRY3009) using Phusion polymerase (NEB). The PCR fragment and EcoRI SalI digested pRS313 were co-transformed into JRY3009. Plasmids were rescued from His^+ tranformants and sequenced. Site-directed mutagenesis was used to generate the *rtt106(69-300)* truncation (pRZ056) as described (*38*). A C-terminal 3xFLAG tag (*39*) was integrated on the plasmid in frame with *RTT106* and *rtt106(69-300)* using homologous recombination, resulting in pRZ093 and pRZ094, respectively. The 72 *RTT106* point mutations were generated on pRZ093 by site-directed mutagenesis performed by the QB3 Macrolab Facility at UC Berkeley. The targeted mutants are described in table 2.3. Follow-up mutants were generated using site-directed mutagenesis (*38*) and Pfu Ultra polymerase (Stratagene) (table 2.4).

Full length *RTT106* was inserted into pET3a Tr by ligation independent cloning (LIC) to generate *His_6-RTT106* expressing plasmids (pRZ044) (*40*). Point mutants were generated using site-directed mutagenesis (*38*) and Pfu Ultra polymerase (Stratagene) (pRZ216, 218, 220). The polycistronic expression plasmid, containing full length, untagged *HHT1* and *HHF1,* was previously described (pRZ047) (*16, 41*).

POB3 and *POB3-13xMYC* were cloned into pRS313 by gap repair to generate pRZ235 and pRZ236 respectively. *POB3* and *POB3-13xMYC::KanMX* were amplified from JRY3009 and RZY1404 (a gift from T. Formosa) genomic DNA using Phusion polymerase (NEB). The PCR fragment and EcoRI SalI digested pRS313 were cotransformed into a wild type strain (JRY3009). Plasmids were rescued from His+ tranformants and sequenced. Point mutants were generated using site-directed mutagenesis (*38*) and Pfu Ultra polymerase (Stratagene) (table 2.5). The RZY1369 background was used for hydroxyurea growth experiments because *POB3* mutants had increased chemical sensitivities in the W303 background compared to S288c.

Histone point mutants (pRZ102, 225) were generated using site-directed mutagenesis with Pfu Ultra polymerase (Stratagene) on pJR2851.

Culture:

To screen *RTT106* and *POB3* mutants for silencing, transcription initiation, and/or chemical sensitivity phenotypes, five-fold serial dilutions of saturated overnight cultures were frogged onto selective media as previously described (*30, 36, 42*). All selective media lacked histidine (-HIS) to maintain selection of *RTT106* or *POB3* plasmids.

Protein analysis and co-purification:

Yeast co-immunoprecipitation:

Rtt106-3xFLAG immunoprecipitations were performed as previously described (*42*). 150 OD_{600} units of mid-log phase cells were harvested by centrifugation and resuspended in Buffer HIP (150 mM Tris-Cl at pH 7.8, 200 mM NaCl, 1.5 mM MgAc, 10 mM NaPPi, 0.1 mM Na_3VO_4, 5 mM NaF, Complete Protease inhibitor cocktail [Roche]). Cells were lysed with acid-washed glass beads and fast prep shaking. Chromatin was digested with 10 U micrococcal nuclease in 1 mM $CaCl_2$ (Sigma) for 10 min at 37 ºC. Insoluble material was pelleted by centrifugation. The supernatant was incubated with 50 µl slurry of anti-FLAG M2 agarose (Sigma) for 2 hrs at 4 ºC. Beads were washed three times with 0.6 ml of HIP buffer. After the final wash, buffer was completely removed with a 30-gauge needle and the beads were resuspended in 25 µl SDS loading buffer. SDS-PAGE and immunoblotting were performed using standard procedures and evaluated with a LiCOR imaging system. Anti-Flag M2 antibody (Sigma) was used to detect Rtt106-3xFLAG and anti-H3 (Ab1791) or anti-H3K56ac (07-677; Millipore) were used to monitor co-purifying proteins.

Pob3-13xMyc immunoprecipitations were performed as described above. Solubilized yeast lysate was incubated with 30 µl anti-c-Myc agarose (Sigma). Anti-c-Myc antibody (M4439; Sigma) was used to detect Pob3-13xMYC and anti-H3 (Ab1791) or anti-H3K56ac (07-677; Millipore) were used to monitor co-purifying proteins. NaCl concentrations were as indicated. 100 mM Na butyrate and 5 mM nicotinamide were included in 50 mM NaCl immunoprecipitations to prevent proteins from sticking to agarose beads non-specifically.

Detection of phosphorylation:

Rtt106-3xFLAG was immunoprecipitated from yeast lysate as described above. The resuspended purified sample was separated by SDS-PAGE supplemented with 30 µM Phos-tag acrylamide (Hiroshima University, Hiroshima, Japan) with 60 µM $MnCl_2$ as described (*43*).

E. coli extract histone binding assays:

Bacterial co-expressions and affinity purifications were performed as described (*16*). Briefly, BL21 (DE3)-Rosetta *E. coli* cells were co-transformed with *HHT1 HHF1* histone (pRZ047) and *His_6-RTT106* (pRZ044, 216, 218, 220) expression plasmids. Protein expression was induced at OD_{600} = 0.5 with 0.5 mM IPTG for 5 hours at 30 ºC. Cell extracts were prepared by sonication in a lysis buffer containing 20 mM Tris pH 7.5, 150 mM NaCl, 0.01% NP-40, 10 mM imidazole, PMSF, leupeptin, pepstatin. 4 mg of soluble extract was incubated with 20 µl Ni-NTA beads (Qiagen) for 2 hr at 4 ºC. Beads were washed three times in 1 ml of lysis buffer. After the final wash, buffer was completely removed with a 30-gauge needle and the beads were resuspended in 25 µl SDS loading buffer. SDS-PAGE and immunoblotting were performed using standard procedures and a LiCOR imaging system. Anti-His (34670; Qiagen) was used to detect His_6-Rtt106 and co-purifying histones were detected with anti-H3 (Ab1791).

2.3 Results

Two regions on Rtt106 were necessary for silencing and nucleosome assembly

Antczak and Berger solved the structure of a truncated version of Rtt106 (2PH), which contained residues 69-300 of the 455 amino acid protein. The N- and C-termini of the full-length protein were predicted to be unstructured and therefore were excluded from the analysis (PFAM). The unstructured C-terminal extension, which is also present in histone chaperones Nap1, Asf1, and Vps75 (*1*), is highly acidic and likely promotes non-specific electrostatic interactions with the highly basic histone proteins (*1, 44*). Although some recombinant truncations of Rtt106 are sufficient to bind H3 *in vitro* (*6, 45*), the 69-300 truncation phenocopied the null allele *in vivo* with respect to silencing (figure 2.3a), nucleosome assembly (figure 2.3b), and H3 binding (figure 2.3c) functions. Therefore, all analyses were conducted using full-length *RTT106*.

To define the Rtt106-H3 interaction surface, we screened 72 *RTT106* point mutants that were designed based either on sequence conservation or on the Rtt106 structure (table 2.3, figure 2.4). Targeted residues were solvent exposed and covered both conserved and non-conserved surfaces. Mutants were screened for defects in two distinct Rtt106-mediated processes: silencing and replication-coupled nucleosome assembly. Since Rtt106-H3 binding is upstream in the nucleosome assembly pathway, we reasoned that Rtt106-H3 binding mutants would likely disrupt multiple processes (figure 2.1).

Mutants were screened for silencing and nucleosome assembly phenotypes by growth on selective media. Silencing at *HMR* was monitored using a *URA3* reporter strain (*HMR-a1Δ::K.l.URA3*). Strains with wild type silencing were able to grow on medium containing 5-fluoroortic acid (FOA), a counter selection for *URA3* expression. Conversely, mutants with silencing defects failed to grow on FOA and gained the ability to grow on medium lacking uracil (-URA). Nucleosome assembly was assayed by growth in the presence of the DNA damaging agent camptothecin (CPT), for which the *cac1*Δ *rtt106*Δ double mutant, and many chromatin assembly mutants are sensitive. All experiments were conducted in a sensitized *cac1Δ* background to expand the sensitivity range of the assays (figure 2.5a). Our results revealed two functionally important clusters of conserved residues, one within each pleckstrin homology (PH) domain (Figure 2.5a,b). We observed a tight correlation between silencing and nucleosome assembly phenotypes, which suggests that these two processes are disrupted by a common mechanism (figure 2.5a). Within each cluster, mutants *S80E*, *R86A* and *T265E* produced the strongest phenotypes and therefore were pursued in further analysis. These results are consistent with a recently published analysis of the Rtt106 structure (*46*). That study used less precise mutations in a truncated form of the protein, limiting confidence in the ability to deduce *in vivo* relevance.

To determine which biochemical properties of S80, R86, and T265 were important for Rtt106 function, we tested the effect of conservative and non-conservative

substitutions at each site (figure 2.6a). S80 and R86 are located within a basic patch on N-terminal PH domain of Rtt106 (figure 2.5b). S80E and S80D mutants resulted in strong silencing and nucleosome assembly phenotypes whereas S80T and S80A mutants behaved like wild type. Similarly, the R86A mutant had severe defects whereas the R86K mutant did not. Therefore, maintaining the charge of this basic surface on Rtt106 is critical for function. T265 is located within a nine residue loop on the C-terminal PH domain of Rtt106 (figure 2.5b). T265E and T265D mutants yielded strong phenotypes whereas T265S and T265A mutants behaved like wild type. However, TT265,268AA double mutants phenocopied T265E suggesting that the proximal T268 may compensate for a T265A mutation. Because S80 and TT265,268 were potentially phosphorylatable, and DNA damaging agents like CPT activate checkpoint protein kinases, we tested whether mutating these residues affected the phosphorylation status of Rtt106.

To determine whether residues S80 or TT265,286 were phosphorylated, Rtt106 S80E and TT265,268EE proteins were purified from yeast and analyzed on a phos-tag gel (figure 2.6b). The phos-tag binds anionic compounds to separate phosphorylated from unphosphorylated proteins. We also analyzed Rtt106 purified from an *rtt109*Δ background, which lacks H3K56ac, to test whether Rtt106-H3 binding affects the phosphorylation profile of Rtt106. Although we did observe a single minor band migrating above the dominant species, which suggests that Rtt106 might be phosphorylated, all mutants behaved identically to wild type. Therefore the phenotypes associated with S80E and TT265,268EE mutants are likely not due to a change in the phosphorylation status of Rtt106.

Both regions defined the Rtt106-H3 interaction surface

During nucleosome turnover, Rtt106 binds H3, in a K56ac-dependent manner, to deposit newly synthesized histones (*6*). Consistent with previous results, we demonstrated that Rtt106-H3 binding was reduced to background levels in strains that lacked the H3K56ac-specific histone acetyl transferase (*rtt109*Δ) or that contained an unmodifiable H3K56R mutation (figure 2.7a,b). Conversely, Rtt106 showed increased H3 binding in strains that lacked the H3K56ac-specific deacetylases (*hst3*Δ *hst4*Δ) or that contained the acetyl-mimic H3K56Q (figure 2.7a,b). Although Rtt106 interacts with other H3/H4 chaperones, *hir1*Δ and *cac1*Δ backgrounds did not alter Rtt106-H3 binding (figure 2.7e). Therefore, the Rtt106-H3 co-purification reflected a direct physical interaction.

Co-immunoprecipitation (CoIP) experiments showed that Rtt106 S80E, R86A, and T265E had significantly reduced H3 binding *in vivo* (figure 2.7c). Additionally, we co-expressed wild type and mutant forms of Rtt106 with *S. cerevisiae* histones H3 and H4 in *E. coli* and monitored binding using affinity purification (figure 2.7d). H3K56ac was required for Rtt106-H3 binding *in vivo,* and H3K56 is not acetylated in *E. coli*. Therefore, it was not surprising that Rtt106 binds recombinant H3 *in vitro* with lower affinity compared to H3 isolated from yeast (*6, 45*). Reduced binding in all three mutants compared to wild type suggests that residues S80, R86, and T265 define an Rtt106-H3

interaction surface that is necessary for silencing and nucleosome assembly. The distance between the two sites suggests that Rtt106 makes multiple contacts with H3. Next, we sought to determine which site specifically recognized K56ac.

To define the origin of H3K56ac specificity in Rtt106, we performed Rtt106-H3 CoIP experiments in yeast strains containing elevated levels of H3K56ac (*hst3*Δ *hst4*Δ or H3K56Q) (figure 2.8a,b). If Rtt106 binds K56ac at one of the two critical sites (site 1) and the other site (site 2) binds another region on H3, point mutants within site 2 might show increased H3 binding in *hst3*Δ *hst4*Δ and H3K56Q backgrounds relative to site 2 mutant binding in an otherwise wild type strain. Mutants within the K56ac binding pocket (site 1) should maintain reduced binding. Surprisingly, all mutants maintained reduced binding, suggesting that either both sites are critical for Rtt106-H3K56ac binding or that changes in binding affinity were too small to be detected by the CoIP experiment.

Pob3 comparative analysis

The relative orientations of the two PH domains of Rtt106 are reminiscent of the two PH domains of Pob3, a member of the chromatin-reorganizing complex, yFACT (*30*) (figure 2.9a). Both Rtt106 and Pob3 bind histones H3/H4, therefore, it is possible that the two regions we have defined on Rtt106 are also important for Pob3 function. To test whether the H3 binding motif is conserved between Pob3 and Rtt106, we generated the analogous mutations in Pob3 and monitored transcription, replication, and H3-binding phenotypes.

Mapping the charge distribution onto the Pob3 structure revealed a basic patch on the N-terminal PH domain in a position analogous to the basic region identified as critical for Rtt106-mediated nucleosome assembly (figure 2.9c). To test whether the charge of this basic patch was necessary for Pob3 function, we generated several glutamate substitutions (F249E, T251E, and T252E) to mimic Rtt106 S80E (figure 2.9d). Analysis of the superimposed structures revealed two candidate arginine residues on Pob3 (R254, R256) that we mutated to alanine to mimic Rtt106 R86A (figure 2.9b). The loop within the C-terminal PH domain of Pob3 is longer (11 residues) than Rtt106 (9 residues) and unlike Rtt106's structure, the loop is not present in the Pob3 structure due to disorder in the crystal (figure 2.9a,b). To test whether the Pob3 loop was critical for function, all 11 residues were mutated to glycine (Pob3 423-433 $(G)_{11}$) and a Pob3 TT428,430EE mutant was constructed to mimic Rtt106 T265E (figure 2.9b).

Pob3 mutants were screened for transcription initiation (Spt^-) phenotypes using the *lys2-128δ* reporter, which contains a Ty1 insertion in the *LYS2* promoter. Mutants with transcription initiation defects bypass the Ty1 insertion, allowing growth on medium lacking lysine (-LYS). Additionally, mutants were screened for replication defects by assaying growth on medium containing hydroxyurea (HU), an S-phase-specific DNA damaging agent.

All observed Pob3 mutant phenotypes were less severe than Pob3 Q308K, a well-studied mutation that disrupts both transcription initiation and replication (figure

2.11a,b) (*30*). Pob3 T252E had the strongest Spt$^-$ phenotype and was the only mutant with any detectable HU sensitivity (figure 2.10a,b). F249E and T251E produced mild Spt$^-$ phenotypes, and RR254,256AA had no phenotype (figure 2.10a.b). Surprisingly, 423-433 $(G)_{11}$ yielded only mild Spt$^-$ phenotypes and the TT428,430EE mutant phenotype was even less severe (figure 2.10a,b). Therefore, whereas the N-terminal basic patch contains residues that are critical for Pob3 function, the C-terminal loop is not important.

To determine whether the targeted Pob3 residues define a conserved H3 interaction surface, we tested the ability of each Pob3 mutant to bind H3 *in vivo*. Co-purification experiments revealed that Pob3-H3 binding defects mirrored the severity of the observed Spt$^-$ phenotypes (figure 2.11). Pob3 T252E had the strongest H3 binding defect, F249E and T251E had slightly reduced binding, and RR254,256AA bound the same amount of H3 as wild type (figure 2.11a). The loop mutants, 423-433 $(G)_{11}$ and TT428,430EE, showed only slightly reduced H3 binding (figure 2.11b). In Rtt106, a single mutant residue within the N-terminal basic patch or the C-terminal loop abolished the interaction with H3. In contrast, the H3 binding function of Pob3 was sensitive only to mutations of the N-terminal basic patch and robust to perturbations of the analogous C-terminal loop. In sum, these results point to distinct mechanisms of H3 binding for Pob3 and Rtt106.

Since Pob3 utilizes different regions to interact with H3, it is possible that unlike Rtt106, Pob3-H3 binding is H3K56ac-independent. CoIP experiments in *rtt109*Δ cells showed that, although binding was reduced, Pob3 still interacted with H3 in the absence of K56ac (figure 2.12). Additionally, *hst3*Δ *hst4*Δ cells, which showed elevated levels of Rtt106-H3 binding, showed reduced Pob3-H3 binding (figure 2.12), indicating differences in Pob3-H3 and Rtt106-H3 recognition. Because the C-terminal loop was not essential for Pob3-H3 binding, and Pob3-H3 binding was H3K56ac independent, we propose that the Rtt106 C-terminal loop provides H3K56ac-specificity.

Residue T252, which gave the strongest phenotype of any mutant we screened, is in close proximity to Q308 (8.69 Å). To determine whether T252E and Q308K mutants disrupted Pob3 function through a common mechanism, we analyzed the double mutant. Surprisingly, the T252E Q308K double mutants suppressed the Spt$^-$ and HU-sensitivity phenotypes of each T252E or Q308K singe mutant (figure 2.13a). Additionally, unlike the T252E mutant, which reduced Pob3-H3 binding, the Q308K mutant had significantly increased Pob3-H3 binding compared to wild type (figure 2.13b). The T252E Q308K double mutant restored Pob3-H3 binding to a level closer to wild type (figure 2.13b). This analysis indicates that a precise level of H3 binding is required for wild type Pob3 function and further implicates this specific region on the N-terminal PH domain in H3 binding.

2.4 Discussion

Rtt106 binds H3 through a tandem pleckstrin homology domain

The x-ray structure of Rtt106 revealed a double pleckstrin homology (PH) architecture (figure 2.2). PH domains have promiscuous targets and do not employ a conserved structural binding mechanism. To identify residues important for Rtt106-H3 binding, which is likely a pre-requisite for all Rtt106 chaperone activity, we screened for mutants that disrupted two distinct branches of the Rtt106-mediated nucleosome assembly pathway: silencing and replication-coupled nucleosome deposition (figure 2.1). Our screen identified two regions, one within each PH domain, in which mutations reduced Rtt106 function (figure 2.5b). As predicted, mutations in both regions were defective for Rtt106-H3 binding, suggesting that these two regions define the Rtt106-H3 interaction surface (figure 2.7c).

The H3 binding surface of Rtt106 was defined by a basic patch on the N-terminal PH domain and a loop within the C-terminal PH domain (figure 2.6). Although it is counterintuitive that a basic surface on Rtt106 could mediate binding with the highly basic histone proteins, histones do contain acidic patches that have previously been implicated in histone-histone interactions (*47*). Therefore, histone chaperones may adopt a similar binding mechanism to regulate nucleosome assembly by occluding these regions prior to histone octamer formation.

The loop within the C-terminal PH domain was consistent with previous reports that the loops connecting β-sheets in PH domains are the source of ligand specificity (*24*). Although, histone chaperones contain diverse structural domains, it is possible that Rtt106 uses a conserved histone binding strategy. Asf1 utilizes anti-parallel β-sheets to sandwich the β-strand of H4 (*17*). Therefore, Rtt106 might bind H3 via a similar mechanism using the loop and the two associated anti-parallel beta sheets (*45*). However, unlike Asf1, Rtt106 binds a different region on H3 and K56ac regulates H3 binding. Therefore, we expect that the C-terminal loop of Rtt106 specifies the H3K56ac interaction by a previously unreported mechanism.

Our results suggest that Rtt106 utilizes both PH domains to make multiple contacts with H3 (figure 2.7c,d). Surprisingly, monitoring mutant Rtt106-H3 binding in backgrounds containing elevated levels of H3K56ac did not reveal which PH domain contained the K56ac-binding pocket (figure 2.8). Therefore, we further defined the separate contributions of each PH domain to Rtt106-H3 binding using a comparative analysis with Pob3, a member of the chromatin reorganizing complex yFACT.

Rtt106 and Pob3 utilize distinct mechanisms to bind H3

Like Rtt106, Pob3 contains a tandem PH domain architecture and has been implicated in H3/H4 binding (*30*). To determine whether Rtt106 and Pob3 bind H3/H4 via a similar mechanism, we mutated the analogous regions within each PH domain on Pob3 and monitored Pob3-H3 binding and Pob3 cellular functions (figure 2.9). A

mutation within the N-terminal basic patch of Pob3 (Pob3 T252E) disrupted Pob3-H3 binding and led to replication and transcription initiation defects (figure 2.10 and 2.11). These phenotypes suggest that the N-terminal PH domains of Rtt106 and Pob3 use a common H3 binding mechanism. This mechanism was highly sensitive to local electrostatics; the addition of a negative charge into the basic region disrupted H3 binding with both Rtt106 and Pob3.

In contrast to the reduced Pob3-H3 binding observed in the Pob3 T252E mutant, a previously characterized Pob3 mutant within the N-terminal PH domain, Q308K, had an increased affinity for H3 (figure 2.13b). Interestingly, both reduced Pob3-H3 binding through addition of a negative charge (T252E), and increased Pob3-H3 binding through addition of a positive charge (Q308K), were deleterious to Pob3 function (figure 2.13a). Combining these mutations in a T252E Q308K double mutant had a neutralizing effect and restored near wild type levels of Pob3-H3 binding and *in vivo* functions (figure 2.13a,b). This suppression may result from a restoration of electrostatics or specific interactions through a neighboring Tyr residue (figure 2.13c). Future studies with Rtt106 should examine whether its function, like that of Pob3, is sensitive to the precise level of bound H3. Mutations in Rtt106 that increase binding affinity may be deficient in silencing and nucleosome assembly, perhaps reflecting evolutionary conservation for an ATP-independent histone release mechanism shared by Pob3 and Rtt106.

In contrast to the conserved H3-binding residues in the N-terminal PH domains of Rtt106 and Pob3, the C-terminal loop, which was critical for Rtt106-H3 binding, was not important for Pob3 function (figure 2.10,11). This divergence suggests that the C-terminal loop may dictate the H3K56ac specificity of Rtt106. H3K56ac is absolutely required for the Rtt106-H3 interaction (figure 2.7a,b) whereas Pob3-H3 binding appears to be H3K56ac-independent (figure 2.12). Pob3-H3 binding was reduced in cells with both increased and decreased levels of H3K56ac (*rtt109Δ* and *hst3Δ hst4Δ*, respectively) (figure 2.12). Reduced Pob3-H3 binding might be due to changes in transcription and replication that result from altered levels of H3K56ac. Additionally, Pob3 may specifically recognize a different H3 modification that is reduced in both *rtt109Δ* and *hst3Δ hst4Δ* backgrounds.

Defining the H3K56ac-specificity of Rtt106-H3 binding

Direct identification of the K56ac binding site on Rtt106 will require a more extensive *in vitro* analysis. Monitoring the K_D of wild type and mutant Rtt106 for unmodified H3 and H3K56ac *in vitro* might be more sensitive than our *in vivo* analysis and therefore might identify the true K56ac binding pocket. Due to the extensive hydrophobic surfaces buried between the two PH domains, we do not expect to be able to express the recombinant PH domains individually. Indeed, others have reported that the individual domains aggregate in solution (*45*). Therefore, future binding experiments will be challenged by the inability to separate the contribution of each PH domain to histone binding. Additionally, we did not observe binding between recombinant Rtt106 and an H3K56ac 18-mer peptide (alreirrfqk*stellirk) (data not shown), indicating that Rtt106 recognizes H3K56ac only in the context of folded H3 or higher order histone

structures. Alternatively, monitoring H3K56ac binding to Rtt106 by NMR or solving an Rtt106-H3K56ac co-crystal structure would fully define the interaction surface.

There many possible models that could explain the distant location of the mutant clusters: 1) The second site on Rtt106 might recognize an additional H3 modification that is coincident with K56ac. 2) The second site on Rtt106 might recognize a region on H4. 3) Allosteric communication (cooperativity) between sites. 4) K56ac induces a conformational change in H3 that is specifically recognized by Rtt106, however, neither site directly interacts with K56ac. Our data, based on a comparative study with the non-K56ac-specific H3 binder Pob3, favor a parsimonious bipartite model of Rtt106 H3-binding, where H3 contacts the N-terminal PH domain and K56ac-specificity is encoded in the C-terminal loop. The nearly unrecognizable sequence divergence of many PH domains and the double PH domain architecture adopted by both Rtt106 and Pob3 suggest that additional proteins with PH domain-dependent histone binding activity have yet to be discovered. The wide variety of ligands recognized by PH domains further suggests that Rtt106 may be the first of many examples of histone modification-specific recognition by this domain architecture.

Here, we have identified the molecular origins of H3 binding by Rtt106 through the tandem PH domain architecture; in the next chapter we will determine the downstream consequences of reduced Rtt06-H3 binding on nucleosome assembly during replication, transcription, and silencing.

2.5 Tables

Table 2.1. Yeast strains used in chapter 2.

Strain	Parent	Genotype	Source
JRY3009	W303	*MATα ade2-1 his3-11 leu2-3,112 trp1-1 ura3-52 can1-100*	R. Rothstein
JRY2334	W303	*MATa ade2-1 his3-11 leu2-3,112 trp1-1 ura3-52 can1-100*	R. Rothstein
JRY8883	W303	*MATa HMR-a1Δ::K.l.URA3*	E. Osbourn (reporter generated by J. Kuei)
RZY150	W303	*MATα rtt106Δ::KanMX*	This study
RZY415	W303	*MATa HMR-a1Δ::K.l.URA3 [pRS313]*	This study
RZY417	W303	*MATa HMR-a1Δ::K.l.URA3 sir3Δ::KanMX [pRS313]*	This study
RZY421	W303	*MATa HMR-a1Δ::K.l.URA3 rtt106Δ::KanMX [pRS313]*	This study
RZY419	W303	*MATa HMR-a1Δ::K.l.URA3 cac1Δ::KanMX [pRS313]*	This study
RZY431	W303	*MATa HMR-a1Δ::K.l.URA3 rtt106Δ::KanMX cac1Δ::HygMX [pRS313]*	This study
RZY433	W303	*MATa HMR-a1Δ::K.l.URA3 rtt106Δ::KanMX cac1Δ::HygMX [pRZ050 HIS3 RTT106]*	This study
RZY435	W303	*MATa HMR-a1Δ::K.l.URA3 rtt106Δ::KanMX cac1Δ::HygMX [pRZ056 HIS3 rtt106(69-300)]*	This study
RZY437	W303	*MATa HMR-a1Δ::K.l.URA3 rtt106Δ::KanMX cac1Δ::HygMX [pRZ093 HIS3 RTT106-3xFLAG::KanMX]*	This study
RZY439	W303	*MATa HMR-a1Δ::K.l.URA3 rtt106Δ::KanMX cac1Δ::HygMX [pRZ094 HIS3 rtt106(69-300)-3xFLAG::KanMX]*	This study
RZY260	W303	*MATα [pRS313]*	This study
RZY220	W303	*MATα rtt106Δ::KanMX [pRS313]*	This study
RZY262	W303	*MATα cac1Δ::HygMX [pRS313]*	This study
RZY228	W303	*MATα rtt106Δ::KanMX cac1Δ::HygMX [pRS313]*	This study
RZY230	W303	*MATα rtt106Δ::KanMX cac1Δ::HygMX [pRZ050 HIS3 RTT106]*	This study
RZY232	W303	*MATα rtt106Δ::KanMX cac1Δ::HygMX [pRZ056 HIS3 rtt106(69 300)]*	This study
RZY234	W303	*MATα rtt106Δ::KanMX cac1Δ::HygMX [pRZ093 HIS3 RTT106-3xFLAG::KanMX]*	This study
RZY236	W303	*MATα rtt106Δ::KanMX cac1Δ::HygMX [pRZ094 HIS3 rtt106(69 300)-3xFLAG::KanMX]*	This study
RZY673	W303	*MATα rtt106Δ::KanMX [pRZ050 HIS3 RTT106]*	This study
RZY226	W303	*MATα rtt106Δ::KanMX [pRZ094 HIS3 rtt106(69-300)-3xFLAG::KanMX]*	This study
RZY675	W303	*MATα rtt106Δ::KanMX [pRZ093 HIS3 RTT106-3xFLAG::KanMX]*	This study
RZY1050	W303	*MATa HMR-a1Δ::K.l.URA3 rtt106Δ::KanMX sir3Δ::NatMX [pRZ093 HIS3 RTT106-3xFLAG::KanMX]*	This study
RZY427	W303	*MATa HMR-a1Δ::K.l.URA3 rtt106Δ::KanMX [pRZ093 HIS3 RTT106-3xFLAG::KanMX]*	This study
RZY250	W303	*MATα rtt106Δ::KanMX rtt109Δ::HygMX [pRZ093 HIS3 RTT106-3xFLAG::KanMX]*	This study
RZY242	W303	*MATα rtt106Δ::KanMX hst3Δ::HygMX hst4Δ::NatMX [pRZ093 HIS3 RTT106-3xFLAG::KanMX]*	This study
JRY7989	W303	*MATα hhf1-hht1Δ::HygMX; hhf2-hht2Δ::NatMX [pJR2657 URA3 HHT2-HHF2]*	O. Rando
RZY363	W303	*MATα hhf1-hht1Δ::HygMX; hhf2-hht2Δ::NatMX rtt106Δ::KanMX [pJR2657 URA3 HHT2-HHF2]*	This study

Table 2.1. Yeast strains used in chapter 2 (cont.).

RZY401	W303	*MATα hhf1-hht1Δ::HygMX; hhf2-hht2Δ::NatMX rtt106Δ::KanMX [pRZ050 HIS3 RTT106 pJR2851 TRP1 HHT2-HHF2]*	This study
RZY403	W303	*MATα hhf1-hht1Δ::HygMX; hhf2-hht2Δ::NatMX rtt106Δ::KanMX [pRZ093 HIS3 RTT106-3xFLAG::KanMX pJR2851 TRP1 HHT2-HHF2]*	This study
RZY409	W303	*MATα hhf1-hht1Δ::HygMX; hhf2-hht2Δ::NatMX rtt106Δ::KanMX [pRZ093 HIS3 RTT106-3xFLAG::KanMX pRZ102 TRP1 hht2K56R-HHF2]*	This study
RZY1158	W303	*MATα hhf1-hht1Δ::HygMX; hhf2-hht2Δ::NatMX rtt106Δ::KanMX [pRZ093 HIS3 RTT106-3xFLAG::KanMX pRZ104 TRP1 hht2K56Q-HHF2]*	This study
RZY679	W303	*MATα rtt106Δ::KanMX [pRZ112 HIS3 rtt106(S80E)-3xFLAG::KanMX]*	This study
RZY702	W303	*MATα rtt106Δ::KanMX [pRZ139 HIS3 rtt106(R86A)-3xFLAG::KanMX]*	This study
RZY700	W303	*MATα rtt106Δ::KanMX [pRZ137 HIS3 rtt106(T265E)-3xFLAG::KanMX]*	This study
RZY1166	W303	*MATα rtt106Δ::KanMX hir1Δ::HygMX [pRZ093 HIS3 RTT106-3xFLAG::KanMX]*	This study
RZY218	W303	*MATα rtt106Δ::KanMX hst3Δ::HygMX hst4Δ::NatMX*	This study
RZY710	W303	*MATα rtt106Δ::KanMX hst3Δ::HygMX hst4Δ::NatMX [pRZ112 HIS3 rtt106(S80E)-3xFLAG::KanMX]*	This study
RZY712	W303	*MATα rtt106Δ::KanMX hst3Δ::HygMX hst4Δ::NatMX [pRZ139 HIS3 rtt106(R86A)-3xFLAG::KanMX]*	This study
RZY716	W303	*MATα rtt106Δ::KanMX hst3Δ::HygMX hst4Δ::NatMX [pRZ137 HIS3 rtt106(T265E)-3xFLAG::KanMX]*	This study
RZY1160	W303	*MATα hhf1-hht1Δ::HygMX; hhf2-hht2Δ::NatMX rtt106Δ::KanMX [pRZ112 HIS3 rtt106(S80E)-3xFLAG::KanMX pRZ225 TRP1 hht2K56Q-HHF2]*	This study
RZY1162	W303	*MATα hhf1-hht1Δ::HygMX; hhf2-hht2Δ::NatMX rtt106Δ::KanMX [pRZ139 HIS3 rtt106(R86A)-3xFLAG::KanMX pRZ225 TRP1 hht2K56Q-HHF2]*	This study
RZY1164	W303	*MATα hhf1-hht1Δ::HygMX; hhf2-hht2Δ::NatMX rtt106Δ::KanMX [pRZ137 HIS3 rtt106(T265E)-3xFLAG::KanMX pRZ225 TRP1 hht2K56Q-HHF2]*	This study
RZY1443	S288c (A364a)	*MATα leu2 trp1 ura3 his3 lys2-128∂ pob3Δ::TRP1 [Ycp URA3 POB3]*	T. Formosa (8190 1 1)
RZY1369	W303	*MATa pob3Δ::KanMX [Ycp URA3 POB3]*	T. Formosa (8190 1 2c)
RZY1404	W303	*MATa lys2-128∂ POB3-13xMYC::KanMX*	T. Formosa (8855 1 3)

Table 2.2. Plasmids used in chapter 2.

Plasmid	Backbone	Yeast Selection	Bacterial Resistance	Insert	Source
pRZ050	pRS313	*HIS3*	*AMP*	*RTT106*	This study
pRZ056	pRS313	*HIS3*	*AMP*	*rtt106(69-300)*	This study
pRZ093	pRS313	*HIS3*	*AMP*	*Rtt106-3xFLAG::KanMX*	This study
pRZ094	pRS313	*HIS3*	*AMP*	*rtt106(69-300)-3xFLAG::KanMX*	This study
pRZ112	pRS313	*HIS3*	*AMP*	*rtt106(S80E)-3xFLAG::KanMX*	This study
pRZ139	pRS313	*HIS3*	*AMP*	*rtt106(R86A)-3xFLAG::KanMX*	This study
pRZ137	pRS313	*HIS3*	*AMP*	*rtt106(T265E)-3xFLAG::KanMX*	This study
pJR2851	pRS314	*TRP1*	*AMP*	*HHT2-HHF2*	C.D Allis
pRZ102	pRS314	*TRP1*	*AMP*	*hht2k56R-HHF2*	This study
pRZ225	pRS314	*TRP1*	*AMP*	*hht2K56Q-HHF2*	This study
pRZ047	pST39	n/a	*KAN*	*HHT1 HHF1*	A. Antczak
pRZ044	pET3a Tr	n/a	*AMP*	*His6-RTT106*	A. Antczak
pRZ216	pET3a Tr	n/a	*AMP*	*His6-rtt106 S80E*	This study
pRZ218	pET3a Tr	n/a	*AMP*	*His6-rtt106 R86A*	This study
pRZ220	pET3a Tr	n/a	*AMP*	*His6-rtt106 T265E*	This study
pRZ235	pRS313	*HIS3*	*AMP*	*POB3*	This study
pRZ236	pRS313	*HIS3*	*AMP*	*POB3-13xMyc::KanMX*	This study
pRZ237	pRS313	*HIS3*	*AMP*	*pob3(Q308K)-13xMyc::KanMX*	This study
pRZ238	pRS313	*HIS3*	*AMP*	*pob3(RR254,256AA)-13xMyc::KanMX*	This study
pRZ239	pRS313	*HIS3*	*AMP*	*pob3(F249E)-13xMyc::KanMX*	This study
pRZ240	pRS313	*HIS3*	*AMP*	*pob3(T251E)-13xMyc::KanMX*	This study
pRZ241	pRS313	*HIS3*	*AMP*	*pob3(T252E)-13xMyc::KanMX*	This study
pRZ257	pRS313	*HIS3*	*AMP*	*pob3(423-433G11)-13xMyc::KanMX*	This study
pRZ250	pRS313	*HIS3*	*AMP*	*pob3(TT428,430EE)-13xMyc::KanMX*	This study
pRZ256	pRS313	*HIS3*	*AMP*	*pob3(T252E Q308K)-13xMyc::KanMX*	This study

Table 2.3. Targeted *RTT106* mutations. 72 *RTT106* mutations were generated for our initial screen. Conservation was calculated based on the sequence entropy of each position, which was calculated based on the frequency of amino acids observed relative to a random distribution. 0 is 100% conserved and 4.2 is a mixture of all amino acids at the frequency observed in a random distribution. Percent solvent exposure was calculated using Mark Gerstein's calc-surface program, with a probe size of 1.4 Å.

Mutated			Conservation		Solvent Exposure (%)	
Residue 1	Residue 2	Substituted Residue(s)	Residue 1	Residue 2	Residue 1	Residue 2
N71	T72	AA	3.2	2.3	0.599	0.374
K75	E77	AA	2.7	3.2	0.493	0.563
S80		E	0.8		0.347	
L82		A	3.2		0.289	
R86	K88	AA	0.7	1.2	0.696	0.571
K87		A	0.7		0.502	
Y94	L95	AA	2.3	2.9	0.354	0.501
N97	D99	AA	-	-	0.581	0.568
S101		A	3.4		0.423	
L107	K108	AA	2.8	2.7	0.207	0.483
N110	D111	AA	3.4	2.8	0.546	0.455
R112	E113	AA	2.7	2.4	0.595	0.408
L114	S115	AA	3.1	2.7	0.183	0.224
Y117	Q118	AA	3.5	3.1	0.480	0.398
N120	K121	AA	3.4	2.7	0.328	0.505
N122	K124	AA	3.2	2.8	0.343	0.560
E133	P135	AA	2.2	2.9	0.556	0.461
K134		A	0.9		0.471	
N136	L137	AA	2.4	3.0	0.305	0.256
Y144	T145	AA	2.7	-	0.417	0.571
E148		A	-		0.478	
F152		A	-		0.494	
E154		A	-		0.345	
T159		E	1.6		0.119	
N161		A	2.3		0.206	
K162		A	3.2		0.264	
E163	N164	AA	2.7		0.417	0.321
N167		A	2.9		0.294	
K170		A	2.7		0.226	
K171	L172	AA	3.0	3.2	0.440	0.353
L174	L175	AA	2.8	2.4	0.252	0.177
D176	S177	AA	2.9	3.1	0.376	0.356
N178	T180	AA	2.8	3.0	0.426	0.376
D181		A	3.2		0.284	
E183	K184	AA	2.6	3.0	0.222	0.332
E187	Y188	AA	2.5	2.9	0.316	0.156
R190	K191	AA	2.9	2.6	0.301	0.360
I194	L195	AA	2.4	2.5	0.343	0.388
K199	S201	AA	2.9	2.1	0.425	0.192

Table 2.3. Targeted *RTT106* mutations (cont.).

F204		A	2.5		0.214	
N218		A	2.8		0.436	
H221	Q223	AA	1.8	2.5	0.219	0.262
H225		A	1.8		0.203	
R226	K229	AA	1.3	1.0	0.210	0.347
T228		A	1.7		0.330	
E230		A	1.3		0.269	
P237	D238	AA	2.5	2.8	0.237	0.283
H239		A	2.3		0.147	
K245		A	1.1		0.356	
K246		A	0.8		0.330	
L250	D252	AA	2.7	2.6	0.202	0.201
S254	D255	AA	2.7	3.1	0.231	0.215
E257		A	3.1		0.295	
T260	S262	EE	1.3	1.7	0.194	0.170
T260	S262	AA	1.3	1.7	0.194	0.170
I264		A	1.4		0.334	
T265	T268	AA	1.4	0.5	0.216	0.099
T265	T268	EE	1.4	0.5	0.216	0.099
R266	L267	AA	1.6	2.0	0.462	0.312
N270		A	1.2		0.060	
K276	D277	AA	3.1	3.1	0.331	0.282
E279	K280	AA	2.5	2.3	0.219	0.324
Y281		A	2.6		0.176	
E282		A	0.7		0.198	
S284		E	1.7		0.061	
S284	M285	AA	1.7	1.0	0.061	0.239
D287		A	0.5		0.186	
Q288		A	0.9		0.181	
T289	Y291	AA	2.4	1.7	0.274	0.241
K293		A	2.4		0.200	
D296		A	2.2		0.255	
K299		A	2.0		0.406	

Table 2.4. Additional targeted *RTT106* mutants. Follow-up *RTT106* mutants were generated based on results from the initial screen.

Mutated		
Residue 1	Residue 2	Substituted Residue(s)
S80		D,T,A
R86		A, K
K88		A
T265		A, S, D, E
T268		A, S, D, E
T265	T268	EA, AE

Table 2.5. Targeted *POB3* mutants.

Mutated		
Residue 1	Residue 2	Substituted Residue(s)
Q308		K
F249		E
T251		E
T252		E
R254	R256	AA
T428	T430	EE
423-433		$(G)_{11}$
T252	Q308	EK

2.6 Figures

Figure 2.1. Rtt106-mediated nucleosome assembly
The histone chaperone Rtt106 delivers H3K56ac to chromatin via several branches of the nucleosome assembly pathway (see text for details). Rtt106 is thought to receive H3K56ac histones from Asf1 and then deposit them into chromatin by interacting with additional chaperone complexes. Rtt106 binds the CAF-1 complex during replication-coupled nucleosome assembly, the HIR complex during replication-independent nucleosome assembly, and Sir4 during silent chromatin formation.

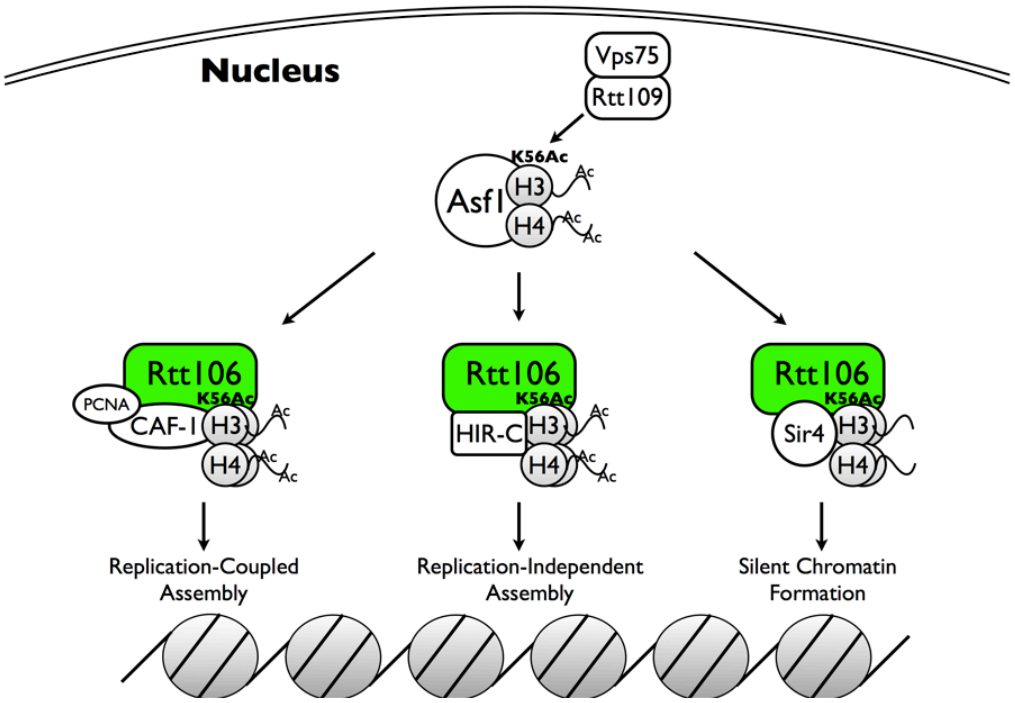

Figure 2.2. Rtt106 structure revealed an unexpected double pleckstrin homology fold.

(A) The secondary structure of Rtt106 is a double pleckstrin homology (PH) fold. An unusual capping alpha helix (magenta) is inserted into the N-terminal PH domain. (B) The structure is shown in cartoon representation. There is an extensive interface between the two PH domains. However, the linker between the N- and C-terminal domains was disordered in our structure. (C) A fungal multiple sequence alignment revealed that only one face of Rtt106 is highly conserved.

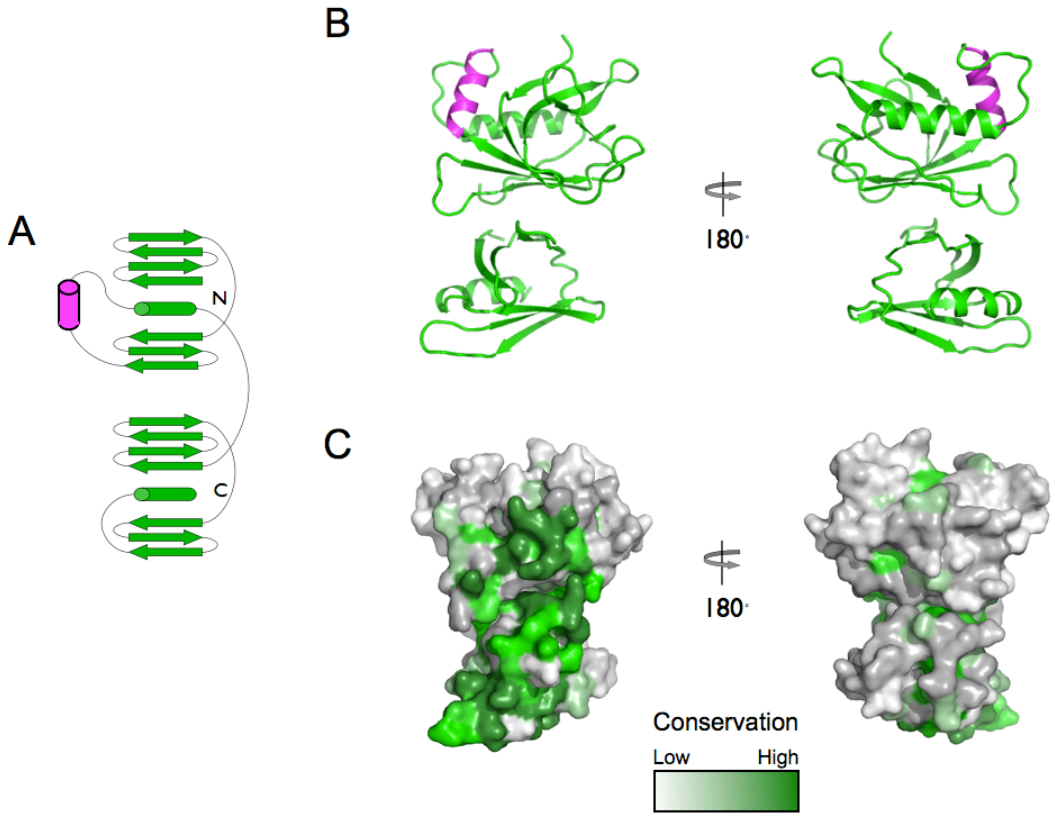

Figure 2.3. Full length *RTT106* was necessary for *in vivo* functions.
(A-C) *RTT106-FLAG* fully complemented the null allele whereas the 69-300 truncation (*2PH-FLAG*) was non-functional. (A) Silencing of the *HMR-a1Δ::URA3* reporter gene, (B) growth on medium containing DNA-damaging agent camptothecin (3.5 ug/mL), and (C) H3 co-purification experiments were performed with full length Rtt106 and the 69-300 (2PH) truncation. (A) To monitor silencing of an *HMR-a1Δ::URA3* reporter gene, five-fold serial dilutions of each mutant were frogged onto medium either containing FOA or lacking uracil. CSM-HIS media maintained selection for *RTT106* plasmids. (B) Growth on medium containing camptothecin (3.5 μg/mL) screened for S-phase DNA damage. CSM-HIS media maintained selection for *RTT106* plasmids. (C) Rtt106-FLAG was immunoprecipitated from yeast whole cell extract with anti-FLAG resin. Co-purifying proteins were detected by immunoblotting with antibodies against the indicated proteins.

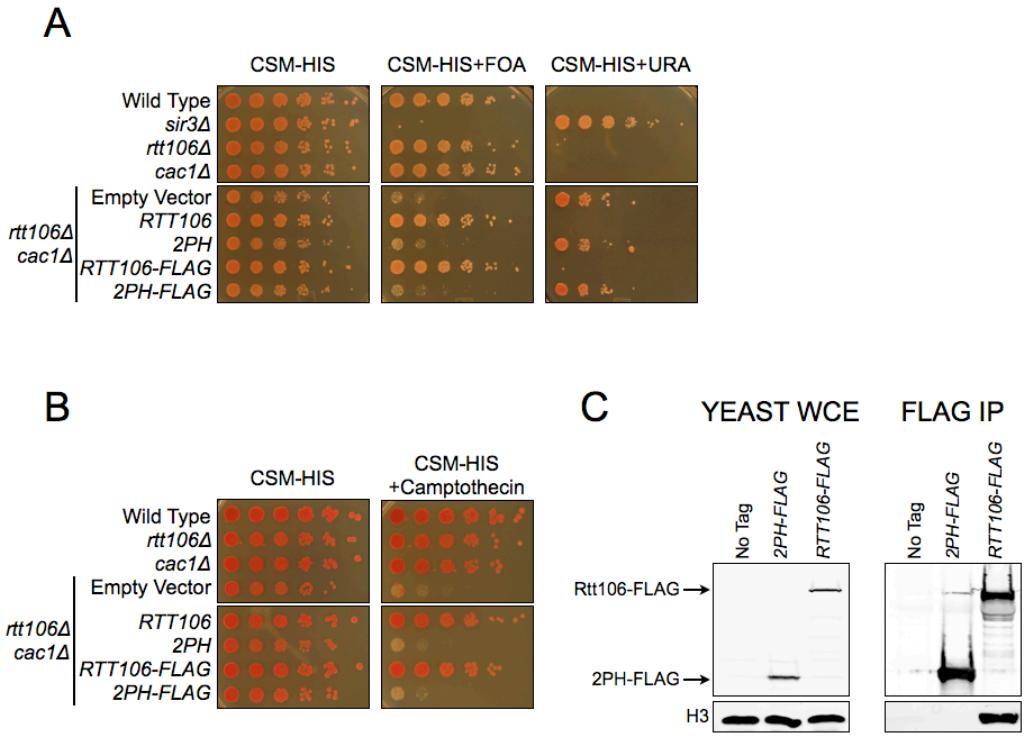

Figure 2.4. Targeted mutational analysis of Rtt106.
Conserved and un-conserved surface exposed residues on Rtt106 were mutated and assayed for function. The X-ray crystal structure of Rtt106 is shown in cartoon representation. Sequence conservation was mapped onto structure as in Figure 2.2. Mutated residues are displayed as spheres.

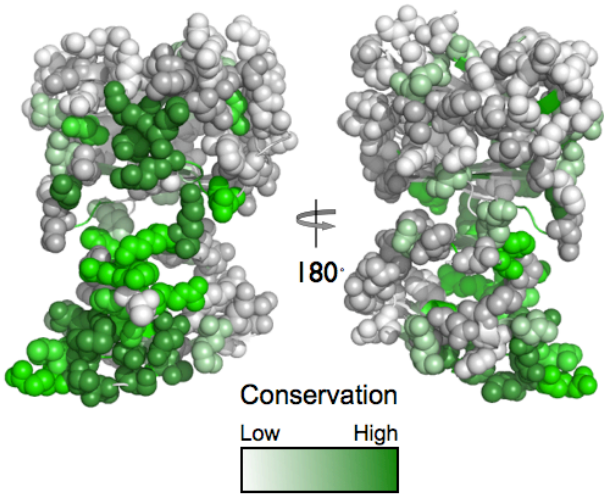

Figure 2.5. Two regions on Rtt106 were necessary for silencing and replication-coupled nucleosome assembly.
(A) Targeted *RTT106* mutants were screened for silencing and nucleosome assembly defects by growth on selective media. Shown are the mutants that yielded phenotypes distinct from wild type. Five-fold serial dilutions were performed as in figure 2.3. (B) Mutations that altered Rtt106-mediated silencing and nucleosome assembly formed two distinct clusters on the N- and C-terminal PH domain surfaces. Shown is a surface representation of the X-ray crystal structure of Rtt106. Residues that, when mutated, impaired Rtt106 function, are highlighted in red (severe), orange (medium), and yellow (mild). Red: S80E, R86A, T265E. Orange: RL266,267AA, SM284,285AA. Yellow: K88A, T268E.

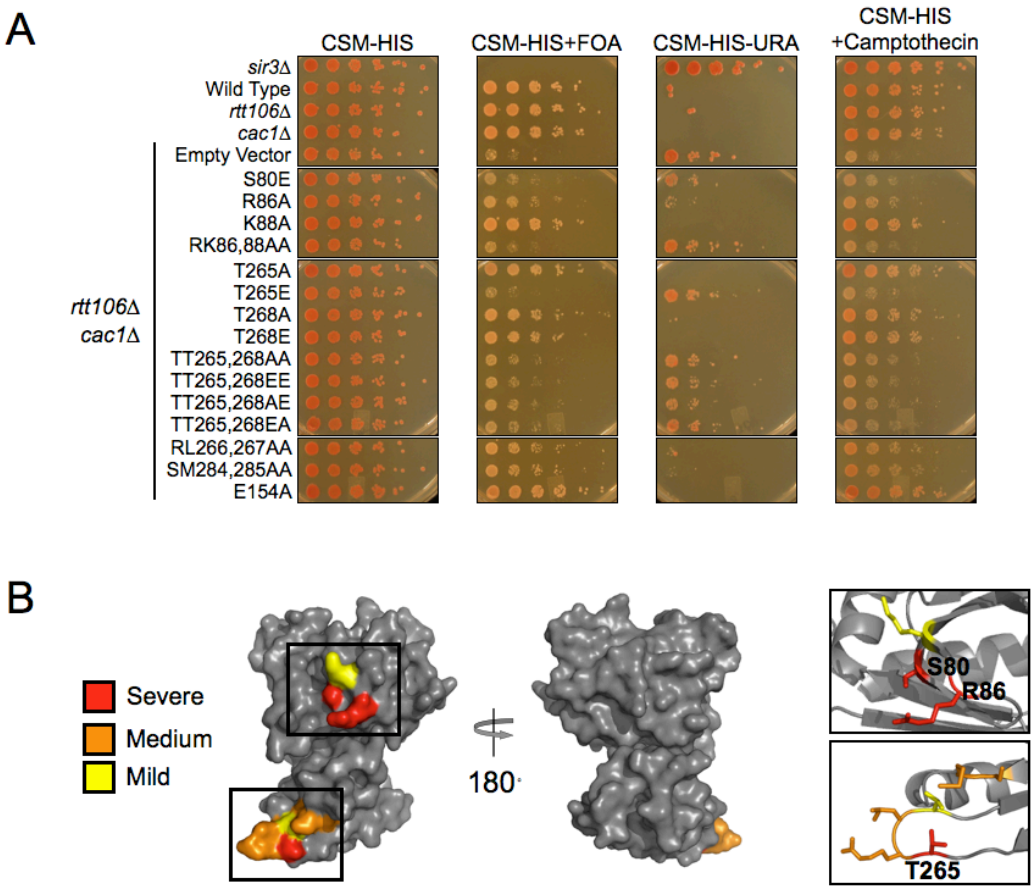

Figure 2.6. S80, R86, and T265 mutational analysis
(A) S80, R86, and T265 residues were mutated to conserved and non-conserved amino acids and assayed for Rtt106 function as in Figure 2.3. (B) S80E and TT265,268EE mutants did not affect the phosphorylation profile of Rtt106. Wild type and mutant Rtt106-FLAG were immunoprecipitated from yeast whole cell extract and separated on a phos-tag gel. Proteins were visualized by immunoblotting with an anti-FLAG antibody.

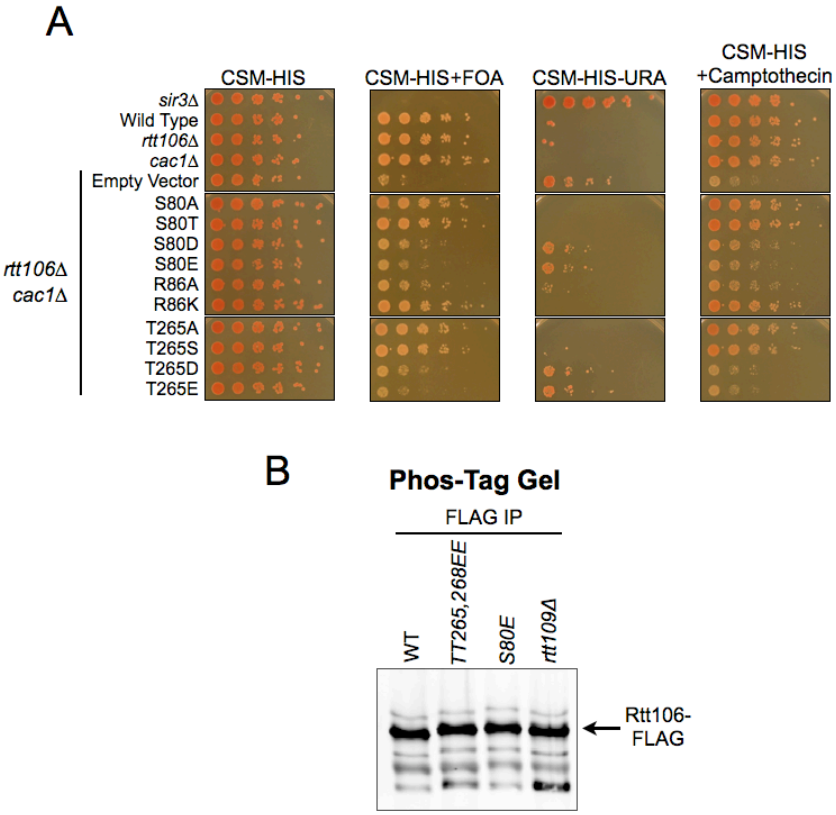

Figure 2.7. S80, R86, and T265 defined the Rtt106-H3 interaction surface.
(A-B) H3K56ac was required for Rtt106-H3 binding *in vivo*. Rtt106-FLAG was immunoprecipitated from yeast whole cell extract in backgrounds with (A) increased or abolished levels of H3K56ac or (B) H3K56 mutated to an unacetylatable (R) or acetyl-mimic (Q) residue. Co-purifying proteins were visualized by immunoblotting with antibodies against the indicated proteins. (C-D) Rtt106 S80E, R86A and T265E mutants disrupted Rtt106-H3 binding *in vivo* (C) and *in vitro* (D). (C) Rtt106 mutants were purified as described in (A). (D) *His6-RTT106* and yeast H3 and H4 were co-expressed in *E.coli*. Binding was monitored by Ni purification and immunoblotting with antibodies against the indicated proteins. (E) Neither CAF-1 nor HIR chaperone complexes were required for Rtt106-H3 binding. Rtt106 was purified as described in (A) in the indicated chaperone mutant backgrounds.

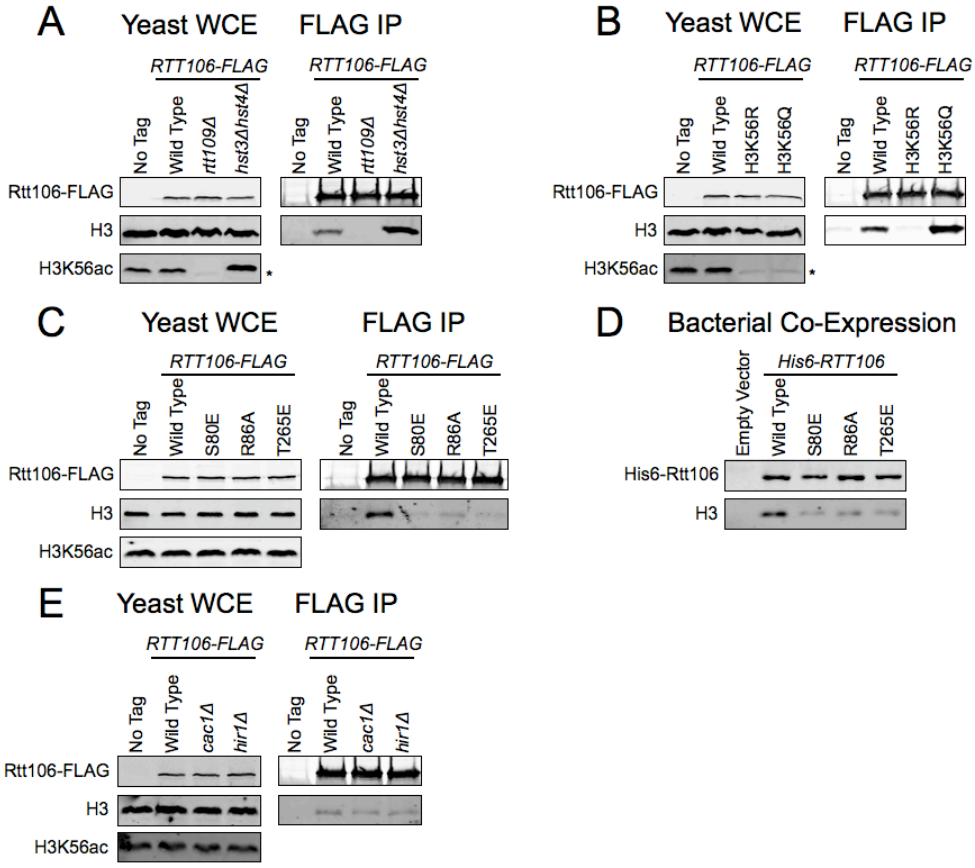

Figure 2.8. Increased cellular H3K56ac did not rescue mutant Rtt106-H3 binding. (A-B) Increased H3K56ac levels did not restore binding in Rtt106 S80E, R86A, or T265E mutants. Rtt106-FLAG was immunoprecipitated from yeast whole cell extract in wild type, (A) *hst3*Δ *hst4*Δ and (B) *H3K56Q* backgrounds as described in Figure 2.3.

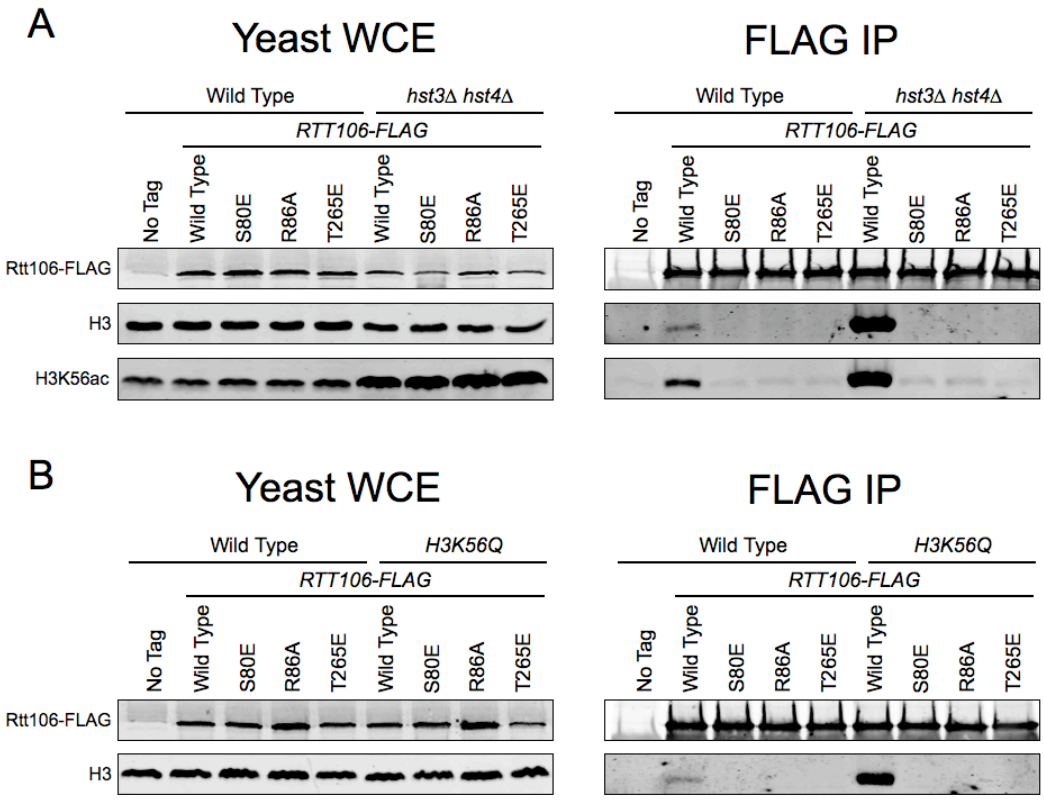

Figure 2.9. Comparative analysis with Pob3
(A) The double PH domain of Rtt106 was similar to Pob3 (PDB 2GCJ). Structures are shown independently and superimposed. (B) Top: Pob3 R254 and R256 (shown in blue sticks) were in structurally conserved positions compared to Rtt106 R86 (shown in green sticks). Bottom: Loop residues for Rtt106 and Pob3. Rtt106 T265 and T268 are highlighted in red. (C) Electrostatics revealed a basic patch on the Pob3 N-terminal PH domain. Rtt106 and Pob3 are shown in the same structural orientation. Electrostatic potential is mapped onto the surface (D) The Cα atoms of residues targeted on Pob3 to mimic Rtt106 S80E are shown in spheres (Pob3 F249, T251, T252). The Cα atom of Pob3 Q308K, a previously described mutation, is shown in spheres.

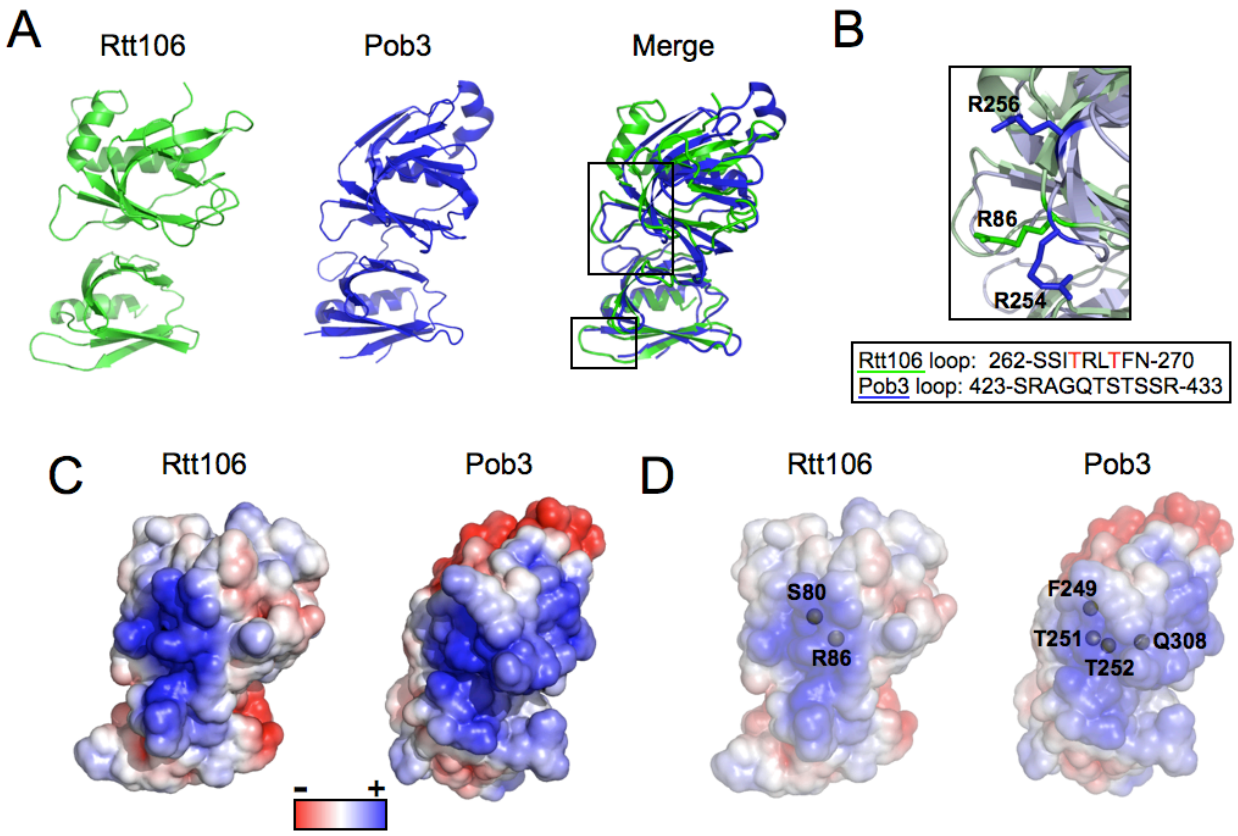

Figure 2.10. A mutation within the basic patch disrupted Pob3 function.
(A) Expression of the Spt- reporter, *lys2-128∂*, was monitored by frogging five-fold serial dilutions onto –LYS media. (B) DNA damage phenotypes were monitored by frogging five-fold serial dilutions onto medium containing hydroxyurea (150 mM). Spt- phenotypes were monitored in an S288c background. Hydroxyurea sensitivity was monitored in a W303 background. Strain backgrounds are described further in materials and methods. CSM-HIS media maintained selection for *POB3* plasmids.

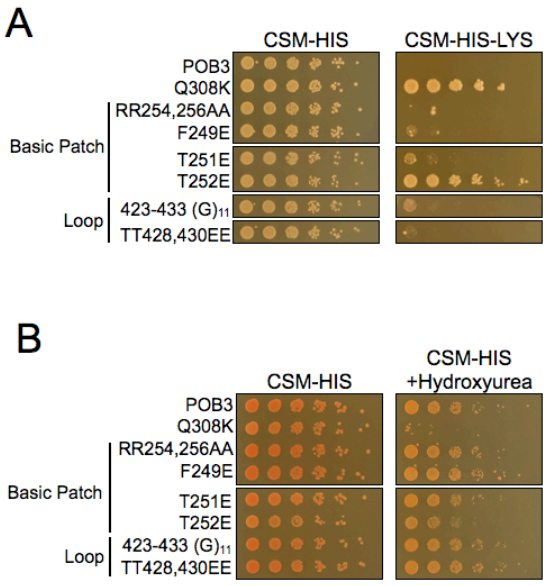

Figure 2.11. Mutations within the basic patch disrupted Pob3-H3 binding.
(A-B) Pob3-MYC was immunoprecipitated as described in figure 2.3 with anti-Myc affinity resin. Purifications contained either (A) 50 mM or (B) 150 mM NaCl as indicated. Immunoblotting with antibodies against the indicated proteins monitored H3 co-purification.

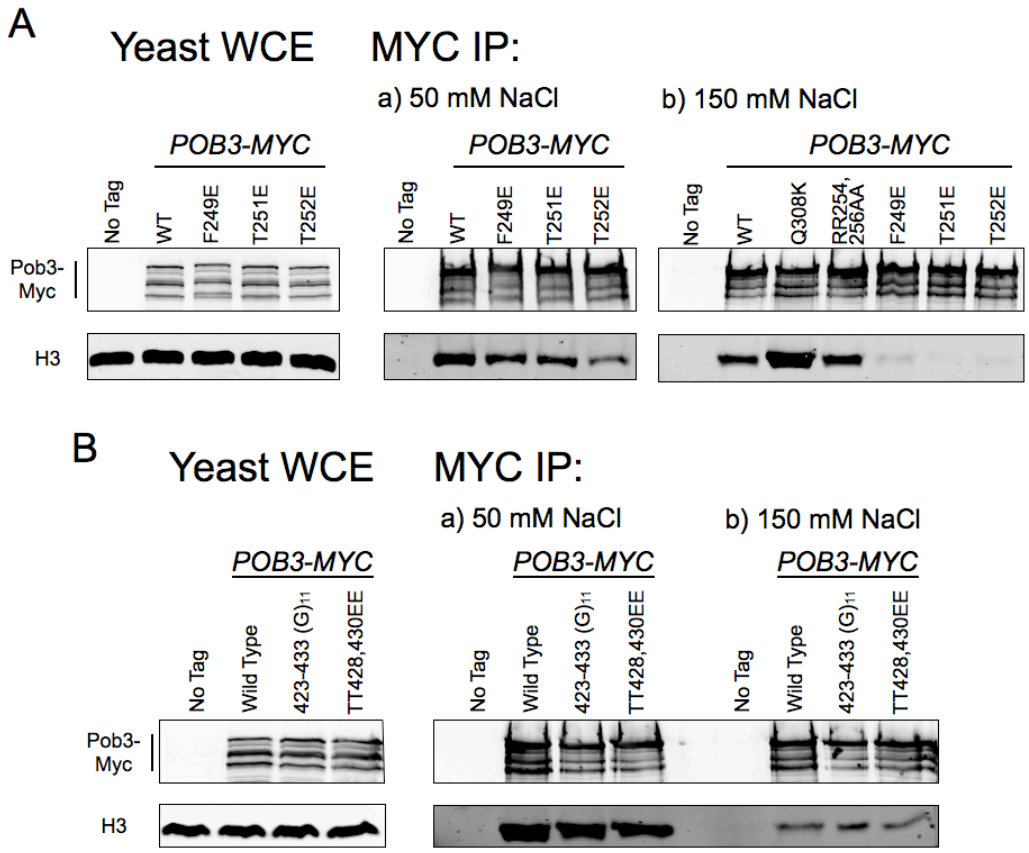

Figure 2.12. Pob3-H3 binding did not correlate with H3K56ac.
Pob3-MYC was immunopurified as described in figure 2.11 from backgrounds containing abolished (*rtt109*Δ) or increased (*hst3*Δ *hst4*Δ) H3K56ac.

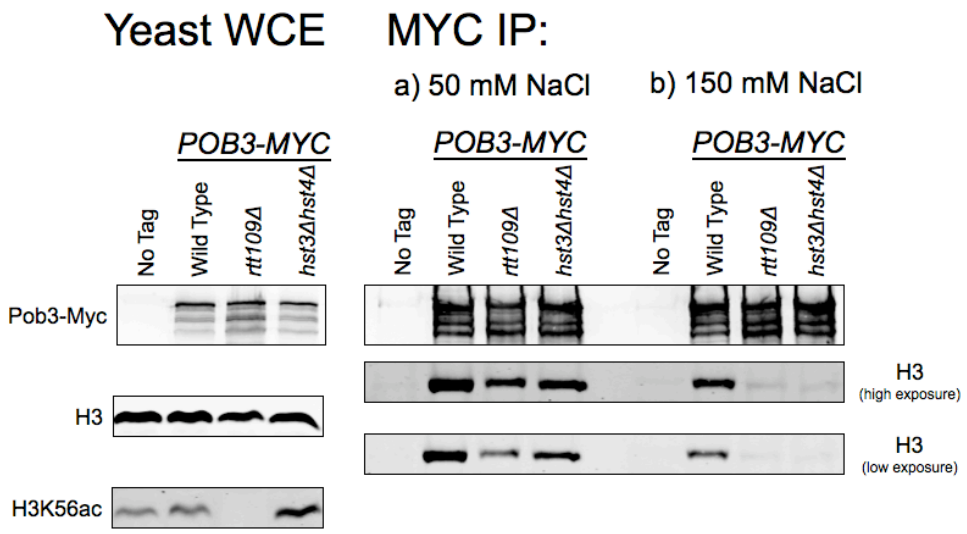

Figure 2.13. Pob3 T252E Q308K double mutant suppressed single mutant phenotypes.
(A) Pob3 T252E Q308K double mutants had suppressed Spt- phenotypes (left) and hydroxyurea sensitivity (right). Frogging was performed as described in figure 2.11. (B) Pob3 T252E Q308K double mutants suppress the single mutant H3 binding defects. Pob3-H3 binding was performed at described in figure 2.11. (C) T252E suppression of Q308K phenotypes may occur though Y313. The Pob3 structure highlights T252E (red) Y313 (cyan) and Q308K (red).

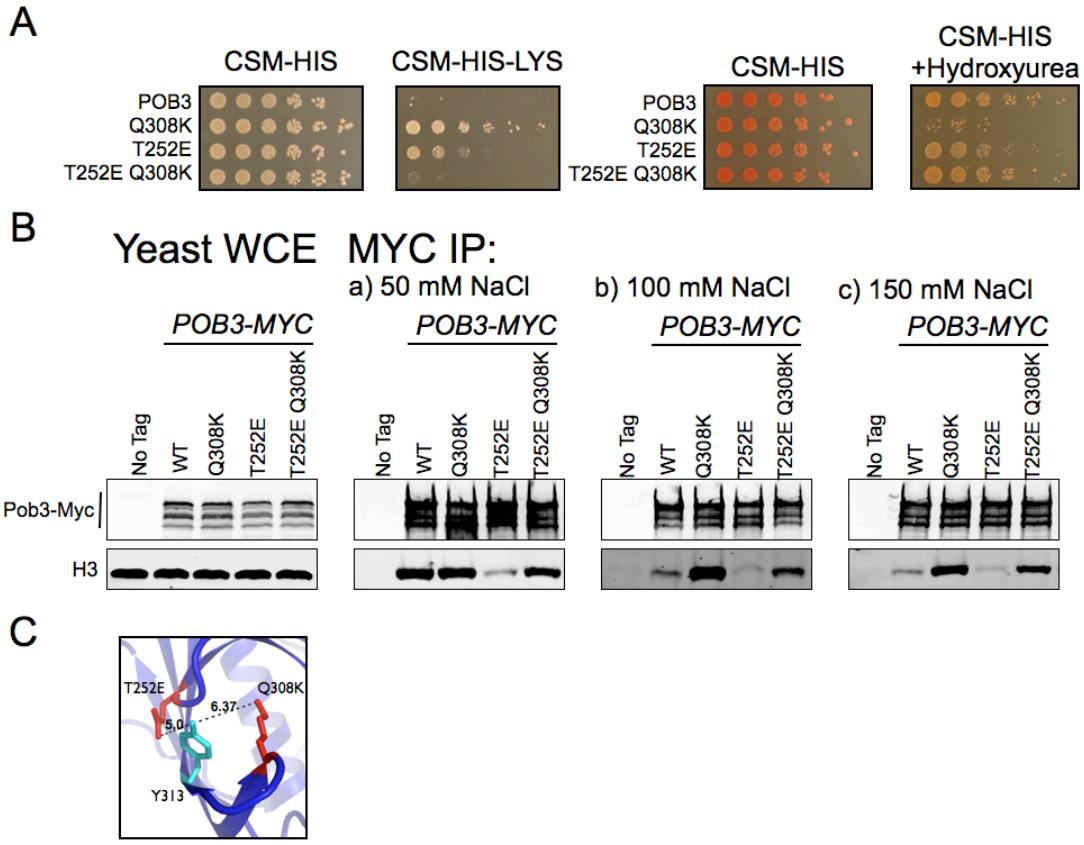

2.7 References

1. Das, C., Tyler, J. K., and Churchill, M. E. (2010) The histone shuffle: histone chaperones in an energetic dance, *Trends in biochemical sciences 35*, 476-489.
2. De Koning, L., Corpet, A., Haber, J. E., and Almouzni, G. (2007) Histone chaperones: an escort network regulating histone traffic, *Nature structural & molecular biology 14*, 997-1007.
3. Avvakumov, N., Nourani, A., and Cote, J. (2011) Histone chaperones: modulators of chromatin marks, *Molecular cell 41*, 502-514.
4. Ransom, M., Dennehey, B. K., and Tyler, J. K. (2010) Chaperoning histones during DNA replication and repair, *Cell 140*, 183-195.
5. Scholes, D. T., Banerjee, M., Bowen, B., and Curcio, M. J. (2001) Multiple regulators of Ty1 transposition in Saccharomyces cerevisiae have conserved roles in genome maintenance, *Genetics 159*, 1449-1465.
6. Li, Q., Zhou, H., Wurtele, H., Davies, B., Horazdovsky, B., Verreault, A., and Zhang, Z. (2008) Acetylation of histone H3 lysine 56 regulates replication-coupled nucleosome assembly, *Cell 134*, 244-255.
7. Fillingham, J., Kainth, P., Lambert, J. P., van Bakel, H., Tsui, K., Pena-Castillo, L., Nislow, C., Figeys, D., Hughes, T. R., Greenblatt, J., and Andrews, B. J. (2009) Two-color cell array screen reveals interdependent roles for histone chaperones and a chromatin boundary regulator in histone gene repression, *Molecular cell 35*, 340-351.
8. Huang, S., Zhou, H., Katzmann, D., Hochstrasser, M., Atanasova, E., and Zhang, Z. (2005) Rtt106p is a histone chaperone involved in heterochromatin-mediated silencing, *Proceedings of the National Academy of Sciences of the United States of America 102*, 13410-13415.
9. Imbeault, D., Gamar, L., Rufiange, A., Paquet, E., and Nourani, A. (2008) The Rtt106 histone chaperone is functionally linked to transcription elongation and is involved in the regulation of spurious transcription from cryptic promoters in yeast, *The Journal of biological chemistry 283*, 27350-27354.
10. Neumann, H., Hancock, S. M., Buning, R., Routh, A., Chapman, L., Somers, J., Owen-Hughes, T., van Noort, J., Rhodes, D., and Chin, J. W. (2009) A method for genetically installing site-specific acetylation in recombinant histones defines the effects of H3 K56 acetylation, *Molecular cell 36*, 153-163.
11. Celic, I., Masumoto, H., Griffith, W. P., Meluh, P., Cotter, R. J., Boeke, J. D., and Verreault, A. (2006) The sirtuins hst3 and Hst4p preserve genome integrity by controlling histone h3 lysine 56 deacetylation, *Curr Biol 16*, 1280-1289.
12. Driscoll, R., Hudson, A., and Jackson, S. P. (2007) Yeast Rtt109 promotes genome stability by acetylating histone H3 on lysine 56, *Science (New York, N.Y 315*, 649-652.
13. Han, J., Zhou, H., Li, Z., Xu, R. M., and Zhang, Z. (2007) Acetylation of lysine 56 of histone H3 catalyzed by RTT109 and regulated by ASF1 is required for replisome integrity, *The Journal of biological chemistry 282*, 28587-28596.
14. Linger, J., and Tyler, J. K. (2005) The yeast histone chaperone chromatin assembly factor 1 protects against double-strand DNA-damaging agents, *Genetics 171*, 1513-1522.

15. Huang, S., Zhou, H., Tarara, J., and Zhang, Z. (2007) A novel role for histone chaperones CAF-1 and Rtt106p in heterochromatin silencing, *The EMBO journal 26*, 2274-2283.
16. Antczak, A. J., Tsubota, T., Kaufman, P. D., and Berger, J. M. (2006) Structure of the yeast histone H3-ASF1 interaction: implications for chaperone mechanism, species-specific interactions, and epigenetics, *BMC structural biology 6*, 26.
17. English, C. M., Adkins, M. W., Carson, J. J., Churchill, M. E., and Tyler, J. K. (2006) Structural basis for the histone chaperone activity of Asf1, *Cell 127*, 495-508.
18. Tang, Y., Holbert, M. A., Delgoshaie, N., Wurtele, H., Guillemette, B., Meeth, K., Yuan, H., Drogaris, P., Lee, E. H., Durette, C., Thibault, P., Verreault, A., Cole, P. A., and Marmorstein, R. (2011) Structure of the Rtt109-AcCoA/Vps75 complex and implications for chaperone-mediated histone acetylation, *Structure 19*, 221-231.
19. Tyers, M., Rachubinski, R. A., Stewart, M. I., Varrichio, A. M., Shorr, R. G., Haslam, R. J., and Harley, C. B. (1988) Molecular cloning and expression of the major protein kinase C substrate of platelets, *Nature 333*, 470-473.
20. Yoon, H. S., Hajduk, P. J., Petros, A. M., Olejniczak, E. T., Meadows, R. P., and Fesik, S. W. (1994) Solution structure of a pleckstrin-homology domain, *Nature 369*, 672-675.
21. Harlan, J. E., Hajduk, P. J., Yoon, H. S., and Fesik, S. W. (1994) Pleckstrin homology domains bind to phosphatidylinositol-4,5-bisphosphate, *Nature 371*, 168-170.
22. Yu, J. W., Mendrola, J. M., Audhya, A., Singh, S., Keleti, D., DeWald, D. B., Murray, D., Emr, S. D., and Lemmon, M. A. (2004) Genome-wide analysis of membrane targeting by S. cerevisiae pleckstrin homology domains, *Molecular cell 13*, 677-688.
23. Jacobs, D. M., Lipton, A. S., Isern, N. G., Daughdrill, G. W., Lowry, D. F., Gomes, X., and Wold, M. S. (1999) Human replication protein A: global fold of the N-terminal RPA-70 domain reveals a basic cleft and flexible C-terminal linker, *Journal of biomolecular NMR 14*, 321-331.
24. Lemmon, M. A. (2004) Pleckstrin homology domains: not just for phosphoinositides, *Biochemical Society transactions 32*, 707-711.
25. Xu, Q., Bateman, A., Finn, R. D., Abdubek, P., Astakhova, T., Axelrod, H. L., Bakolitsa, C., Carlton, D., Chen, C., Chiu, H. J., Chiu, M., Clayton, T., Das, D., Deller, M. C., Duan, L., Ellrott, K., Ernst, D., Farr, C. L., Feuerhelm, J., Grant, J. C., Grzechnik, A., Han, G. W., Jaroszewski, L., Jin, K. K., Klock, H. E., Knuth, M. W., Kozbial, P., Krishna, S. S., Kumar, A., Marciano, D., McMullan, D., Miller, M. D., Morse, A. T., Nigoghossian, E., Nopakun, A., Okach, L., Puckett, C., Reyes, R., Rife, C. L., Sefcovic, N., Tien, H. J., Trame, C. B., van den Bedem, H., Weekes, D., Wooten, T., Hodgson, K. O., Wooley, J., Elsliger, M. A., Deacon, A. M., Godzik, A., Lesley, S. A., and Wilson, I. A. (2010) Bacterial pleckstrin homology domains: a prokaryotic origin for the PH domain, *Journal of molecular biology 396*, 31-46.
26. Marchler-Bauer, A., Anderson, J. B., Cherukuri, P. F., DeWeese-Scott, C., Geer, L. Y., Gwadz, M., He, S., Hurwitz, D. I., Jackson, J. D., Ke, Z., Lanczycki, C. J.,

Liebert, C. A., Liu, C., Lu, F., Marchler, G. H., Mullokandov, M., Shoemaker, B. A., Simonyan, V., Song, J. S., Thiessen, P. A., Yamashita, R. A., Yin, J. J., Zhang, D., and Bryant, S. H. (2005) CDD: a Conserved Domain Database for protein classification, *Nucleic acids research 33*, D192-196.

27. Jacobson, R. H., Ladurner, A. G., King, D. S., and Tjian, R. (2000) Structure and function of a human TAFII250 double bromodomain module, *Science (New York, N.Y 288*, 1422-1425.
28. Zeng, L., Zhang, Q., Li, S., Plotnikov, A. N., Walsh, M. J., and Zhou, M. M. (2010) Mechanism and regulation of acetylated histone binding by the tandem PHD finger of DPF3b, *Nature 466*, 258-262.
29. Matangkasombut, O., Buratowski, R. M., Swilling, N. W., and Buratowski, S. (2000) Bromodomain factor 1 corresponds to a missing piece of yeast TFIID, *Genes & development 14*, 951-962.
30. VanDemark, A. P., Blanksma, M., Ferris, E., Heroux, A., Hill, C. P., and Formosa, T. (2006) The structure of the yFACT Pob3-M domain, its interaction with the DNA replication factor RPA, and a potential role in nucleosome deposition, *Mol Cell 22*, 363-374.
31. Formosa, T. (2008) FACT and the reorganized nucleosome, *Molecular bioSystems 4*, 1085-1093.
32. Orphanides, G., LeRoy, G., Chang, C. H., Luse, D. S., and Reinberg, D. (1998) FACT, a factor that facilitates transcript elongation through nucleosomes, *Cell 92*, 105-116.
33. Rhoades, A. R., Ruone, S., and Formosa, T. (2004) Structural features of nucleosomes reorganized by yeast FACT and its HMG box component, Nhp6, *Molecular and cellular biology 24*, 3907-3917.
34. Goldstein, A. L., and McCusker, J. H. (1999) Three new dominant drug resistance cassettes for gene disruption in Saccharomyces cerevisiae, *Yeast (Chichester, England) 15*, 1541-1553.
35. Longtine, M. S., McKenzie, A., 3rd, Demarini, D. J., Shah, N. G., Wach, A., Brachat, A., Philippsen, P., and Pringle, J. R. (1998) Additional modules for versatile and economical PCR-based gene deletion and modification in Saccharomyces cerevisiae, *Yeast (Chichester, England) 14*, 953-961.
36. Zill, O. A., Scannell, D., Teytelman, L., and Rine, J. (2010) Co-evolution of transcriptional silencing proteins and the DNA elements specifying their assembly, *PLoS biology 8*, e1000550.
37. Gietz, R. D., and Woods, R. A. (2002) Transformation of yeast by lithium acetate/single-stranded carrier DNA/polyethylene glycol method, *Methods in enzymology 350*, 87-96.
38. Makarova, O., Kamberov, E., and Margolis, B. (2000) Generation of deletion and point mutations with one primer in a single cloning step, *BioTechniques 29*, 970-972.
39. Gelbart, M. E., Rechsteiner, T., Richmond, T. J., and Tsukiyama, T. (2001) Interactions of Isw2 chromatin remodeling complex with nucleosomal arrays: analyses using recombinant yeast histones and immobilized templates, *Molecular and cellular biology 21*, 2098-2106.

40. Aslanidis, C., and de Jong, P. J. (1990) Ligation-independent cloning of PCR products (LIC-PCR), *Nucleic acids research 18*, 6069-6074.
41. Tan, S. (2001) A modular polycistronic expression system for overexpressing protein complexes in Escherichia coli, *Protein expression and purification 21*, 224-234.
42. Babiarz, J. E., Halley, J. E., and Rine, J. (2006) Telomeric heterochromatin boundaries require NuA4-dependent acetylation of histone variant H2A.Z in Saccharomyces cerevisiae, *Genes & development 20*, 700-710.
43. Woodruff, J. B., Drubin, D. G., and Barnes, G. (2010) Mitotic spindle disassembly occurs via distinct subprocesses driven by the anaphase-promoting complex, Aurora B kinase, and kinesin-8, *The Journal of cell biology 191*, 795-808.
44. Mehrotra, P. V., Ahel, D., Ryan, D. P., Weston, R., Wiechens, N., Kraehenbuehl, R., Owen-Hughes, T., and Ahel, I. (2011) DNA repair factor APLF is a histone chaperone, *Molecular cell 41*, 46-55.
45. Liu, Y., Huang, H., Zhou, B. O., Wang, S. S., Hu, Y., Li, X., Liu, J., Zang, J., Niu, L., Wu, J., Zhou, J. Q., Teng, M., and Shi, Y. (2010) Structural analysis of Rtt106p reveals a DNA binding role required for heterochromatin silencing, *The Journal of biological chemistry 285*, 4251-4262.
46. Liu, Y., Huang, H., Zhou, B. O., Wang, S. S., Hu, Y., Li, X., Liu, J., Zang, J., Niu, L., Wu, J., Zhou, J. Q., Teng, M., and Shi, Y. Structural analysis of Rtt106p reveals a DNA binding role required for heterochromatin silencing, *The Journal of biological chemistry 285*, 4251-4262.
47. Luger, K., Mader, A. W., Richmond, R. K., Sargent, D. F., and Richmond, T. J. (1997) Crystal structure of the nucleosome core particle at 2.8 A resolution, *Nature 389*, 251-260.

Chapter 3

Rtt106 mediates H3K56ac-dependent nucleosome assembly during replication, transcription, and silencing

3.1 Introduction

Rtt106 chaperones H3K56ac during nucleosome turnover

Packaging DNA into chromatin is a dynamic, reversible process essential for eukaryotic cell viability. The principle packaging unit of chromatin is the nucleosome, consisting of two H2A/H2B dimers and one H3/H4 tetramer wrapped in 146-bp of DNA (*1*). During chromatin formation, a network of histone chaperones guide histones into the nucleus and promote nucleosome assembly during replication, transcription, and repair (*2-5*). Although extensive work has identified which chaperones coordinate each DNA-dependent process, many details of how and when specific chaperones function in the chromatin assembly pathway remain unresolved.

During nucleosome assembly, newly synthesized histone H3/H4 dimers are bound by the chaperone Asf1, acetylated at H3K56 (H3K56ac) by the Rtt109-Vps75 complex, and incorporated into chromatin along with two H2A/H2B dimers by one of several other histone chaperone complexes (*4*). Here we focus on the newest H3/H4 histone chaperone to enter the scene, Rtt106, which is thought to receive H3K56ac histones from Asf1, and facilitate both replication-dependent and replication-independent nucleosome assembly (*6-10*). To determine how the interactions of Rtt106 with H3K56ac and other binding partners are regulated, we performed a targeted mutational screen to define the Rtt106-H3K56ac interaction surface (described in chapter 2). In the work described in this chapter, we utilized mutants that specifically disrupt Rtt106-H3 binding to examine the importance of Rtt106-mediated H3K56ac delivery during replication, transcription, and silencing.

Rtt106 regulates nucleosome assembly during replication

During replication, histone chaperones promote both the disassembly of nucleosomes ahead of the DNA polymerase and the incorporation of histones onto replicated DNA (*5*). Throughout S-phase, all newly synthesized H3 proteins are acetylated at K56 (*11*). As replication begins, H3K56ac is enriched at origins of replication and then as replication proceeds spreads throughout the genome (*12, 13*). As the cell passes through G_2, H3K56ac is globally deacetylated by the NAD-dependent histone deacetylases (HDACs) Hst3 and Hst4 (*14*). Cells lacking H3K56ac have reduced PCNA at origins of replication and are sensitive to S-phase-specific DNA damaging agents (*15, 16*). These phenotypes suggest that H3K56ac is critical for DNA replication.

During replication-coupled nucleosome assembly, the histone chaperones Rtt106 and the CAF-1 complex (Cac1, Cac2, Msi1) are thought to deliver H3K56ac to sites of DNA synthesis (*6*). Rtt106 and CAF-1 interact physically, and both chaperones bind H3 in a K56ac-dependent manner (*6, 9*). The synergistic reduction in H3K56ac enrichment at origins and the increased sensitivity to S-phase-specific genotoxic agents in *cac1*Δ *rtt106*Δ cells suggests that Rtt106 and CAF-1 perform overlapping functions during replication (*6, 9*). At present, it has been difficult to disentangle the contribution of

Rtt106 to replication-dependent delivery of H3K56ac from other phenotypes associated with cells lacking Rtt106, including defects in silencing and mis-regulation of histone gene transcription.

Rtt106 mediates silent chromatin formation

In *S. cerevisiae*, the mating-type loci (*HMR* and *HML*) and the telomeres form a heterochromatin-like structure, referred to as silent chromatin, that represses transcription of genes within or near these regions (*17*). The major structural and enzymatic components of silent chromatin are the Sir proteins (silent information regulator), which form a repressive complex throughout silent regions (*18*). The inheritance of silent chromatin is likely mediated by replication-coupled nucleosome assembly. Double-mutant analyses revealed that the histone chaperones Rtt106, Asf1, and the HIR complex (Hir1, Hir2, Hir3, Hpc2) function in the same silencing pathway, whereas CAF-1 mediates a genetically distinct, partially redundant, silencing pathway (*9, 10, 19*). Although histone chaperones are required for silencing, the mechanism of histone chaperone activity within silent chromatin is unknown.

Rtt106 interacts physically with Sir4, and is required for the initial recruitment of Sir2 and Sir3, but not Sir4, to silent loci (*10*). Subsequent spreading of the Sir2/3/4 complex is reduced in *rtt106*Δ *cac1*Δ mutants, suggesting the chaperoning H3K56ac is necessary for silent chromatin formation (*9, 10*). However, the role of H3K56ac in silencing is paradoxical. Cells that lack H3K56ac (*rtt109*Δ) have fully functional silent chromatin, suggesting that the modification is not critical for silencing (*20, 21*). However, cells with elevated levels of H3K56ac (*hst3*Δ *hst3*Δ) have telomeric silencing defects that are suppressible by an *rtt109*Δ mutation, suggesting that excess H3K56ac is antagonistic to silencing (*21*). Intriguingly, these silencing defects occur post-Sir spreading. In contrast to telomeres, *HMR* and *HML* remain silenced in an *hst3*Δ *hst4*Δ background indicating that the role of H3K56ac in silencing is locus-dependent (*21*). Although this modification is important for silencing, the molecular mechanisms of histone chaperones and H35K6ac deposition at silent loci are poorly defined.

Rtt106 represses histone gene transcription

Cell cycle regulated transcription is a hallmark of eukaryotic organisms. This precise control is exemplified by transcription of the canonical histone genes. To ensure that large amounts of new histones are available during DNA replication, histone transcription is coordinated with S-phase (*22*). To prevent transcription outside of S-phase, several histone chaperones form a repressive complex at histone gene promoters. In *S. cerevisiae*, three of the four histone gene pairs, *HTA1-HTB1*, *HHT1-HHF1*, and *HHT2-HHF2,* contain similar regulatory sequences and are regulated by the same set of proteins, whereas transcription of the fourth pair, *HTA2-HTB2*, is regulated by a distinct, unknown mechanism (*23, 24*). Repression of *HTA1-HTB1*, *HHT1-HHF1*, and *HHT2-HHF2* outside of S-phase is mediated by the histone chaperones Rtt106, Asf1, and the HIR complex (*8, 23, 25, 26*).

HIR proteins localize to the negative regulatory element (NEG) sequences located in histone gene promoters (*23, 27*). Rtt106 recruitment is both HIR- and Asf1-dependent, and together Rtt106 and HIR are thought to form a repressive complex over the promoter that coordinates transcription with the cell cycle (*8*). Because *asf1*Δ cells lack H3K56ac (*8*), it is possible that Rtt106-H3 binding, rather than Asf1 directly, regulates Rtt106 recruitment to histone gene promoters. In the absence of Rtt106, Asf1 or HIR, the histone genes are transcribed outside of S-phase leading to an increase in the total level of histone mRNA (*8, 23, 25*).

In addition to replication-coupled deposition at origins during S-phase, H3K56ac is also enriched at the promoters of highly expressed genes, including the histone genes, and is necessary for transcription-dependent rapid nucleosome turnover (*12, 13*). Although H3K56 is hyperacetylated at histone gene promoters and has been implicated in regulating expression (*28*), it is unclear whether Rtt106 mediates histone gene repression through its role in H3K56ac-driven nucleosome assembly, or by an H3K56ac-independent mechanism. The specificity of chaperones for histone modifications may provide an additional layer of transcriptional control at the histone gene loci.

Summary of findings

Here we analyzed whether the histone-binding activity of Rtt106 was required for Rtt106 localization and H3K56ac incorporation during replication, transcription, and silencing. Our results suggest that Rtt106 localizes properly to origins of replication and silent chromatin even in cells with mutant forms of Rtt106 defective in H3 binding. However, such mutant forms of Rtt106 cannot deliver H3K56ac. Reductions in H3K56ac incorporation were detrimental to replication, whereas within silent chromatin excess unincorporated H3K56ac was antagonistic to silencing. In contrast to origins and silent chromatin, binding to H3K56ac was required for recruitment of Rtt106 to histone gene promoters, subsequent H3K56ac incorporation, and histone gene repression. This work demonstrates that the Rtt106-mediated escort of H3K56ac into chromatin is necessary during all known branches of the Rtt106-mediated nucleosome assembly pathway, but the localization cues are pathway dependent.

3.2 Materials and Methods

Yeast strains, plasmids, culture, and genetic manipulations:

Yeast:

All yeast strains were generated in *S. cerevisiae* W303 and its derivatives (table 3.1). Gene deletions were generated by one-step integration of knock-out cassettes (*29, 30*). PCR analysis of the 5' and 3' end of each targeted gene verified complete knock-outs. The *HMR-a1Δ::K.l.URA3* reporter strain used to screen *RTT106* mutants for silencing defects was previously described (*31*). *RTT106* plasmids were introduced into each mutant strain using the standard plasmid transformation protocol (*32*). *HHT2-HHF2* plasmids harboring mutations of interest were introduced into strains containing

wild type versions of the relevant gene (RZY363) by plasmid swap using FOA counter selection. Plasmids are described in table 3.2.

Plasmids:

RTT106 was cloned into pRS313 using gap repair and C-terminally FLAG tagged to generate pRZ050 and pRZ093, respectively, as described in chapter 2. *RTT106* point mutants (pRZ112, 139, 137) were generated on pRZ093 using site-directed mutagenesis (*33*) and Pfu Ultra polymerase (Stratagene). Histone point mutants (pRZ102, 225) were generated using site-directed mutagenesis of pJR2851.

Culture:

To screen *RTT106* mutants for silencing or chemical sensitivity phenotypes, five-fold serial dilutions of saturated overnight cultures were frogged onto selective media as previously described (*31, 34, 35*). All selective media lacked histidine (-HIS) to maintain selection of *RTT106* plasmids.

Protein analysis

Yeast whole-cell extracts were precipitated using 20% trichloroacetic acid (TCA) and solubilized in SDS loading buffer. SDS-PAGE and immunoblotting were performed using standard procedures and evaluated with a Li-COR Odyssey imaging system. Anti-H3 (Ab1791) or anti-H3K56ac (07-677; Millipore) were used to monitor bulk or modified H3. Anti-Pgk1 (Invitrogen) was used as a loading control.

RNA preparation and analysis

RNA analysis was performed as described (*36*). Total RNA was prepared using an RNeasy mini kit (Qiagen). Genomic DNA was digested on the column using RNase-free DNase (Qiagen). Oligo(dT) primer-directed cDNA was synthesized using the SuperScript III first-strand synthesis system for reverse transcriptase PCR kit (Invitrogen). qPCR was performed on an Mx3000P machine (Stratagene) using a DyNAmo HS SYBR Green qPCR kit (New England Biolabs). Amplification values for all primer sets were normalized to actin (*ACT1*) cDNA amplification values. Samples were analyzed in triplicate for at least three independent RNA preparations unless otherwise indicated. Oligonucleotide sequences are listed in table 3.3.

Rtt106-FLAG chromatin immunoprecipitation

Chromatin immunoprecipitation (ChIP) analyses were performed as previously described (*36*) with minor modifications. 50 OD_{600} units of log-phase cells were cross-linked with 1% formaldehyde for 30 minutes at room temperature. Chromatin was sheared by sonication to an average size of 500 bp. Rtt106-FLAG was immunoprecipitated using anti-FLAG M2 agarose (Sigma). Precipitated DNA fragments were analyzed by qPCR using an Mx3000P qPCR system (Stratagene) and a DyNAmo HS qPCR kit (New England Biolabs). Amplification values for all primer sets were normalized to percent input or a previously described reference primer set, which amplifies an un-transcribed region on chromosome V in the S. *cerevisiae* genome (*8*).

Samples were analyzed in triplicate for at least three independent chromatin preps. Oligonucleotide sequences are listed in table 3.4.

H3K56ac chromatin immunoprecipitation

ChIP analyses were performed as previously described (*37*) with minor modifications. 50 OD_{600} units of log-phase cells were cross-linked with 1% formaldehyde for 20 minutes at room temperature. Chromatin was sheared by sonication to an average size of 500 bp. 1.2 μg of H3 antibody (Ab1791) or 1 μl H3K56acetyl antibody (07-677; Millipore) was coupled to a 30 μl slurry of Protein A Sepharose (17-5280-01; GE healthcare). The sonicated sample was split in half and each half was incubated with either H3- or H3K56ac-coupled beads. Precipitated DNA fragments were analyzed by qPCR as described above. Amplification values for all primer sets were normalized to a previously described reference primer set that amplifies *SSC1* (*21*). Samples were analyzed in triplicate for at least three independent chromatin preps. Statistical comparisons were performed using a 2-tailed unpaired t-test. Oligonucleotide sequences are listed in table 3.4.

3.3 Results

Rtt106 delivered H3K56ac to origins during replication-coupled nucleosome assembly

During S phase, H3K56ac is thought to be incorporated at origins of replication by the histone chaperones Rtt106 and CAF-1 (*12*). An *rtt109*Δ strain that cannot acetylate H3K56 was sensitive to the S-phase-specific genotoxic agent camptothecin (CPT), suggesting that the modification plays an important role during replication (figure 3.1a). In a *cac1*Δ-sensitized background, the *rtt106(S80E*, *R86A*, and *T265E*) mutants, which have reduced H3-binding activity, were also CPT-sensitive, suggesting that Rtt106-H3 binding is necessary for DNA replication (figure 3.1a). To analyze the nature of the replication defect, we used chromatin immunoprecipitation (ChIP) to monitor Rtt106 localization and H3K56ac incorporation at origins of replication in each mutant background.

We observed no difference in localization between wild type and mutant Rtt106 protein at early and late origins of replication in asynchronously dividing cells (figure 3.1b). However, in the *RTT106* mutant backgrounds, H3K56ac-enrichment was significantly reduced compared to wild type (figure 3.1c). Reduced H3K56ac-enrichment at a sequence downstream of origins (*ARS305* +1kb) suggests that Rtt106 and CAF-1 are required for H3K56ac incorporation during replication initiation and as the replication complex travels throughout the genome. In *cac1*Δ *rtt106*Δ mutants, the total cellular level of H3K56ac was similar to that of wild type (figure 3.1d), suggesting that the CPT-sensitivity was due to the inability of each Rtt106 mutant to deliver free H3K56ac to origins during S-phase.

Rtt106 chaperoned H3K56ac within silent chromatin

RTT106 mutants with compromised H3-binding, in combination with the *cac1Δ* mutation, were initially characterized as silencing defective by monitoring growth of a *URA3* reporter strain *(HMR-a1Δ::URA3)* on media lacking uracil (figure 3.2a, also described in chapter 2). In agreement with the growth assay, qRT-PCR of *URA3* mRNA verified that *cac1Δ rtt106*(*S80E*, *R86A* and *T265E*) mutants were 71, 54 and 67% derepressed, respectively, compared to the *cac1Δ rtt106Δ* strain (figure 3.2b). At *HMR*, Rtt106 mutant proteins were recruited to the locus (figure 3.3a), however, like at origins of replication, the inability of each mutant to bind H3, in combination with the *cac1Δ* mutation, resulted in H3K56 hypoacetylation throughout the region (figure 3.3b).

Intriguingly, unlike defects in replication-coupled nucleosome assembly, *rtt109Δ* strains do not have silencing defects, indicating that the H3K56ac modification is not required for silencing (figure 3.3c) (*21*). We hypothesized that the silencing defects in *cac1Δ rtt106Δ* mutants were likely due to mis-regulation of H3K56ac in addition to the observed reduction in chromatin incorporation. This model predicts that the absence of this modification may alleviate the *cac1Δ rtt106Δ* silencing defect. Indeed, the *HMR* silencing defects observed in *cac1Δ rtt106*(*Δ*, *S80E*, *R86A*, and *T265E*) mutants were all partially suppressed by an *rtt109Δ* null mutation (figure 3.3c). Suppression of the silencing defect was also observed at endogenous *HMRa1* indicating that the phenotype was not due to the *URA3* reporter (figure 3.4a). These results suggest that although H3K56ac is not required for silencing, if H3K56ac is present, it must be properly chaperoned within *HMR* to maintain the silent state.

Surprisingly, an H3K56R mutation, which mimics the unacetylated state, did not suppress the *cac1Δ rtt106Δ* silencing defect at *HMR* (figure 3.4b). However, the lack of suppression was likely due to a novel *RTT106*-associated phenotype in the histone point-mutant backgrounds rather than the *rtt109Δ* suppression occurring through an H3K56ac-independent mechanism (histone point-mutant strains described in materials and methods, novel phenotype described in figure 3.9 and associated text).

Unlike the mild silencing defects observed at *HMR*, silenced genes were fully derepressed at the telomeres in *RTT106* mutants. For example, in *cac1Δ rtt106Δ* strains, *HMRa1* was 3.7% derepressed compared to a *sir3Δ* strain (figure 3.2b), whereas the endogenous sub-telomeric gene *YFR057W* was 110% derepressed compared to a *sir3Δ* strain (figure 3.5a). Each Rtt106 mutant protein properly localized to *YFR057W* (figure 3.5b); however, unlike at *HMR* where H3K56ac-occupancy was reduced compared to wild type (figure 3.3b), at *YFR057W* H3K56ac was increased in the *RTT106* mutant backgrounds (figure 3.5c). Since the *RTT106* mutants were more silencing defective at the telomeres than at *HMR*, the H3K56ac enrichment may have resulted from increased *YFR057W* transcription, and the transcription-coupled delivery of H3K56ac by Asf1, HIR, or FACT (*7*). Active transcription is correlated with an increase in H3K56ac incorporation at the promoter (*12*). A challenge in interpreting H3K56ac incorporation at some derepressed loci is to de-convolute the *cac1Δ rtt106Δ* silencing defect from the transcription-dependent increase that results from the silencing

defect. Thus, a transcription-dependent increase in incorporation may mask the possible defects in H3K56ac incorporation in the *cac1Δ rtt106Δ* mutants. Consistently, *Sir⁻* strains, with fully derepressed *HMR* and *YFR057W*, showed strong enrichment of H3K56ac at both loci (figure 3.5.d). Unlike at *HMR*, the telomeric silencing defects of *cac1Δ rtt106Δ* strains were not suppressed by an *rtt109Δ* null mutation (figure 3.5.e). This may be due to the increased expression of *YFR057W* compared to *HMRa1*, or the role of H3K56ac in silencing may be locus-dependent.

Rtt106-H3 binding was required for histone gene repression

In addition to replication-coupled nucleosome turnover, H3K56ac is also incorporated during transcription-coupled turnover at active promoters and other sites of rapid nucleosome exchange (*8, 12*). H3K56ac enrichment and rapid nucleosome turnover is thought to be important at the core histone genes, where Rtt106 is recruited to the promoters by the HIR complex and represses histone gene expression outside of S-phase (*8*). Unlike other regions of the genome, where mutant Rtt106 localization profiles were similar to wild type (figures 3.1b, 3.3a, and 3.5b), Rtt106 (S80E, R86A and T265E) mutants showed reduced occupancy at core histone gene promoters *HTA1-HTB1*, *HHT1-HHF1*, and *HHT2-HHF2* (figure 3.6a and figure 3.7a,b). Rtt106 enrichment was strongest at the *HTA1-HTB1* promoter; therefore all further analysis focused on this histone gene pair. The reduction of mutant Rtt106 at all Rtt106-occupied histone gene promoters, suggests that Rtt106 is recruited by a similar mechanism at all histone genes.

This reduced occupancy suggests that Rtt106 must bind H3 for proper recruitment to histone gene promoters and may provide a feedback mechanism to regulate histone gene expression as a function of cellular histone protein levels. Consistent with this hypothesis, Rtt106 occupancy at histone gene promoters was similarly reduced in *rtt109*Δ and H3K56R backgrounds (figure 3.6a,b), which also disrupted Rtt106-H3 binding (figure 2.7a,b). Surprisingly, *hst3*Δ *hst4*Δ and H3K56Q backgrounds, which increased Rtt106-H3 binding (figure 2.7a,b), also reduced Rtt106 occupancy at histone gene promoters (figure 3.6a,b). Therefore, a specific level of Rtt106-H3 binding, which is modulated by the amount of acetylation at H3K56, is required for Rtt106 to localize and regulate histone gene expression. Alternatively, mislocalized Rtt106 may be due to the transcriptional changes associated with the *rtt109*Δ and *hst3*Δ *hst4*Δ backgrounds rather than changes in Rtt106-H3 binding.

To determine whether Rtt106 regulates histone gene expression by delivering H3K56ac to the promoter, we monitored H3K56ac enrichment at the *HTA1-HTB1* promoter in backgrounds with reduced Rtt106 occupancy (figure 3.8a). A previously published ChIP analysis revealed that *rtt106*Δ and *rtt109*Δ backgrounds have reduced and increased enrichment of H3 at the *HTA1-HTB1* promoter, respectively (figure 3.8b) (*8*). To distinguish between loss of H3K56ac and loss of H3, we normalized all H3K56ac ChIP analyses to total H3 (figure 3.8c). H3K56ac incorporation was reduced in all backgrounds with mislocalized Rtt106 ($p<0.05$), suggesting that Rtt106 delivers H3K56ac to histone gene promoters. In the absence of Rtt106, H3 is likely incorporated

by other transcription-coupled histone chaperones such as Asf1, HIR, and FACT. Reduced H3K56ac at the *HTA1-HTB1* promoter was particularly striking in the *hst3*Δ *hst4*Δ background (figure 3.8a,c), which had elevated total cellular levels of H3K56ac (figure 3.1c). This reduction further supports our hypothesis that without Rtt106, H3K56ac is not delivered to the histone gene promoters.

Previous work has shown increased histone gene transcription in *rtt106*Δ strains (*8*). *rtt106*(*S80E*, *R86A* and *T265E*) mutants showed increased *HTA1* transcription similar to the null allele (figure 3.8d). This suggests that Rtt106 represses histone transcription outside of S-phase by delivering H3K56ac to the promoters of histone genes. Surprisingly, *rtt109*Δ and *hst3*Δ *hst4*Δ backgrounds, which did not target Rtt106 to histone gene promoters (figure 3.6a), did not have increased histone mRNA (figure 3.8d). These results suggest that *rtt109*Δ and *hst3*Δ *hst4*Δ mutants are epistatic to *rtt106*Δ mutants with respect to histone gene transcription and do not require proper Rtt106 localization to repress histone transcription outside of S-phase. This result was unanticipated and will be explored further in the discussion.

An Rtt106-dependent distinction between the H3-H4 histone gene copies

It is possible that the silencing and chemical sensitivity phenotypes observed in the *cac1Δ rtt106Δ* background were partially due to inappropriate histone gene expression throughout the cell cycle, a phenotype that is also present in *cac1Δ rtt106Δ* strains. If this were true, a reduction in histone gene dosage, and presumably histone expression, might suppress the silencing defects and chemical sensitivities found in *cac1Δ rtt106Δ* strains. To test this hypothesis, we monitored silencing at *HMR* and CPT-sensitivity in *cac1Δ rtt106Δ* backgrounds with one of the two H3-H4 histone gene copies knocked-out (*hht1-hhf1Δ* or *hht2-hhf2Δ*). This reduction in histone gene dosage did not suppress the *cac1Δ rtt106Δ* phenotypes (figure 3.9a,b), suggesting that Rtt106-mediated delivery of H3K56ac to ARSs and *HMR* was necessary for proper replication and silencing, respectively, independently of Rtt106's role in histone gene repression.

Surprisingly, rather than suppression, a synergistic increase in CPT-sensitivity and silencing defects was observed in *hht1-hhf1Δ rtt106Δ* but not *hht2-hhf2Δ rtt106Δ* strains. This differential phenotype was unexpected; the two loci encode identical H3 and H4 proteins that are thought to be completely functionally redundant (*38*) and Rtt106 localizes equally to both promoters (figure 3.7a,b). RNA analysis of total H3 and H4 revealed that *hht1-hhf1Δ* strains had an increased H3:H4 ratio compared to wild type whereas *hht2-hhf2Δ* strains had a decreased H3:H4 ratio (figure 3.9c). These data suggest that more H3 and/or less H4 may be detrimental in the absence of Rtt106. These findings unveil a previously unappreciated distinction between the two copies of H3 and H4. The unique function of each core histone gene copy is a theme I return to in chapter 4 where we examine the two copies of H2B.

3.4 Discussion

Chaperone-histone binding interactions are essential for nucleosome turnover during all DNA-dependent processes. Although histone chaperones act at distinct locations throughout the genome, it remains unclear whether the localization signals are encoded in the chaperone itself or in its histone cargo. Here, we observed that the histone chaperone Rtt106 was localized by both mechanisms in a context-dependent manner. During replication and silencing, if Rtt106's affinity for histones was comprised, Rtt106 was properly localized, but it could not deliver H3K56ac. In contrast, during histone gene repression feedback, Rtt106 required H3 binding for recruitment to histone gene promoters. These results highlight how plasticity in recruitment signals can expand the potential functions of a single histone chaperone.

Rtt106 mutants localized but did not deliver H3K56ac during DNA replication

Rtt106 plays a key role delivering newly synthesized H3K56ac molecules into chromatin during DNA replication. Once incorporated into chromatin, the acetylation of H3 on K56 disrupts histone-DNA contacts, which creates a looser nucleosome structure (*39*). These loosely assembled nucleosomes are thought to reduce the energetic costs of ATP-dependent remodeling, which slides nucleosomes along newly replicated DNA. In the absence of H3K56ac, nucleosomes may be less accessible to remodelers leading to stalled replication and subsequent damage. Our results show that Rtt106 localized to origins independently of its H3-binding activity, possibly through a direct interaction with PCNA (figure 3.1b) (*8*). Although Rtt106 localized to ARS sequences, mutations that reduced binding to H3 led to decreased H3K56 deposition and sensitivity to S-phase-specific DNA damaging agents (figure 3.1a,c). Strains lacking H3K56ac (*rtt109Δ*) had similar genotoxic-sensitivities (figure 3.1a), suggesting that reduced H3K56ac incorporation caused the replication defects of *RTT106* mutants.

Silencing defects resulted from unchaperoned H3K56ac

Similar to replication-coupled nucleosome assembly, H3 binding was not required for Rtt106 localization within silent chromatin (figure 3.3a and 3.5b). Because Sir4 recruitment to silencers and telomere ends is not affected in *cac1Δ rtt106Δ* strains, Rtt106 is likely targeted to silent chromatin by its direct physical interaction with Sir4 (*10*). Our results suggest that silencing requires either Rtt106- or CAF-1-mediated recruitment of H3K56ac into silent chromatin, which promotes Sir spreading and gene repression. However, the importance of chaperoning H3K56ac into silent chromatin was locus-dependent.

Surprisingly, *cac1Δ rtt106Δ* strains had severe silencing defects at telomeres, but only mild silencing defects at *HMR* (figure 3.3 and figure 3.5). A similar pattern of increased silencing defects at telomeres compared to *HMR* was shown in *hst3Δ hst4Δ* strains, which have increased levels of H3K56ac (*21*). Both *cac1Δ rtt106Δ* and *hst3Δ hst4Δ* strains likely increase the level of H3K56ac in the free-histone pool, which may underlie the telomere-specific silencing defects. Consistent with this hypothesis, an

rtt109Δ mutation suppressed *cac1Δ rtt106Δ* and *hst3Δ hst4Δ* silencing defects, which will be discussed more below (figure 3.3c) (*21*). Additionally, Sir1 nucleates silencing at the *HM* loci, but not at the telomeres (*17*). Perhaps Sir1 may act as a histone chaperone in the absence of Rtt106 and CAF-1, or in the presence of excess H3K56ac. Indeed, *sir1Δ cac1Δ rtt106Δ* strains show a synergistic increase in expression of an *HMR::GFP* reporter compared to *sir1Δ* and *cac1Δ rtt106Δ* mutants alone (*10*). This model predicts that a *sir1Δ* mutation might lead to *HMR* silencing defects in an *hst3Δ hst4Δ* background.

Our results suggest that in the absence of Rtt106 and CAF-1, there is an initial defect in the recruitment of H3K56ac that reduces Sir spreading, which leads to increased transcription. When analyzing *cac1Δ rtt106Δ*-associated silencing phenotypes in large populations of cells, it is challenging to de-couple the initial reduction in chromatin-bound H3K56ac from the transcription-coupled increase in chromatin-bound H3K56ac that results from the silencing defect. At *HMR*, *cac1Δ rtt106Δ* strains had only mild silencing defects, which allowed us to visualize the initial reduction in H3K56ac (figure 3.3b). At telomeres, a strong transcription-dependent increase in H3K56ac enrichment, which was likely facilitated by Asf1, HIR or FACT, masked our ability to detect H3K56ac recruitment defects associated with the *cac1Δ rtt106Δ* background (figure 3.5c). However, we predict that monitoring H3K56ac enrichment at telomeres during the establishment of silencing over time would reveal an initial reduction in H3K56ac in *cac1Δ rtt106Δ* strains. In sum, our results support a model where Sir4, bound to telomere ends or silencers, is recognized by Rtt106, which, in turn, recruits H3K56ac, and that H3K56ac promotes silencing, potentially by providing a target for Sir2 or for Hst3 Hst4 deacetylase activity.

Because strains that lacked H3K56ac (*rtt109Δ* and H3K56R) maintained silencing, H3K56ac is not strictly required for silent chromatin formation (figure 3.3c and 3.4a,b). However, if a cell makes H3K56ac, yet does not incorporate it during replication (as in *cac1Δ rtt106Δ* mutants), or allows it to accumulate (as in *hst3Δ hst4Δ* mutants), then silencing is disrupted. Consistent with these results, *cac1Δ rtt106Δ* silencing defects at *HMR* and *hst3Δ hst4Δ* silencing defects at telomeres were both suppressed by an *rtt109Δ* mutation (figure 3.3) (*21*). The telomeric silencing defects in *cac1Δ rtt106Δ* strains were not suppressed by an *rtt109Δ* mutation (figure 3.5e). This may be due to increased transcription in the *cac1Δ rtt106Δ* background compared to the *hst3Δ hst4Δ* background (figure 3.5a) (*21*). Because H3K56ac is not essential for silencing, these data suggest that the role of Rtt106 and CAF-1 in silencing is either to remove excess H3K56ac from the free histone pool through nucleosome assembly and/or to create an arrangement of H3K56ac-containing nucleosomes that is compatible with Sir spreading.

Surprisingly, unlike the *rtt109Δ* mutation, H3K56R mutations did not suppress *cac1Δ rtt106Δ* silencing defects (figure 3.4b). The strain used to analyze the silencing phenotype of the H3K56R *cac1Δ rtt106Δ* triple mutant was *hht1-hhf1Δ* and already contained more severe *rtt106Δ*-associated phenotypes (figure 9b). Due to the supposed functional redundancy of the H3 and H4 histone gene copies, histone point-mutants are

typically studied by knocking-out both endogenous copies and adding back mutant *hht2-hhf2* on a plasmid. These strains are effectively *hht1-hhf1Δ*. Therefore the lack of suppression of *cac1Δ rtt106Δ* silencing defects by H3K56R may be due to the sensitized *hht1-hhf1Δ* background rather than the *cac1Δ rtt106Δ* silencing phenotype occurring through H3K56ac-independent mechanisms. Dissecting these roles will require strains with integrated point-mutants at the endogenous locus for both histone gene copies.

Rtt106 highlighted a lack of redundancy between histone gene copies

Increased expression of histone genes may contribute to the observed replication and silencing defects associated with *RTT106* mutant strains. However, strains carrying a reduced H3-H4 histone gene dosage (*hht1-hhf1Δ* or *hht2-hhf2Δ*) did not suppress the Rtt106-associated phenotypes, suggesting that Rtt106 plays direct roles in replication and silencing (figure 3.9a,b). Intriguingly, *rtt106Δ hht1-hhf1Δ* double mutants had a synergistic increase in silencing and replication defects compared to the single mutants whereas *rtt106Δ hht2-hhf2Δ* double mutants did not. These results suggest that Rtt106 either plays a distinct role at the *HHT1-HHF1* promoter or that Rtt106 mutant cells are more sensitive to the increased H3:H4 ratio of histone mRNA associated with the *hht1-hhf1Δ* background (figure 3.9c). It is possible that other histone chaperones, such as CAF-1, will have similar genetic interactions with the *HHT1-HHF1* histone gene copy. Because CAF-1 does not affect histone gene transcription, but binds to H3 in a K56ac-dependent manner (*6*), *cac1Δ hht1-hhf1Δ* synergistic phenotypes would support a previously unappreciated relationship between histone chaperones that bind H3/H4 protein and the two H3-H4 histone gene pairs.

H3 bridged Rtt106 and the HIR complex to provide feedback at histone promoters

In contrast to replication and silencing, where Rtt106 was properly localized in the absence of H3 binding, Rtt106 recruitment to histone gene promoters was dependent on Rtt106's H3-binding function (figure 3.6 and 3.7). Because Rtt106 localization is also dependent on the HIR complex, mislocalized Rtt106-H3 binding mutants could result from mislocalized HIR. However, preliminary results show that the enrichment of HIR complex at histone gene promoters does not require Rtt106 (data not shown), further suggesting that both HIR and H3 recruit Rtt106 to the promoter. Rtt106 and HIR co-purify *in vivo*, however a direct interaction has not been demonstrated *in vitro* (*8*). The HIR complex is thought to contact both H3/H4 histones and the negative regulatory sequences within the histone gene promoters (*26, 27*). Our results support a model where distinct surfaces of one H3 molecule act as interaction bridge between Rtt106 and HIR (figure 3.6c). This model predicts that either Rtt106-H3 binding mutants or HIR-H3 binding mutants will disrupt the Rtt106-HIR interaction, leading to Rtt106 mislocalization at histone gene promoters. Our data implicate this histone bridging interaction as an indirect recruitment signal for Rtt106 to DNA and a general structural mechanism for histone hand-off between different chaperones.

In addition to Rtt106 mislocalization at histone gene promoters in strains with reduced Rtt106-H3 binding, Rtt106 was also mislocalized in strains with excess H3K56ac, which increased Rtt106-H3 binding (*hst3Δ hst4Δ* and H3K56Q) (figure 3.6). Therefore, Rtt106 requires a specific level of H3 binding for recruitment to the histone genes. Increased H3K56ac may titrate Rtt106 off of histone gene promoters and into other areas of the genome with elevated levels of H3K56ac. Alternatively, increased H3K56ac within the free histone pool may titrate Rtt106 off chromatin. Chromatin association assays and ChIP of Rtt106 at additional genomic loci in the *hst3Δ hst4Δ* and H3K56Q backgrounds will distinguish between these possibilities.

In the absence of Rtt106, H3K56ac was reduced at histone gene promoters, leading to histone gene derepression (figure 3.8c,d). Although, *rtt109*Δ and *hst3*Δ *hst4*Δ backgrounds had mislocalized Rtt106, and reduced H3K56ac at the promoter, histone mRNA levels were equal to those of wild type (figure 3.6a and 3.8c,d). Mislocalization of the Spt10 activator of histone transcription would be epistatic to mislocalized Rtt106. However, preliminary ChIP results suggest that Spt10 localization is equal to that in wild type in the *rtt109*Δ and *hst3*Δ *hst4*Δ backgrounds (data not shown). Strains lacking either Rtt106 or Rtt109 had opposite effects on bulk H3 within the promoter, further revealing their antagonistic effects on histone gene transcription (figure 3.8b). Additionally, others have categorized Rtt109 as an activator of histone gene transcription and shown that *HTA1* transcription is reduced in *rtt109*Δ strains (*8*). We did not observe this reduction in histone mRNA (figure 3.8), which may reflect a difference in the parent strains used in each study (we used W303 rather than S288c). If Rtt109 were an activator of histone gene transcription, then mislocalized Rtt106 repressor in the absence of Rtt109 would not result in increased histone gene transcription.

Because all newly synthesized H3 molecules are acetylated on K56, and Rtt106-H3 binding is K56ac-dependent, our results suggest that Rtt106 may act as a sensor to regulate histone gene transcription as a function of histone protein levels. In wild type cells, Rtt106 binds H3K56ac and is recruited to histone gene promoters to repress transcription outside of S-phase. Reduced H3K56ac disrupts Rtt106-H3 binding, which leads to Rtt106 mislocalization at the histone gene promoters and increased histone gene expression. This feedback structure positions the Hir-Rtt106 interaction as a critical node in regulating histone transcription. Since histone gene promoters are sites of rapid histone turnover (*8*), monitoring Rtt106 occupancy at other sites in the genome with similar histone dynamics, possibly at genes where expression is sensitive to the cellular level of histone protein, will reveal whether the Rtt106-HIR repressive complex represents a new general mechanism of transcriptional control.

The evolution of H3K56ac interactions

Although H3K56ac plays a critical role in yeast chromatin metabolism, the roles of H3K56ac in other eukaryotes are still emerging. The hierarchy of Asf1-mediated H3K56 acetylation by p300/CBP (a functional analogue of Rtt109-Vps75) followed by CAF-1-mediated deposition into chromatin is conserved in both human and fly cells (*40*). Additionally, H3K56ac localizes to DNA repair foci and elevated levels of H3K56ac

are observed in cancer cell lines, suggesting that H3K56ac has a conserved role in the DNA damage response (*40*). Recent studies show that H3K56ac is more prevalent in human embryonic stem cells (hESCs) than human somatic cells (*41*). Unlike in yeast, H3K56ac occupancy in hESCs is restricted to specific genes, rather than globally enriched (*12*). Intriguingly, the genomic profile of H3K56ac overlaps with the enrichment patterns of transcription factors NANOG, SOX2, and OCT4, suggesting that H3K56ac may regulate pluripotency (*41*). Although the roles of H3K56ac appear to be at least partially conserved, further analysis is necessary to uncover the distinct regulatory controls afforded by this modification in other eukaryotes. Rtt106 provides insight into a novel architecture that can interact with H3K56ac, suggesting that additional organism-specific chaperones have yet to be discovered. These chaperones will likely rely on the same general principles of modification specificity, localization, and transcriptional feedback that we have revealed for Rtt106 in yeast.

Tables 3.5

Table 3.1. Yeast strains used in chapter 3.

Strain	Genotype	Source
JRY3009	*MATα ade2-1 his3-11 leu2-3,112 trp1-1 ura3-52 can1-100*	R. Rothstein
JRY2334	*MATa ade2-1 his3-11 leu2-3,112 trp1-1 ura3-52 can1-100*	R. Rothstein
JRY8883	*MATa HMR-a1Δ::K.l.URA3*	E. Osbourn (reporter generated by J. Kuei)
RZY673	*MATα rtt106Δ::KanMX [pRZ050 HIS3 RTT106]*	This study
RZY675	*MATα rtt106Δ::KanMX [pRZ093 HIS3 RTT106-3xFLAG::KanMX]*	This study
RZY234	*MATα rtt106Δ::KanMX cac1Δ::HygMX [pRZ093 HIS3 RTT106-3xFLAG::KanMX]*	This study
RZY525	*MATα rtt106Δ::KanMX cac1Δ::HygMX [pRZ112 HIS3 rtt106(S80E)-3xFLAG::KanMX]*	This study
RZY663	*MATα rtt106Δ::KanMX cac1Δ::HygMX [pRZ139 HIS3 rtt106(R86A)-3xFLAG::KanMX]*	This study
RZY661	*MATα rtt106Δ::KanMX cac1Δ::HygMX [pRZ137 HIS3 rtt106(T265E)-3xFLAG::KanMX]*	This study
RZY1166	*MATα rtt106Δ::KanMX hir1Δ::HygMX [pRZ093 HIS3 RTT106-3xFLAG::KanMX]*	This study
RZY679	*MATα rtt106Δ::KanMX [pRZ112 HIS3 rtt106(S80E)-3xFLAG::KanMX]*	This study
RZY702	*MATα rtt106Δ::KanMX [pRZ139 HIS3 rtt106(R86A)-3xFLAG::KanMX]*	This study
RZY700	*MATα rtt106Δ::KanMX [pRZ137 HIS3 rtt106(T265E)-3xFLAG::KanMX]*	This study
RZY250	*MATα rtt106Δ::KanMX rtt109Δ::HygMX [pRZ093 HIS3 RTT106-3xFLAG::KanMX]*	This study
RZY242	*MATα rtt106Δ::KanMX hst3Δ::HygMX hst4Δ::NatMX [pRZ093 HIS3 RTT106-3xFLAG::KanMX]*	This study
RZY363	*MATα hhf1-hht1Δ::HygMX; hhf2-hht2Δ::NatMX rtt106Δ::KanMX [pJR2657 URA3 HHT2-HHF2]*	This study
RZY401	*MATα hhf1-hht1Δ::HygMX; hhf2-hht2Δ::NatMX rtt106Δ::KanMX [pRZ050 HIS3 RTT106 pJR2851 TRP1 HHT2-HHF2]*	This study
RZY403	*MATα hhf1-hht1Δ::HygMX; hhf2-hht2Δ::NatMX rtt106Δ::KanMX [pRZ093 HIS3 RTT106-3xFLAG::KanMX pJR2851 TRP1 HHT2-HHF2]*	This study
RZY409	*MATα hhf1-hht1Δ::HygMX; hhf2-hht2Δ::NatMX rtt106Δ::KanMX [pRZ093 HIS3 RTT106-3xFLAG::KanMX pRZ102 TRP1 hht2K56R-HHF2]*	This study
RZY1158	*MATα hhf1-hht1Δ::HygMX; hhf2-hht2Δ::NatMX rtt106Δ::KanMX [pRZ093 HIS3 RTT106-3xFLAG::KanMX pRZ104 TRP1 hht2K56Q-HHF2]*	This study
RZY220	*MATα rtt106Δ::KanMX [pRS313]*	This study
RZY228	*MATα rtt106Δ::KanMX cac1Δ::HygMX [pRS313]*	This study
RZY1046	*MATα rtt106Δ::KanMX sir3Δ::NatMX [pRZ093 HIS3 RTT106-3xFLAG::KanMX]*	
RZY427	*MATa HMR-a1Δ::K.l.URA3 rtt106Δ::KanMX [pRZ093 HIS3 RTT106-3xFLAG::KanMX]*	This study
RZY1050	*MATa HMR-a1Δ::K.l.URA3 rtt106Δ::KanMX sir3Δ::NatMX [pRZ093 HIS3 RTT106-3xFLAG::KanMX]*	This study
RZY1066	*MATa HMR-a1Δ::K.l.URA3 rtt106Δ::KanMX rtt109Δ::HygMX [pRZ093 HIS3 RTT106-3xFLAG::KanMX]*	
RZY421	*MATa HMR-a1Δ::K.l.URA3 rtt106Δ::KanMX [pRS313]*	This study
RZY437	*MATa HMR-a1Δ::K.l.URA3 rtt106Δ::KanMX cac1Δ::HygMX [pRZ093 HIS3 RTT106-3xFLAG::KanMX]*	This study
RZY431	*MATa HMR-a1Δ::K.l.URA3 rtt106Δ::KanMX cac1Δ::HygMX [pRS313]*	This study
RZY573	*MATa HMR-a1Δ::K.l.URA3 rtt106Δ::KanMX cac1Δ::HygMX [pRZ112 HIS3 rtt106(S80E)-3xFLAG::KanMX]*	This study
RZY669	*MATa HMR-a1Δ::K.l.URA3 rtt106Δ::KanMX cac1Δ::HygMX [pRZ139 HIS3 rtt106(R86A)-3xFLAG::KanMX]*	This study
RZY1052	*MATa HMR-a1Δ::K.l.URA3 rtt106Δ::KanMX cac1Δ::HygMX [pRZ137 HIS3 rtt106(T265E)-3xFLAG::KanMX]*	This study

Table 3.1. Yeast strains used in chapter 3 (cont.).

RZY1054	*MATa HMR-a1Δ::K.l.URA3 rtt106Δ::KanMX cac1Δ::HygMX rtt109Δ::NatMX [pRS313]*	This study
RZY1004	*MATa HMR-a1Δ::K.l.URA3 rtt106Δ::KanMX cac1Δ::HygMX rtt109Δ::NatMX [pRZ112 HIS3 rtt106(S80E)-3xFLAG::KanMX]*	This study
RZY1056	*MATa HMR-a1Δ::K.l.URA3 rtt106Δ::KanMX cac1Δ::HygMX rtt109Δ::NatMX [pRZ139 HIS3 rtt106(R86A)-3xFLAG::KanMX]*	This study
RZY1008	*MATa HMR-a1Δ::K.l.URA3 rtt106Δ::KanMX cac1Δ::HygMX rtt109Δ::NatMX [pRZ137 HIS3 rtt106(T265E)-3xFLAG::KanMX]*	This study
RZY202	*MATα rtt109Δ::HygMX*	This study
RZY212	*MATα rtt106Δ::KanMX cac1Δ::HygMX*	This study
RZY1198	*MATα rtt106Δ::KanMX cac1Δ::HygMX rtt109Δ::NatMX*	This study
RZY1126	*MATα HMR-a1Δ::K.l.URA3 hhf1-hht1Δ::HygMX; hhf2-hht2Δ::NatMX [pJR2851 TRP1 HHT2-HHF2]*	This study
RZY1182	*MATα HMR-a1Δ::K.l.URA3 sir3Δ::KanMX hhf1-hht1Δ::HygMX; hhf2-hht2Δ::NatMX [pJR2851 TRP1 HHT2-HHF2]*	This study
RZY1138	*MATα HMR-a1Δ::K.l.URA3 hhf1-hht1Δ::HygMX; hhf2-hht2Δ::NatMX [pRZ102 TRP1 hht2K56R-HHF2]*	This study
RZY1178	*MATα HMR-a1Δ::K.l.URA3 rtt106Δ::KanMX cac1Δ::loxP-LEU2-loxP hhf1-hht1Δ::HygMX; hhf2-hht2Δ::NatMX [pJR2851 TRP1 HHT2-HHF2]*	This study
RZY1144	*MATα HMR-a1Δ::K.l.URA3 rtt106Δ::KanMX cac1Δ::loxP-LEU2-loxP hhf1-hht1Δ::HygMX; hhf2-hht2Δ::NatMX [pRZ102 TRP1 hht2K56R-HHF2]*	This study
RZY369	*MATa HMR-a1Δ::K.l.URA3 sir3Δ::KanMX*	This study
RZY1234	*MATa HMR-a1Δ::K.l.URA3 hht1-hhf1Δ::KanMX*	This study
RZY1236	*MATa HMR-a1Δ::K.l.URA3 hht2-hhf2Δ::KanMX*	This study
RZY1242	*MATa HMR-a1Δ::K.l.URA3 rtt106Δ::KanMX hht1-hhf1Δ::HygMX*	This study
RZY1244	*MATa HMR-a1Δ::K.l.URA3 rtt106Δ::KanMX hht2-hhf2Δ::HygMX*	This study
RZY399	*MATa HMR-a1Δ::K.l.URA3 rtt106Δ::KanMX cac1Δ::HygMX*	This study
RZY1252	*MATa HMR-a1Δ::K.l.URA3 rtt106Δ::KanMX cac1Δ::HygMX hht1-hhf1Δ::NatMX*	This study
RZY1253	*MATa HMR-a1Δ::K.l.URA3 rtt106Δ::KanMX cac1Δ::HygMX hht2-hhf2Δ::NatMX*	This study

Table 3.2. Plasmids used in chapter 3.

Plasmid	Backbone	Yeast Selection	Bacterial Resistance	Insert	Source
pRZ050	pRS313	*HIS3*	*AMP*	*RTT106*	This study
pRZ093	pRS313	*HIS3*	*AMP*	*Rtt106-3xFLAG::KanMX*	This study
pRZ112	pRS313	*HIS3*	*AMP*	*rtt106(S80E)-3xFLAG::KanMX*	This study
pRZ139	pRS313	*HIS3*	*AMP*	*rtt106(R86A)-3xFLAG::KanMX*	This study
pRZ137	pRS313	*HIS3*	*AMP*	*rtt106(T265E)-3xFLAG::KanMX*	This study
pJR2851	pRS314	*TRP1*	*AMP*	*HHT2-HHF2*	C.D Allis
pRZ102	pRS314	*TRP1*	*AMP*	*hht2k56R-HHF2*	This study
pRZ225	pRS314	*TRP1*	*AMP*	*hht2K56Q-HHF2*	This study

Table 3.3. Oligos used for qRT-PCR.

Name	Amplified Target	Forward Oligo	Reverse Oligo
oRZ375, 376	*ACT1*	GGC ATC ATA CCT TCT ACA ACG AAT TG	CTA CCG GAA GAG TAC AAG GAC AAA AC
oMS69, 70	*HMR-a1Δ::K.l.URA3*	CTT CCA AGG GTT CTC TAG CAC ACG	CTG TAC TGC TGA CCC AAT GCA TCG
oRZ358, 359	*HMRa1*	TTT AGA AGA AAG CAA AGC CTT AAT TCC	CTT GAA GTG GAG TAA TGC CAC ATT
oRZ369, 370	*YFR057W*	GCC AAG CTT CCA ATA TCA CGA	GGA ATG ATC TTG GAA ATC GAT CA
oRZ472, 473	*HTA1*	TCC GGT GGT AAA GGT GGT AA	TGG AGC ACC AGA ACC AAT TC
oRZ459, 460	*HHT*	GGT GGT GTT AAG AAG CCT CA	CTT GAG CGA TTT CTC TGA CC
oRZ461, 462	*HHF*	AGC TAG AAG AGG TGG TGT CA	TCT TTC TCT TGG CGT GTT CG

Table 3.4. Oligos used for ChIP.

Name	Amplified Target	Forward Oligo	Reverse Oligo
oRZ397, 398	*SSC1*	GTG CCT TAG ATG CGC TGA AT	AGA GGA GGA CAG CAA CGT AT
oRZ310, 311	Chromosome V UTR	GCA ATC AAC ATC TGA AGA AAA GAA AGT AGT	CAT AAT CTG CGT AAA AAT GGC GTA AAT
oRZ407, 408	*ARS305*	AGC AAG ACC GGC CAG TTT GA	GCA CTT TGA TGA GGT CTC TAG CAA
oRZ409, 410	*ARS305* +1kb	ACC GGA CCC TCT TGC GTA AAG TAT	ATA TGC ATC AGC TGG CCC TGT TTG
oRZ415, 416	*ARS607*	CGG CTC GTG CAT TAA GCT TG	TGC CGC ACG CCA AAC ATT GC
oRZ419 420	*ARS501*	GAA TGT GTC TAC GTA ATT GG	CCT TTC TTT TGG AGC TGC TA
oRZ336, 337	*HMRa1*	TGG ATG ATA TTT GTA GTA TGG CGG A	TCC CTT TGG GCT CTT CTC TT
oRZ362, 363	*YFR057W*	GTG CTA AAG GAA TCC CCA GAG A	TCT GTC CAT TTT CCC TCT GCT C
oRZ298, 299	*HTA1-HTB1* Promoter	ACG GGC GTT TCT TCA ACA ACG A	ATA GTT AAC GAC CCA ACC GCG T
oRZ467, 468	*HHT1-HHF1* Promoter	AGG TGC AGA GCA AGG AAA TG	ATT TAC CAC CGT ATT CGC GG
oRZ469, 470	*HHT2-HHF2* Promoter	AAA TGA CCA ACT CCC ATC CG	TTT GTT CTG GTC TGG TCT GC

Figures 3.7

Figure 3.1. Rtt106 delivered H3K56ac to origins of replication.
(A) *RTT106* mutants were sensitive to S-phase DNA damaging agents. Five-fold serial dilutions of each strain were spotted on camptothecin (3.5 μg/mL) and hydroxyurea (150 mM) containing media. CSM-HIS medium maintained selection of the mutant *RTT106* plasmids. (B) Rtt106 mutants localized to origins of replication. ChIP analysis of wild type and mutant Rtt106-FLAG at early and late origins of replication compared to an untagged control. IP/input ratios of amplified DNA for *ARS305*, *ARS305* +1kb, *ARS607*, and *ARS501* primer sets are shown for each strain. Error bars here and elsewhere represent standard deviations (n = 3). (C) H3K56ac occupancy was reduced at early and late origins of replication in Rtt106 mutant backgrounds. ChIP analysis used antibodies against H3K56ac and total H3. Amplified DNA from *ARS305*, *ARS305* +1kb, *ARS607*, and *ARS501* was normalized to a previously described control gene, *SSC1*. (D) Total cellular H3K56ac was not altered in *rtt106*Δ *cac1*Δ backgrounds. H3K56ac levels were detected by immunoblotting whole-cell extract with antibodies against either H3K56ac or total H3, normalized to an anti-Pgk1 loading control. Immunoblot quantifications were calculated using Li-COR Odyssey software.

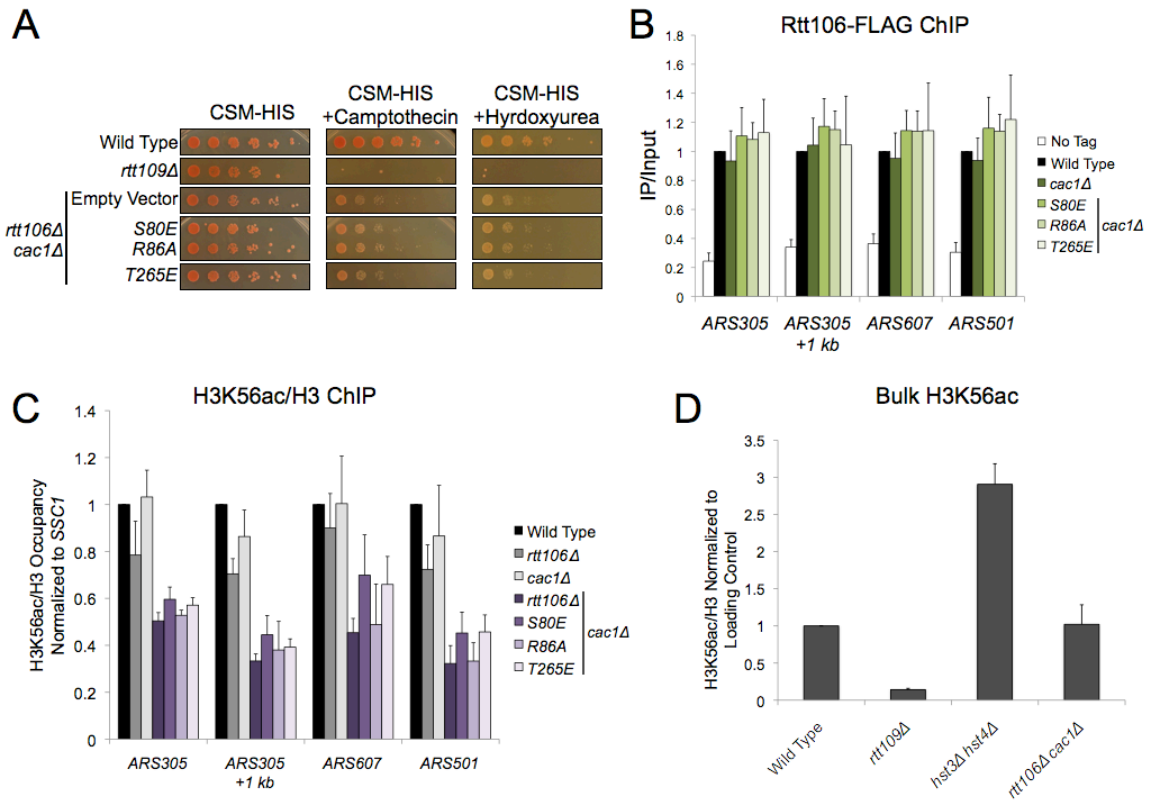

Figure 3.2. Rtt106-H3 binding was required for silencing at *HMR*.
(A) *RTT106* mutants had silencing defects at *HMR*. To monitor silencing of an *HMR-a1Δ::URA3* reporter gene, five-fold serial dilutions of each *RTT106* mutant were spotted onto medium either containing FOA or lacking uracil. CSM-HIS media maintained selection of the mutant *RTT106* plasmids. (B) qRT-PCR analysis of *HMR-a1Δ::URA3* expression normalized to *ACT1*.

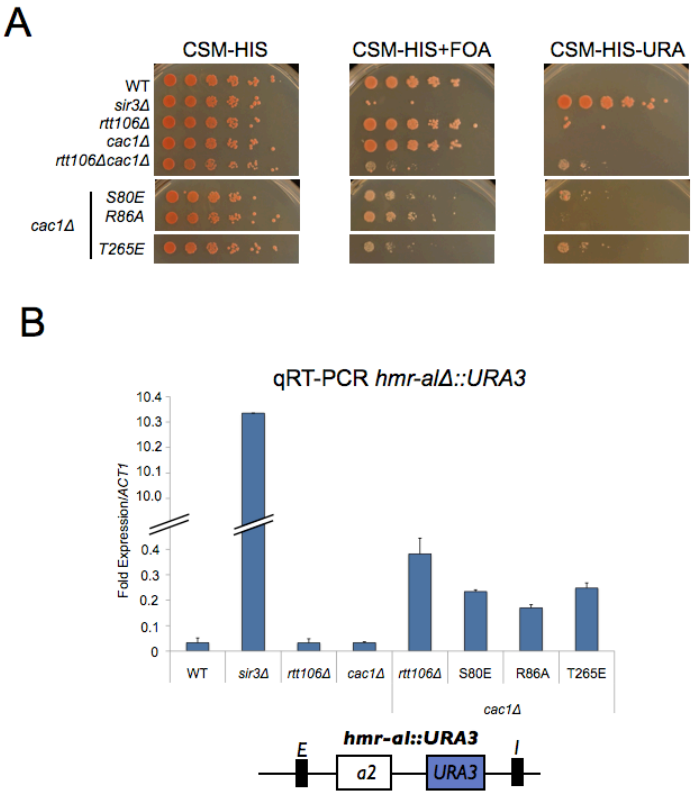

Figure 3.3. Unchaperoned H3K56ac was antagonistic to silencing.
(A) Rtt106 mutant proteins localized to *HMR*. ChIP analysis of Rtt106-FLAG was performed as in figure 3.1b with a primer set amplifying *HMRa1*. (B) H3K56ac was reduced at *HMRa1* in each *RTT106* mutant background. ChIP analysis of H3K56ac was performed as in Figure 3.1c with a primer set amplifying *HMRa1.* (C) The *rtt109*Δ mutation partially suppressed *rtt106*Δ *cac1*Δ silencing defects at *HMRa1*. qRT-PCR analysis of *HMR-a1*Δ*::URA3* expression was performed as described in figure 3.2b.

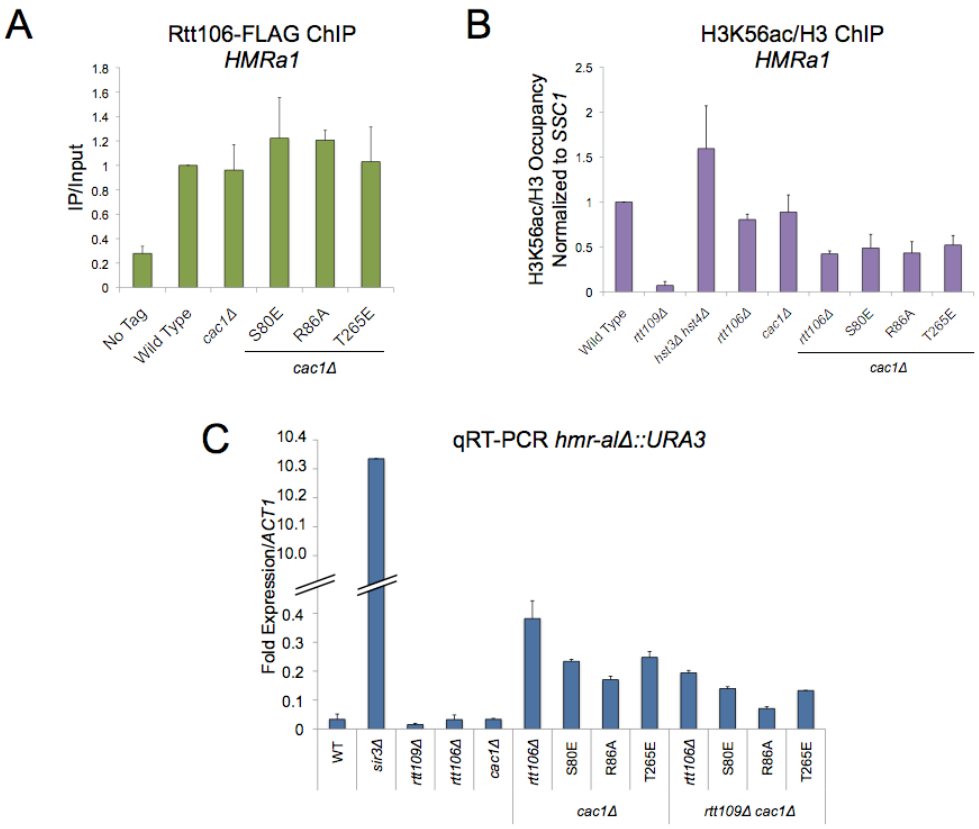

Figure 3.4. Further analysis of *rtt109*Δ suppression *rtt106*Δ *cac1*Δ silencing defects.

(A) An *rtt109*Δ mutation partially suppressed *rtt106*Δ *cac1*Δ silencing defects at endogenous *HMRa1*. (B) An H3K56R mutation did not suppress the *rtt106*Δ *cac1*Δ silencing defects. qRT-PCR analyses of *HMRa1* (A) and *HMR-a1*Δ*::URA3* (B) were performed as described in figure 3.2b.

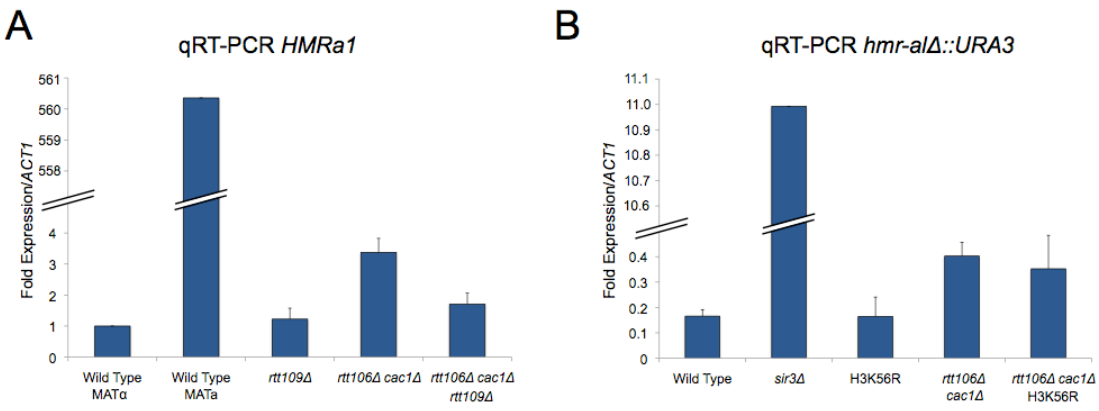

Figure 3.5. Rtt106-mediated delivery of H3K56ac was essential for telomeric silencing.

(A) *RTT106* mutants had silencing defects at *YFR057W*. qRT-PCR analysis of *YFR057W* expression was performed as described in figure 3.2b. (B) Rtt106 mutants localized to *YFR057W*. ChIP analysis of Rtt106-FLAG was performed as in figure 3.1b with a primer set amplifying *YFR057W*. (C) H3K56ac was enriched in *RTT106* mutant backgrounds at *YFR057W*. ChIP analysis of H3K56ac was performed as in Figure 3.1c with a primer set amplifying *YFR057W.* (D) H3K56ac was enriched in *Sir*⁻ backgrounds at *HMRa1* and *YFR057W*. ChIP analysis of H3K56ac was performed as in Figure 3.1c with primer sets amplifying *HMRa1* and *YFR057W*. (E) An *rtt109*Δ mutation did not suppress *rtt106*Δ *cac1*Δ silencing defects at *YFR057W*. qRT-PCR analysis of *YFR057W* expression was performed as described in figure 3.2b.

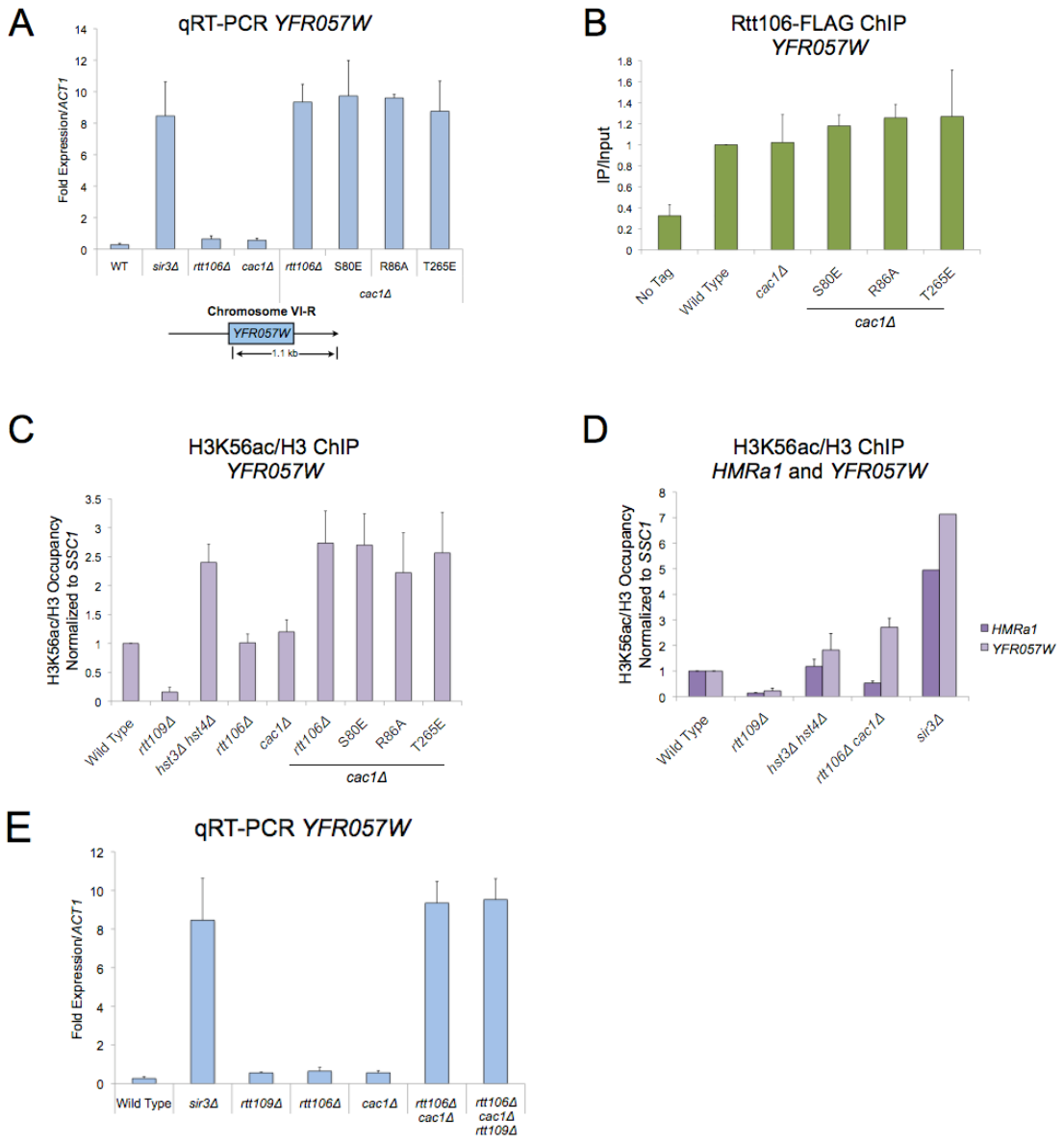

Figure 3.6. Rtt106-H3 binding was necessary for Rtt106 localization to histone gene promoters.
(A) Rtt106-H3 binding mutants did not localize to histone gene promoters. ChIP analysis of wild type and mutant Rtt106-FLAG strains at the *HTA1-HTB1* promoter compared to an untagged control. Amplified DNA from the *HTA1-HTB1* promoter was normalized to a previously described control region on an untranscribed region (UTR) of chromosome V. (B) ChIP analysis of Rtt106-FLAG was performed as in figure 3.6a in a histone point mutant background (described in materials and methods). (C) The regulation of Rtt106 recruitment at histone gene promoters (described in the text). Rtt106 localization to histone gene promoters was HIR-dependent. Mutant backgrounds that increased or decreased Rtt106-H3 binding reduced Rtt106 localization at histone gene promoters.

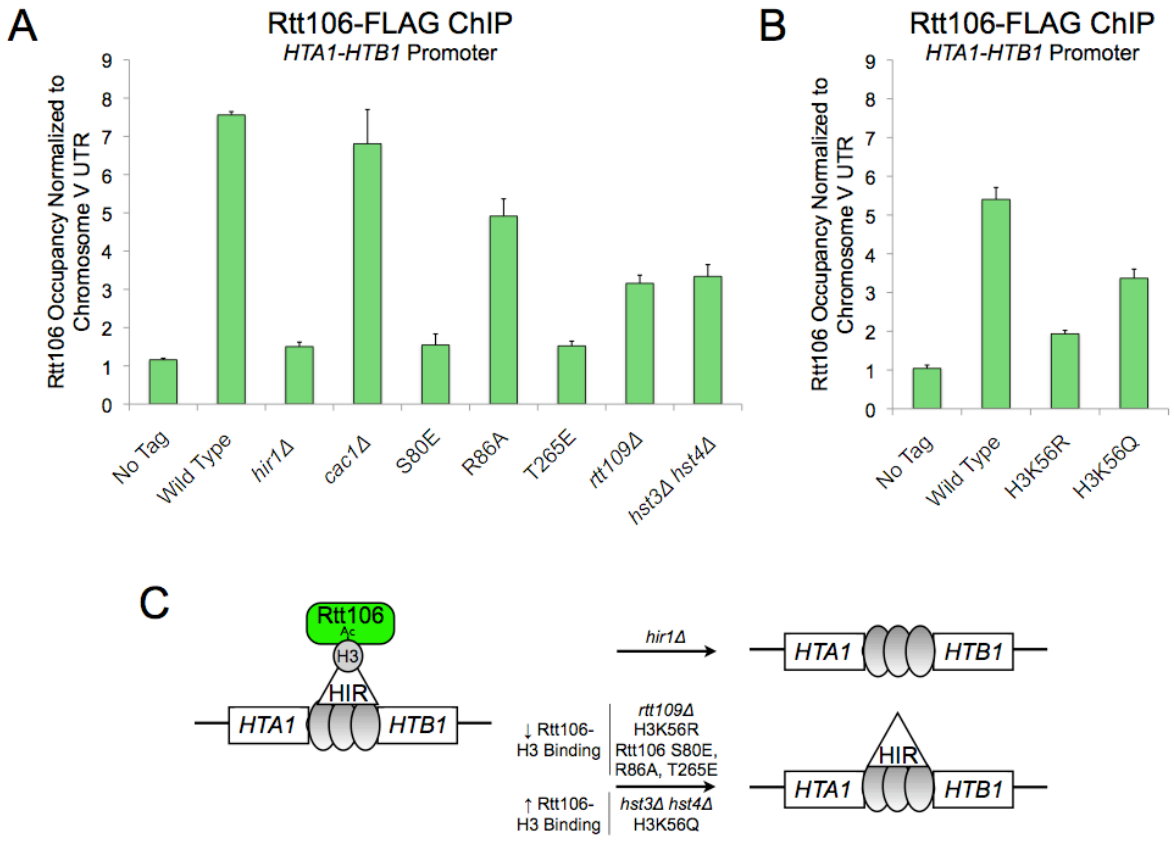

Figure 3.7. Further analysis of Rtt106-H3 binding and localization at histone gene promoters.

(A,B) Rtt106 mutants did not localize to H3-H4 histone gene promoters. ChIP analysis of Rtt106-FLAG was performed as in figure 3.6a with primer sets amplifying the *HHT1-HHF1* (A) or *HHT2-HHF2* (B) promoter.

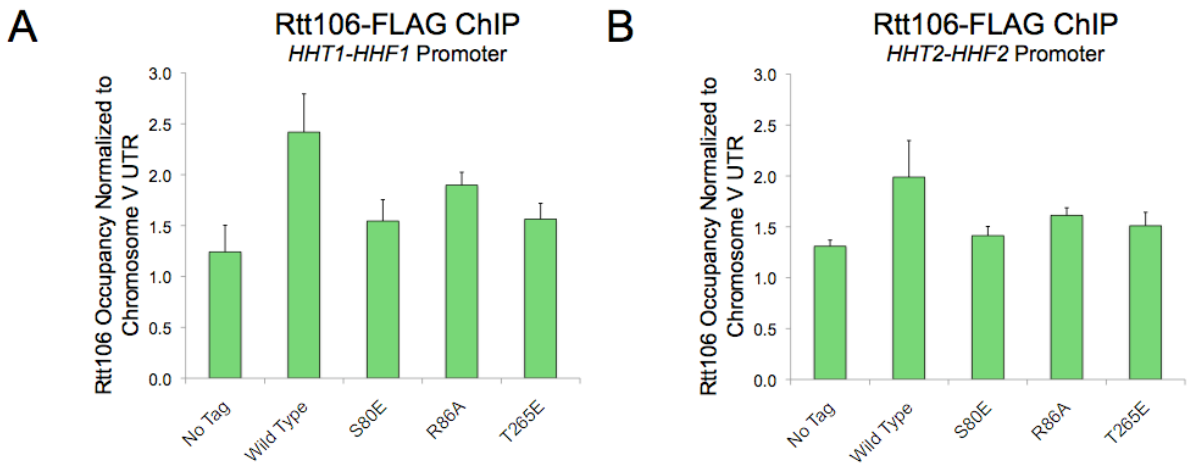

Figure 3.8. Rtt106 delivered H3K56ac to histone gene promoters to repress transcription.

H3K56ac occupancy was reduced at histone gene promoters in backgrounds with mis-localized Rtt106. (A) ChIP analysis was performed with antibodies against H3K56ac. Amplified DNA from the *HTA1-HTB1* promoter was normalized to a previously described control region on chromosome V. (B) ChIP analysis was performed as in figure 3.8a with antibodies against H3. (C) H3K56ac occupancy was reduced in *rtt106Δ* strains ($p<0.05$). ChIP analysis of H3K56ac from figure 3.8a normalized to total H3 from figure 3.8b. (D) *RTT106* mutants had increased histone gene expression. qRT-PCR analysis of *HTA1* expression was performed as described in figure 3.2b. Data shown represents one biological replicate.

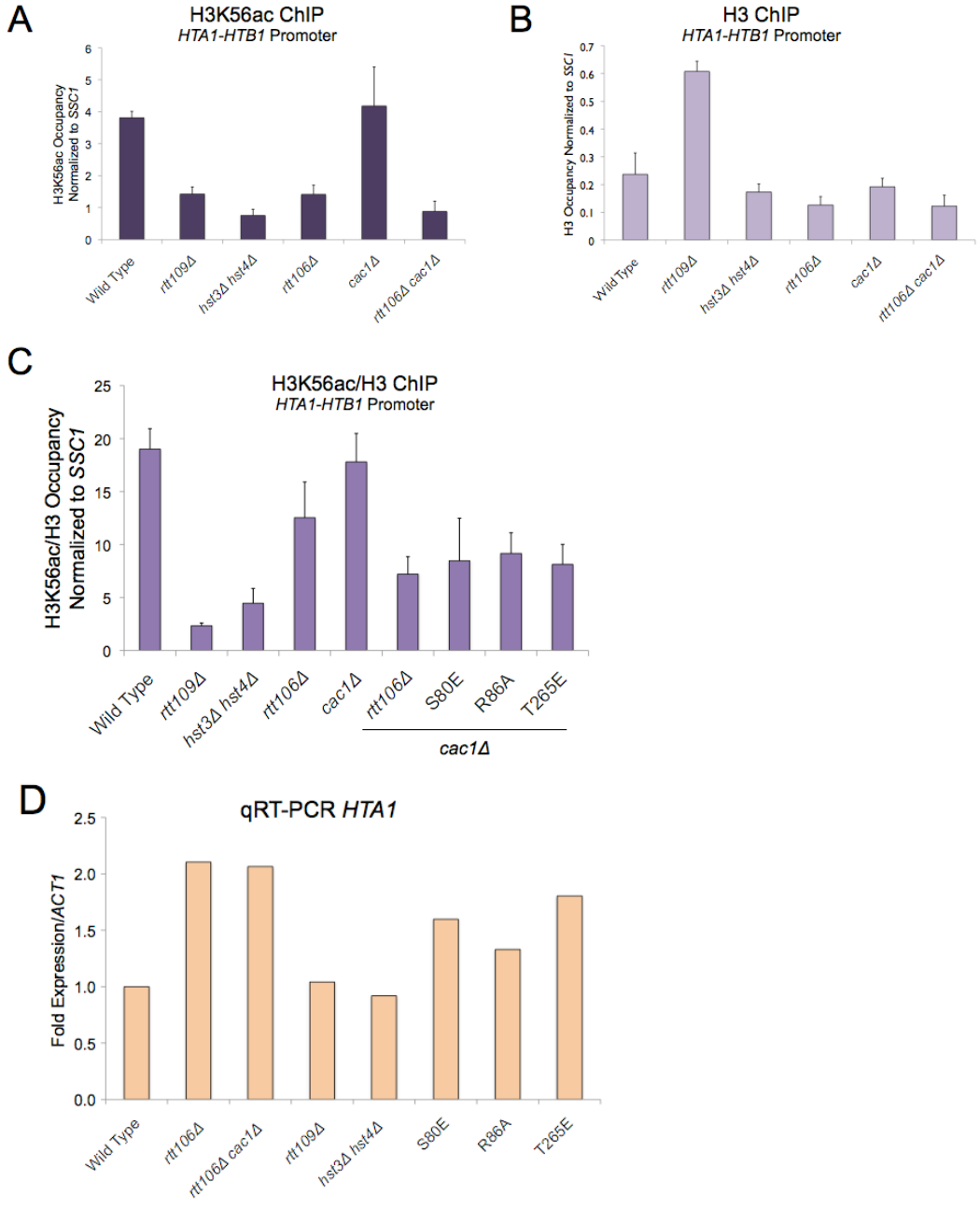

Figure 3.9. Distinct regulation of H3 and H4 histone gene copies.
(A) *rtt106*Δ *hht1-hhf1*Δ strains were synergistically sensitive to DNA damaging agents. Five fold serial dilutions of each strain were spotted onto medium containing camptothecin (3.5 μg/ml), methyl-methanesulfonate (0.005%), or hydroxyurea (150 mM). (B) *rtt106*Δ *hht1-hhf1*Δ strains had synergistic silencing defects at *HMR*. qRT-PCR analysis of *HMR-a1*Δ*::URA3* expression was performed as described in figure 3.2b. Data shown represent a single biological replicate. (C) *hht1-hhf1*Δ and *hht2-hhf2*Δ strains had distinct ratios of H3:H4 mRNA. qRT-PCR analysis of *HHT and HHF* expression was performed as described in figure 3.2b. Data shown represent the average of two biological replicates.

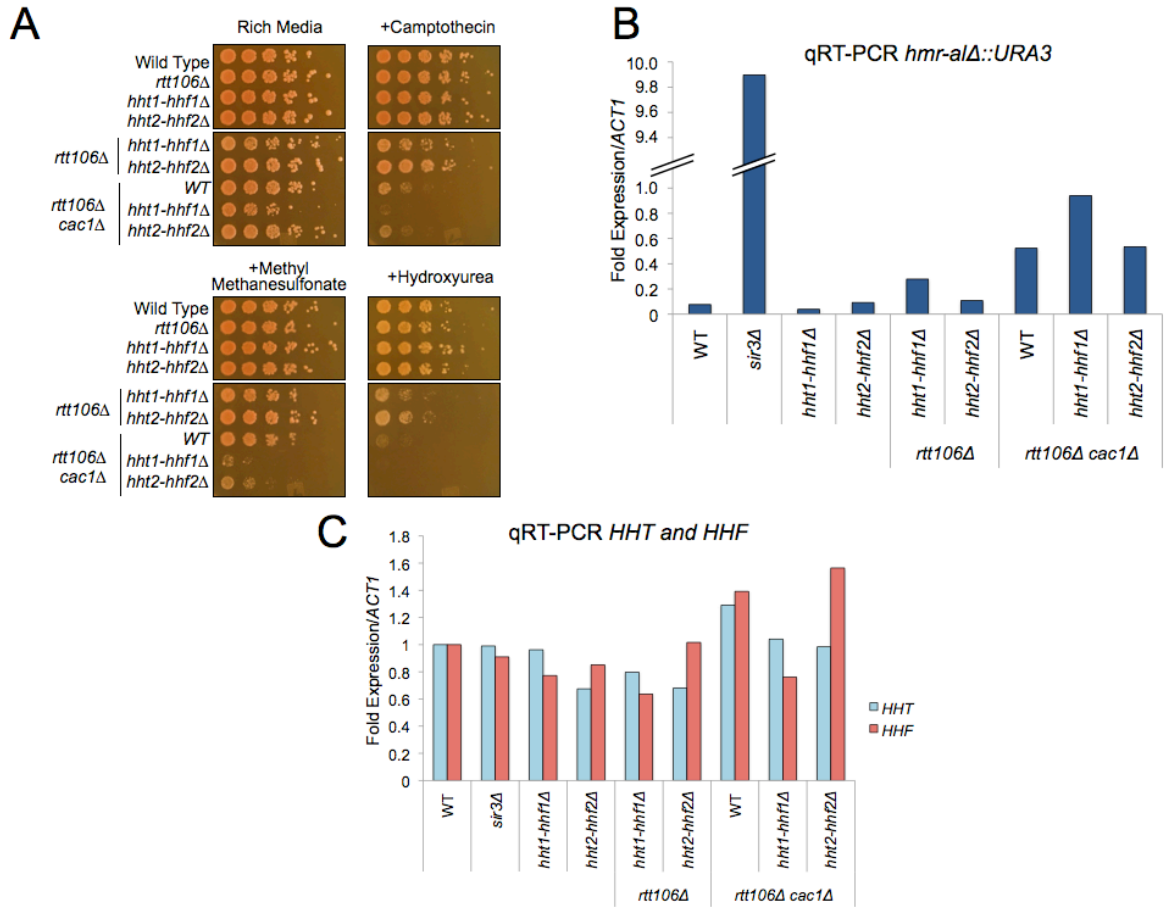

3.7 References

1. Luger, K., Mader, A. W., Richmond, R. K., Sargent, D. F., and Richmond, T. J. (1997) Crystal structure of the nucleosome core particle at 2.8 A resolution, *Nature 389*, 251-260.
2. Avvakumov, N., Nourani, A., and Cote, J. (2011) Histone chaperones: modulators of chromatin marks, *Molecular cell 41*, 502-514.
3. Das, C., Tyler, J. K., and Churchill, M. E. (2010) The histone shuffle: histone chaperones in an energetic dance, *Trends in biochemical sciences 35*, 476-489.
4. De Koning, L., Corpet, A., Haber, J. E., and Almouzni, G. (2007) Histone chaperones: an escort network regulating histone traffic, *Nature structural & molecular biology 14*, 997-1007.
5. Ransom, M., Dennehey, B. K., and Tyler, J. K. (2010) Chaperoning histones during DNA replication and repair, *Cell 140*, 183-195.
6. Li, Q., Zhou, H., Wurtele, H., Davies, B., Horazdovsky, B., Verreault, A., and Zhang, Z. (2008) Acetylation of histone H3 lysine 56 regulates replication-coupled nucleosome assembly, *Cell 134*, 244-255.
7. Imbeault, D., Gamar, L., Rufiange, A., Paquet, E., and Nourani, A. (2008) The Rtt106 histone chaperone is functionally linked to transcription elongation and is involved in the regulation of spurious transcription from cryptic promoters in yeast, *The Journal of biological chemistry 283*, 27350-27354.
8. Fillingham, J., Kainth, P., Lambert, J. P., van Bakel, H., Tsui, K., Pena-Castillo, L., Nislow, C., Figeys, D., Hughes, T. R., Greenblatt, J., and Andrews, B. J. (2009) Two-color cell array screen reveals interdependent roles for histone chaperones and a chromatin boundary regulator in histone gene repression, *Molecular cell 35*, 340-351.
9. Huang, S., Zhou, H., Katzmann, D., Hochstrasser, M., Atanasova, E., and Zhang, Z. (2005) Rtt106p is a histone chaperone involved in heterochromatin-mediated silencing, *Proceedings of the National Academy of Sciences of the United States of America 102*, 13410-13415.
10. Huang, S., Zhou, H., Tarara, J., and Zhang, Z. (2007) A novel role for histone chaperones CAF-1 and Rtt106p in heterochromatin silencing, *The EMBO journal 26*, 2274-2283.
11. Celic, I., Masumoto, H., Griffith, W. P., Meluh, P., Cotter, R. J., Boeke, J. D., and Verreault, A. (2006) The sirtuins hst3 and Hst4p preserve genome integrity by controlling histone h3 lysine 56 deacetylation, *Curr Biol 16*, 1280-1289.
12. Kaplan, T., Liu, C. L., Erkmann, J. A., Holik, J., Grunstein, M., Kaufman, P. D., Friedman, N., and Rando, O. J. (2008) Cell cycle- and chaperone-mediated regulation of H3K56ac incorporation in yeast, *PLoS genetics 4*, e1000270.
13. Williams, S. K., Truong, D., and Tyler, J. K. (2008) Acetylation in the globular core of histone H3 on lysine-56 promotes chromatin disassembly during transcriptional activation, *Proceedings of the National Academy of Sciences of the United States of America 105*, 9000-9005.
14. Masumoto, H., Hawke, D., Kobayashi, R., and Verreault, A. (2005) A role for cell-cycle-regulated histone H3 lysine 56 acetylation in the DNA damage response, *Nature 436*, 294-298.

15. Franco, A. A., Lam, W. M., Burgers, P. M., and Kaufman, P. D. (2005) Histone deposition protein Asf1 maintains DNA replisome integrity and interacts with replication factor C, *Genes & development 19*, 1365-1375.
16. Han, J., Zhou, H., Li, Z., Xu, R. M., and Zhang, Z. (2007) Acetylation of lysine 56 of histone H3 catalyzed by RTT109 and regulated by ASF1 is required for replisome integrity, *The Journal of biological chemistry 282*, 28587-28596.
17. Rusche, L. N., Kirchmaier, A. L., and Rine, J. (2003) The establishment, inheritance, and function of silenced chromatin in Saccharomyces cerevisiae, *Annual review of biochemistry 72*, 481-516.
18. Rine, J., and Herskowitz, I. (1987) Four genes responsible for a position effect on expression from HML and HMR in Saccharomyces cerevisiae, *Genetics 116*, 9-22.
19. Sharp, J. A., Fouts, E. T., Krawitz, D. C., and Kaufman, P. D. (2001) Yeast histone deposition protein Asf1p requires Hir proteins and PCNA for heterochromatic silencing, *Curr Biol 11*, 463-473.
20. Xu, F., Zhang, Q., Zhang, K., Xie, W., and Grunstein, M. (2007) Sir2 deacetylates histone H3 lysine 56 to regulate telomeric heterochromatin structure in yeast, *Molecular cell 27*, 890-900.
21. Yang, B., Miller, A., and Kirchmaier, A. L. (2008) HST3/HST4-dependent deacetylation of lysine 56 of histone H3 in silent chromatin, *Molecular biology of the cell 19*, 4993-5005.
22. Gunjan, A., Paik, J., and Verreault, A. (2005) Regulation of histone synthesis and nucleosome assembly, *Biochimie 87*, 625-635.
23. Osley, M. A., and Lycan, D. (1987) Trans-acting regulatory mutations that alter transcription of Saccharomyces cerevisiae histone genes, *Molecular and cellular biology 7*, 4204-4210.
24. Xu, H., Kim, U. J., Schuster, T., and Grunstein, M. (1992) Identification of a new set of cell cycle-regulatory genes that regulate S-phase transcription of histone genes in Saccharomyces cerevisiae, *Molecular and cellular biology 12*, 5249-5259.
25. Sutton, A., Bucaria, J., Osley, M. A., and Sternglanz, R. (2001) Yeast ASF1 protein is required for cell cycle regulation of histone gene transcription, *Genetics 158*, 587-596.
26. Green, E. M., Antczak, A. J., Bailey, A. O., Franco, A. A., Wu, K. J., Yates, J. R., 3rd, and Kaufman, P. D. (2005) Replication-independent histone deposition by the HIR complex and Asf1, *Curr Biol 15*, 2044-2049.
27. Osley, M. A., Gould, J., Kim, S., Kane, M. Y., and Hereford, L. (1986) Identification of sequences in a yeast histone promoter involved in periodic transcription, *Cell 45*, 537-544.
28. Xu, F., Zhang, K., and Grunstein, M. (2005) Acetylation in histone H3 globular domain regulates gene expression in yeast, *Cell 121*, 375-385.
29. Goldstein, A. L., and McCusker, J. H. (1999) Three new dominant drug resistance cassettes for gene disruption in Saccharomyces cerevisiae, *Yeast (Chichester, England) 15*, 1541-1553.
30. Longtine, M. S., McKenzie, A., 3rd, Demarini, D. J., Shah, N. G., Wach, A., Brachat, A., Philippsen, P., and Pringle, J. R. (1998) Additional modules for

versatile and economical PCR-based gene deletion and modification in Saccharomyces cerevisiae, *Yeast (Chichester, England) 14*, 953-961.
31. Zill, O. A., Scannell, D., Teytelman, L., and Rine, J. (2010) Co-evolution of transcriptional silencing proteins and the DNA elements specifying their assembly, *PLoS biology 8*, e1000550.
32. Gietz, R. D., and Woods, R. A. (2002) Transformation of yeast by lithium acetate/single-stranded carrier DNA/polyethylene glycol method, *Methods in enzymology 350*, 87-96.
33. Makarova, O., Kamberov, E., and Margolis, B. (2000) Generation of deletion and point mutations with one primer in a single cloning step, *BioTechniques 29*, 970-972.
34. Babiarz, J. E., Halley, J. E., and Rine, J. (2006) Telomeric heterochromatin boundaries require NuA4-dependent acetylation of histone variant H2A.Z in Saccharomyces cerevisiae, *Genes & development 20*, 700-710.
35. VanDemark, A. P., Blanksma, M., Ferris, E., Heroux, A., Hill, C. P., and Formosa, T. (2006) The structure of the yFACT Pob3-M domain, its interaction with the DNA replication factor RPA, and a potential role in nucleosome deposition, *Molecular cell 22*, 363-374.
36. Ozaydin, B., and Rine, J. (2010) Expanded roles of the origin recognition complex in the architecture and function of silenced chromatin in Saccharomyces cerevisiae, *Molecular and cellular biology 30*, 626-639.
37. Aparicio, O., Geisberg, J. V., Sekinger, E., Yang, A., Moqtaderi, Z., and Struhl, K. (2005) Chromatin immunoprecipitation for determining the association of proteins with specific genomic sequences in vivo, *Current protocols in molecular biology / edited by Frederick M. Ausubel ... [et al Chapter 21*, Unit 21 23.
38. Dollard, C., Ricupero-Hovasse, S. L., Natsoulis, G., Boeke, J. D., and Winston, F. (1994) SPT10 and SPT21 are required for transcription of particular histone genes in Saccharomyces cerevisiae, *Molecular and cellular biology 14*, 5223-5228.
39. Neumann, H., Hancock, S. M., Buning, R., Routh, A., Chapman, L., Somers, J., Owen-Hughes, T., van Noort, J., Rhodes, D., and Chin, J. W. (2009) A method for genetically installing site-specific acetylation in recombinant histones defines the effects of H3 K56 acetylation, *Molecular cell 36*, 153-163.
40. Das, C., Lucia, M. S., Hansen, K. C., and Tyler, J. K. (2009) CBP/p300-mediated acetylation of histone H3 on lysine 56, *Nature 459*, 113-117.
41. Xie, W., Song, C., Young, N. L., Sperling, A. S., Xu, F., Sridharan, R., Conway, A. E., Garcia, B. A., Plath, K., Clark, A. T., and Grunstein, M. (2009) Histone h3 lysine 56 acetylation is linked to the core transcriptional network in human embryonic stem cells, *Molecular cell 33*, 417-427.

Chapter 4

Investigating the distinct roles of two H2B isotypes in *S. cerevisiae*

4.1 Introduction

Eukaryotic DNA is packaged into chromatin, which compacts the genome and regulates gene expression. The fundamental unit of chromatin is the nucleosome, consisting of an octamer core of the four canonical histones (H2A, H2B, H3, and H4) wrapped in 146-bp of DNA (*1*). The surface of the nucleosome is studded with a plethora of post-translational modifications, including acetylation, methylation, phosphorylation, and ubiquitinylation. In addition to chemical modifications, the nucleosome structure can also be altered by replacing canonical histones with histone variants. The pattern of histone modifications and variants partitions the genome into defined regions of euchromatin and heterochromatin. These modifications are essential for orchestrating DNA-dependent processes such as replication, transcription, and repair.

In the *S. cerevisiae* genome, each canonical histone gene is present in two non-allelic isotypes that are expressed in divergently transcribed gene pairs of H2A-H2B or H3-H4 (*HTA1-HTB1, HTA2-HTB2, HHT1-HHF1*, and *HHT2-HHF2*) (figure 4.1a). The H3 and H4 isotypes encode identical proteins. The two H2A isotypes, Hta1 and Hta2, differ by an AT inversion within the globular domain. The two H2B isotypes, Htb1 and Htb2, differ at four residues within the N-terminal tail (figure 4.1b). Two of these substitutions (A2, K3 in Htb1 and S2, A3 in Htb2) are completely conserved across the *Saccharomyces sensu stricto* clade (figure 4.1c) (*2, 3*). The other two differences are strongly but incompletely conserved (27T, 35A in Htb1 and 27V, 35V in Htb2). The preservation of these substitutions over ~20 million years suggests that they represent a functional divergence between Htb1 and Htb2.

In other eukaryotes, four amino acid substitutions distinguish the canonical H3 protein from the transcription-specific variant H3.3 (*4*). Compared to canonical H3, H3.3 associates with unique histone chaperones that promote transcription-coupled nucleosome assembly (*5, 6*). H3.3 incorporation into chromatin influences both histone modifications and nucleosome structure to promote active transcription (*7, 8*). Based on the functional diversity between H3 and H3.3, we predict that the four amino acid changes between Htb1 and Htb2 might be sufficient to establish unique biochemical properties that lead to distinct functions.

In addition to changes at the protein level, *HTB1* and *HTB2* contain unique promoter sequences that lead to distinct transcriptional regulation. Both H2B isotypes are expressed exclusively during S-phase (*9*). However, like the H3-H4 gene pairs (*HHT1-HHF1* and *HHT2-HHF2*), *HTA1-HTB1* transcription is regulated by Rtt106 and the HIR histone chaperone complex whereas the mechanism of *HTA2-HTB2* transcriptional regulation is unknown (*10-12*). Further, *HTB1* gene expression auto-regulates based on H2B dosage (*13*). Therefore, in *htb2Δ* cells *HTB1* expression is up-regulated two-fold. The *HTB2* gene does not auto-regulate expression; therefore, *htb1Δ* cells are inviable due to the reduced level of H2B protein. Although these isotype-specific changes in H2B expression are important for cellular viability, the unique functions of the two H2B proteins remain unclear.

H2B contains a variety of post-translational modifications and associates with the histone variant H2A.Z, however, it is unknown whether any modifications or interactions are isotype-specific. Multiple lysine-acetylations within the H2B N-terminal tail and ubiquitinylation of lysine 123 within the globular domain are associated with active transcription (*14, 15*). H2B serine 10 phosphorylation promotes a yeast form of apoptosis by inducing chromatin condensation (*16*). Additionally, H2B exists in a dimer with either the canonical histone H2A or the histone variant H2A.Z. In *S. cerevisiae*, H2A.Z (encoded by the *HTZ1* locus) plays multiple roles in genome regulation. Acetylation of H2A.Z maintains the boundary between euchromatin and heterochromatin (referred to as silent chromatin) (*17*). Additionally, H2A.Z is enriched within nucleosomes at the promoter regions of active genes and is lost upon transcription initiation (*18, 19*). Interplay between modification, variants, and H2B isotypes would provide an additional level of genomic control.

To investigate the distinct functions of the two H2B isotypes, we examined differences in the modification patterns and histone variant associations between Htb1 and Htb2. Additionally, we analyzed the effects of *htb1*- and *htb2*- mutations on cellular fitness. Mass spectrometry analysis was performed by the Freitas lab at the Ohio State University. Although we found that H2A.Z showed a slight preference for Htb2 in H2A.Z-H2B dimers, H2A.Z and Htb2 did not directly affect one another's expression, chromatin incorporation, or modification profile. The Htb1 and Htb2 isotypes contained unique modifications that were H2A.Z-independent, but the role of these modifications in chromatin function remains elusive. To identify chemicals that relate to functional differences between the two H2B proteins rather than expression differences, the Giaever lab at the University of Toronto re-screened the top hits identified in their chemical-genomic analysis of the yeast heterozygous knock-out collection with strains we constructed that express an equal amount of only Htb1 or Htb2 (*20*). In our strains, the chemical sensitivities were equal to wild type, suggesting that the phenotypes of the hemizygous strains were likely due to changes in histone H2B expression rather than protein function.

4.2 Materials and Methods

Yeast Strains, Plasmids, and Culture

Yeast:

All yeast strains were generated in the *S. cerevisiae* W303 background unless otherwise indicated (table 4.1). Gene deletions were generated by one-step integration of knock-out cassettes (*21, 22*). PCR analysis of the 5' and 3' end of each targeted gene verified complete knock-outs. The C-terminal 3xFLAG tag (*23*) was integrated in frame using homologous recombination and verified by colony PCR and expression analysis. *HTA1-HTB1* and *HTA2-HTB2* plasmids harboring mutations of interest were introduced into strains containing wild type versions of the relevant gene by plasmid swap using 5-floroortic acid (FOA) counter selection. Strains harboring integrated *HTB* mutants were generated using the pRS400 series of integrating plasmids as described (RZY186 and RZY344) (*24*). Briefly, pRZ088 and pRZ062 were digested with MluI and

BclI, respectively, and transformed into wild type yeast (JRY3009) using the standard plasmid transformation protocol (*25*). Transformants were selected on CSM-URA medium and colony-PCR verified for plasmid integration at the intended *HTB* locus. Colonies with integrated plasmids were grown in YPD liquid culture and plated on FOA to select for mutants that looped-out the integrated plasmid in such as way as to replace the wild type allele with the mutant allele of interest. Colonies were screened for integrated mutants by sequencing the targeted *HTB* locus. Plasmids are described in table 4.2.

Plasmids:

HTA1-HTB1 was cloned into pRS313 and pRS316 using gap repair to generate pRZ001 and pRZ015, respectively. *HTA1-HTB1* was amplified from wild-type genomic DNA (JRY3009) using Phusion polymerase (NEB). The PCR fragment and EcoRI SalI digested pRS313 were co-transformed into JRY3009. Plasmids were rescued from *His*+ (pRS313) or *Ura*+ (pRS316) transformants and sequenced. The Htb1-specific residues on *HTB1* were sequentially mutated to the Htb2-specific residues (mutant referred to as *HTB2**) using site-directed mutagenesis (*26*) and Pfu Ultra polymerase (Stratagene) to generate pRZ018 (pRS313) and pRZ027 (pRS316). *htb1 K3A, K37A*, and *R102A* point mutants were also generated using site-directed mutagenesis on pRZ001 to generate pRZ040, pRZ002, and pRZ005, respectively. *HTA2-HTB2* was cloned into pRS313 using gap repair to generate pRZ008 as described above. The Htb2-specific residues on *HTB2* were sequentially mutated to the Htb1-specific residues (mutant referred to as *HTB1**) using site-directed mutagenesis to generate pRZ092.

*HTB1** and *HTB2** were each cloned into pRS406 to generate pRZ088 and pRZ062, respectively. *HTB1** and *HTB2** were PCR amplified with primers containing EcoRI and NotI overhangs from pRZ018 and pRZ092, respectively, using Phusion polymerase (NEB). The PCR fragments and pRS406 were each double digested with EcoRI and NotI and gel purified. Digested *HTB1** and *HTB2** were each ligated into digested pRS406 plasmid using a Rapid DNA Ligation kit (Roche). Plasmids were verified by sequencing.

Culture:

To screen *htb1K3A, K37A,* and *R102A* mutants for chemical sensitivity phenotypes, five- or ten-fold serial dilutions of saturated overnight cultures were spotted onto selective media as previously described (*27-29*). All selective media lacked histidine (-HIS) to maintain selection of *HTA1-HTB1* plasmids.

Purification of H2A-H2B and H2A.Z-H2B dimers from *S. cerevisiae* for acetic acid-urea gels.

HTB1-3xFLAG, HTB2-3xFLAG, or *HTZ1-3xFLAG* was purified from *S. cerevisiae* as previously described (*27*). Briefly, 100 OD_{600} units of mid-log phase cells were harvested by centrifugation and resuspended in Buffer HIP (150 mM Tris-HCl at pH 7.8, 200 mM NaCl, 1.5 mM MgAc, 10 mM NaPPi, 0.1 mM Na_3VO_4, 5 mM NaF, Complete Protease inhibitor cocktail (Roche)). Cells were lysed with acid-washed glass beads and fast-prep shaking. Chromatin was digested with 10 U micrococcal nuclease (Sigma) in 1

mM $CaCl_2$ for 10 min at 37 ºC. Insoluble material was pelleted by centrifugation. The supernatant was incubated with 25 µl slurry of anti-FLAG M2 agarose (Sigma) for 1.5 hrs at 4 ºC. Beads were washed three times with 0.6 ml of HIP buffer. After the final wash, buffer was completely removed with a 30-gauge needle and the beads were resuspended in AU gel-loading buffer (6 M urea, 5% acetic acid, 0.02% Pyronin Y). Samples were resolved on an acetic acid urea (AU) gel as previously described (*27*). Immunoblotting was performed using standard procedures and evaluated with a Li-COR Odyssey imaging system. Anti-Flag M2 antibody (Sigma) was used to detect Htb1-FLAG, Htb2-FLAG or H2A.Z-FLAG.

Chromatin association assays

Chromatin association assays were carried out exactly as described (*27*). The soluble fractions and MNase-digested fractions were either loaded directly on SDS-PAGE gels or affinity-purified using anti-Flag M2 resin (Sigma) and resolved on an AU gel as described above.

Purification of H2A-H2B and H2A.Z-H2B dimers from *S. cerevisiae* for Mass Spectrometry

12 L of *S. cerevisiae* containing *HTA1-3xFLAG* or *HTZ1-3xFLAG* was grown to mid-log phase (OD_{600} ~ 1.0). The cells were pelleted and frozen in liquid nitrogen. Pellets were lysed, as previously described, in coffee grinders with dry ice (*30*). The lysate was resuspended in 0.8 volumes of Buffer A (50 mM Tris-Cl at pH 7.8, 150 mM NaCl, 1.5 mM MgAc, 100 mM Na butyrate, 0.5 mM nicotinamide, 10 mM NaPPi, 5 mM EGTA, 5 mM EDTA, 0.1 mM Na_3VO_4, 5 mM NaF, Complete Protease inhibitor cocktail (Roche). Chromatin was digested with DNase I (Sigma) at 0.2 mg/ml for 10 minutes on ice. Insoluble material was removed by centrifugation at 25,000 x g for 20 minutes at 4 ^oC. Supernatant was the whole cell extract. Whole cell extract was incubated with 250 µl of αFLAG M2 affinity resin (Sigma) for 1.5 hours at 4^oC. The resin was washed once in Buffer A, and transferred to a 500 µl gravity column. The resin was washed on the column with 20 column volumes of Buffer A, followed by 20 column volumes of Buffer A + 300 mM NaCl (to dissociate the nucleosomes). H2A-H2B or H2A.Z-H2B dimers were eluted in four 250 µl fractions of 100 mM glycine, pH 2.5. Following elution, the fractions were neutralized with 25 µl of 500 mM Tris-Cl pH 7.5, 1.5 M NaCl. A small portion of each fraction was analyzed on an SDS-PAGE gel and stained with Coomassie Brilliant Blue. Peak fractions containing H2A-H2B or H2A.Z-H2B dimers were pooled and concentrated to ~ 20 µl. Purified samples were analyzed by LC-MS as described (*31*) or resolved on an AU gel as described above. The gel was stained with Coomassie Brilliant Blue and H2B bands were cut out and analyzed by LC-MS/MS as described (*31*). Additional LC-MS/MS replicates of H2B were performed as described above but purified dimers were resolved on an SDS-PAGE gel, rather than an AU gel to increase the concentration of the sample. All mass spectrometry experiments and data analysis were performed by Xiaodan Su, Bei Zhao, and Michael Freitas at the Ohio State University.

Purifying bulk histones from *S. cerevisiae* for mass spectrometry

Bulk histones were purified from *S. cerevisiae* as described (*32*). Briefly, 200 OD_{600} units of cells were pelleted and washed in 30 ml cold sterile water. All centrifugation was performed for 10 minutes at 6,500 RPM with an SS-34 rotor at 4 ^{o}C unless otherwise indicated. Cells were pelleted and resuspended in 5 ml Buffer A (50 mM Tris-HCl pH 7.5, 30 mM DTT). Resuspended cells were incubated at 30 ^{o}C for 15 minutes with gentle shaking and spun as above. Pelleted cells were resuspended in 10 ml Buffer S (20 mM HEPES pH 7.4, 1.2 M sorbitol) and spun. Pellet was weighed and resuspended in 5 ml Buffer S with 2 mg Zymolyase 100T (Seikagaku America Inc.) per gram of yeast cells and incubated at 30 ^{o}C for 60 minutes with gentle shaking. 10 ml ice cold Buffer B (20 mM PIPES pH 6.8, 1.2 M sorbitol, 1 mM $MgCl_2$) was added and cells were spun. Three successive times, the pellet was resuspended in 5 ml ice cold Buffer NIB (15 mM MES pH 6.6, 0.25 M sucrose, 60 mM KCl, 15 mM NaCl, 5 mM $MgCl_2$, 1 mM $CaCl_2$, 0.8% Triton X-100, 1 mM PMSF, 1 mM NaF), incubated on ice for 20 minutes and spun. Three successive times, the pellet was resuspended in 5 ml Wash Buffer A (10 mM Tris-HCl pH 8.0, 0.5% NP-40, 75 mM NaCl, 30 mM Na butyrate, 1 mM PMSF, 1 mM NaF), incubated on ice for 15 minutes and spun. Two successive times, the pellet was resuspended in 5 ml Wash Buffer B (10 mM Tris-HCl pH 8.0, 0.4 M NaCl, 30 mM Na butyrate, 1 mM PMSF, 1 mM NaF), incubated on ice for 5 minutes, and spun. Histones were extracted by resuspending the pellet in 1 ml 0.4 N H_2SO_4 and incubating on ice for 1 hour with occasional vortexing. Extracts were spun at 10,000 RPM for 10 minutes in a tabletop centrofuge at 4 ^{o}C. The supernatant was transferred to a new tube and trichloroacetic acid (TCA) was added to a final concentration of 20%. The sample was incubated on ice overnight. Histones were pelleted at 12,000 RPM for 30 minutes at 4 ^{o}C. The pellet was washed in 500 µl of acidified acetone (0.1% HCl in acetone) and spun for 5 minutes at 12,000 RPM. The pellet was washed in 100% acetone (no HCl) and spun as before. Acetone was poured off and the pellet was air-dried at 4 ^{o}C. Isolated histones were stored at -20 ^{o}C. The bulk histone analysis by LC-MS was performed by the Freitas lab as described (*31*).

Protein analysis

Yeast whole-cell extracts were precipitated using 20% TCA and solubilized in SDS loading buffer. SDS-PAGE and immunoblotting were performed using standard procedures and evaluated with a Li-COR imaging system. Anti-H2B (Ab1790) was used to monitor total H2B expression. Anti-actin (a gift from the G. Barnes lab) was used as a loading control.

Competitive growth experiments

Growth conditions:

50 ml of non-selective YPD medium was inoculated to 0.01 OD_{600} with equal amounts of *htb1*- and *htb2*- (non-integrated) strains. Cultures were shaken at 180 RPM for 24 hours at 30 ^{o}C. After 24 hours a portion of the culture was removed for restriction fragment length polymorphism (RFLP) analysis and/or auxotrophic selection. The culture was diluted to OD_{600} 0.01 in 50 ml fresh YPD media. Cells were grown as before and the analysis was repeated every 24 hours for 10 days or as indicated.

Auxotrophic selection:
Every 24 hours, 300 µl of 10^{-4} and 5 x 10^{-5} dilutions of the saturated culture were plated on YPD, CSM-HIS and CSM-URA media. Colonies were counted manually after 3 days of growth at 30 ^{o}C. Percent abundance for each strain was calculated as # of colonies on selective media / # of colonies on YPD.

RFLP analysis:
Every 24 hours, total gDNA was extracted from 1 ml of the saturated culture using a standard phenol extraction protocol (*33*). The *HTB* gene was PCR-amplified with Expand Long Template polymerase (Roche) using primers that target sequence common to both *HTB1* and *HTB2**. Samples were purified using a PCR purification spin kit (Qiagen). 2 µg of purified PCR product was digested with PstI (NEB) for 2 hours at 37 ^{o}C. Digests were heat inactivated at 80 ^{o}C for 20 minutes and resolved on a 1.5% agarose gel. Gels were stained with EtBr and imaged with a Gel Doc XR system (Bio-Rad). Bands were quantified using ImageJ software.

Chemical genomic profiling:
Strains were grown in parallel in a 96-well Genios Plate-reader (Tecan) in liquid media containing the indicated drugs. Growth experiments and data analysis were performed by Marinella Gebbia and Guri Giaever at the University of Toronto as previously described (*34*). Percent fitness was calculated based on the doubling time of the mutant strain compared to a wild type strain grown in liquid media +/- the drug of interest. Chemicals were obtained from the following sources: NSC 693632 and NSC 604586 (Developmental Therapeutics Program NCI/NIH, the challenge set), distamycin a and streptovitacin (Developmental Therapeutics Program NCI/NIH, the natural products set), cloxiquin, acriflavinium hydrochloride, and sanguinarine sulfate (Microsource Inc., the spectrum collection), and FK506 (LC Laboratories).

Halo Assay
Approximately 10^{6} cells from a saturated overnight culture were plated onto YPD medium. Plates were dried for 5 minutes. 10 µl of a 10 mM solution of the indicated drug in DMSO was spotted onto the middle of the plate and dried for an additional 5 minutes. Plates were grown for 2 days at 30 ^{o}C. Halo size was measured by taking pictures of the plates with a Canon Powershot camera. Halo images were analyzed manually in Keynote.

4.3 Results

H2B isotype-specific modifications and histone variant associations

To examine the relationship between H2A.Z and each H2B isotype, we tested whether H2A.Z preferentially associated with either Htb1 or Htb2 in H2A.Z-H2B dimers. H2A.Z-H2B dimers were purified from *S. cerevisiae,* and the Freitas lab performed LC-MS (Liquid Chromatography followed by Mass Spectrometry) to determine the ratio of Htb1 to Htb2. A previous Rine lab member, in collaboration with the Freitas lab,

reported a ten-fold increase in Htb2 over Htb1 in H2A.Z-H2B dimers (figure 4.2a). However, in a second biological replicate, I observed only a two-fold increase in Htb2 over Htb1 (figure 4.2b). Although we found equal amounts of Htb1 and Htb2 in canonical H2A-H2B dimers (figure 4.2c), LC-MS of total cellular histones showed a 1:2 ratio of Htb1 to Htb2 (figure 4.3c). This suggests that the 1:2 ratio observed in H2A.Z-H2B dimers may not represent an enrichment of Htb2. However, it is difficult to reconcile why the ratio of Htb1 to Htb2 in canonical H2A-H2B dimers was different than the ratio observed in bulk histones. Because the experiments described above were each only performed once, additional replicates will be required to make strong conclusions about the H2B isotype ratios. Due to the inconsistency between the LC-MS analysis of two H2A.Z-H2B biological replicates, and the discrepancy between the LC-MS analysis of H2A-H2B dimers and bulk histones, we performed additional analyses (described below) to test whether there is functional linkage between H2A.Z and Htb2.

To analyze the relationship between H2A.Z and Htb2, we monitored expression, chromatin incorporation, and modification profile of H2A.Z in *htb2*- strains and of Htb2 in *htz1Δ* strains. Chromatin-association assays revealed that neither expression, nor chromatin incorporation of H2A.Z was dependent upon Htb2 and vice versa (figure 4.3a,b). LC-MS of bulk histones showed that the cellular ratio of Htb1 to Htb2 was not H2A.Z-dependent (figure 4.3c).

Next, we examined whether the modification profile of H2A.Z was H2B isotype-dependent and whether the modification profiles of the Htb1 and Htb2 were H2A.Z-dependent. First, we purified H2A-H2B and H2A.Z-H2B dimers and analyzed the banding pattern of each sample on an acetic acid-urea (AU) gel (figure 4.4a). AU gels separate differentially modified histones based on both size and charge (*35*). Lysine acetylation neutralizes a positive charge and results in slower migration through an AU gel. Each unique band represents a single additional acetyl group present on the protein. Phosphorylation and ubiquitination also affect protein migration through an AU gel but methylation, which does not significantly alter protein size or charge, does not. The H2B (Htb1 and Htb2) associated with H2A or H2A.Z produced identical AU banding patterns (figure 4.4a). Further, the H2B bands from each gel were extracted and analyzed by LC-MS/MS (tandem mass spectrometry), and we were unable to identify any H2B modifications that were unique to H2A.Z-H2B dimers (data not shown). The AU banding patterns of purified H2B and H2A.Z from *htz1Δ* and *htb1*- or *htb2*- strains, respectively, suggest that there is no relationship between H2A.Z and H2B modifications (figure 4.4b).

Although we did not identify any H2B modifications that were H2A.Z-dependent, we did observe an H2A.Z-independent difference in the AU banding patterns of the two H2B isotypes, suggesting that they may be differentially modified (figure 4.4b). Surprisingly, Htb2 contained a significantly smaller fraction of unmodified protein (the fastest migrating band) compared to Htb1. This difference was observed in both the free histone pool and in chromatin (figure 4.4c). The requirement for more unmodified Htb1 may reflect a functional difference between the two H2B isotypes. Additionally, we identified three new H2B modifications: H2B-K3ac, -K37me$_{2,3}$, and -R102me$_2$ (figure

4.5a-c). Since Htb2 contains a K3A substitution, H2B-K3ac represents a novel Htb1-specific modification (figure 4.5b). H2B-K37me$_{2,3}$ was observed on both Htb1 and Htb2 peptides. Peptides containing H2B-R102me$_2$ did not include isotype-specific residues and hence we cannot exclude the possibility that this modification is isotype specific. H2B-K37 and -R102 are conserved through humans, suggesting that these modifications may exist in other eukaryotes (figure 4.5d). The X ray crystal structure of the *S. cerevisiae* nucleosome reveals that H2B-K37 is located within the two gyres of DNA and R102 is at the H2B-H4 interface (figure 4.5e) (*36*). These positions suggest that H2B-K37me$_{2,3}$, and -R102me$_2$ may influence nucleosome stability. Alanine point mutations at each of the modified sites failed to yield any chemical sensitivities, suggesting that these modifications are not necessary for the majority of chromatin-associated processes. It was possible that the modifications may have more subtle functional roles (figure 4.6a,b), which motivated the experiments in the next section.

The unique cellular functions of Htb1 and Htb2

To explore the functional differences between the two H2B isotypes, we generated two strains that expressed either Htb1 or Htb2 protein as the only source of H2B. The strains were constructed by knocking-out both endogenous copies of H2A-H2B (*HTA1-HTB1* and *HTA2-HTB2*) and expressing either wild type *HTA1-HTB1* on a plasmid or a version of *HTA1-HTB1* where the Htb1-specific residues were mutated to the Htb2-specific residues (mutant *HTB1* gene is referred to as *HTB2**). I will refer to these strains as *htb2-* and *htb1-*, respectively. Both isotypes were expressed off the *HTA1-HTB1* promoter to control for any differences that might arise due to changes in expression (figure 4.7a) (*13*). To determine whether the absence of either subtype affects cellular fitness, we performed competitive growth experiments (figure 4.7b). Briefly, we inoculated non-selective liquid media with equal amounts of each *htb1-* and *htb2-* strain. After 24 hours of growth, we diluted the culture into fresh media and allowed it to grow for an additional 24 hours. We continued to grow and dilute the culture for 10 days. At the end of each 24-hour growth period, the ratio of each strain within the culture was determined by exploiting both the unique auxotrophic markers within each strain and an RFLP site within the *HTB* gene.

Preliminary results suggested that *htb2-* strains were at a fitness disadvantage compared to *htb1-* strains (figure 4.8). In 4 out of 5 biological replicates, *htb1-* strains out-competed *htb2-* strains in ~7 days (figure 4.8b,c). However, in these experiments the *htb1-* and *htb2-* strains contained distinct *HIS3* and *URA3* markers, respectively (figure 4.8a). Competitive growth experiments with *htb1-* and *htb2-* strains where the auxotrophic markers were reversed did not reveal a similar *htb1-* fitness advantage (figure 4.9a). These results suggest that the original competitive growth experiment was confounded by either an increase in fitness associated with *HIS3* or a decrease in fitness associated with *URA3*. To control for these artifacts, we performed competitive growth experiments with *htb1-* and *htb2-* strains containing identical auxotrophic markers and monitored the ratio of each strain within the culture using only the RFLP analysis (figure 4.9b). Unfortunately, the results were inconsistent. Strains with either *HTA1-HTB1* or *HTA1-HTB2** expressed off the pRS313 (*HIS3*) plasmid did not produce

a clear winner, even after 20 days of competitive growth (figure 4.9b top panel). Strains with either *HTA1-HTB1* or *HTA1-HTB2** expressed off the pRS316 (*URA3*) plasmid showed an *htb1-* strain victory in two out of three biological replicates (figure 4.9b bottom panel). Because these experiments were inconsistent and time consuming, we pursued chemicals that would sensitize the competition experiment and potentially reveal unique functions of the two H2B isotypes.

Just as genome-wide synthetic lethality has been instrumental in uncovering genetic interactions, the Giaever lab at the University of Toronto pioneered the use of chemical genomic profiling with the yeast knockout collection to reveal many important drug sensitivities for mutants lacking a phenotype under standard growth conditions (*20*). Their study identified many compounds to which diploids hemizygous for *HTB1* or *HTB2* had increased sensitivity upon exposure in growth media. Our analysis of these data identified 40 compounds with a significant difference in sensitivity between *htb1Δ* /*HTB1* and *htb2Δ* /*HTB2* heterozygotes, with p-values ranging from 0.01 to 10^{-10} (figure 4.10). Of particular interest to us was compound NSC 693632. Of the ~1000 chemicals tested, *htb1Δ* /*HTB1* diploid cells, which rely more on their two copies of the *HTB2* encoded-isotype, were most sensitive to compound NSC 693632. This compound is a potential inhibitor of S-adenosyl-methionine biosynthesis, which is the methyl-donor for histone methylation. NSC 693632 was also among the 10 most effective at reducing fitness of diploid cells individually hemizygous for *HTZ1*, *SET3,* or *SET4* (encoding two histone methyltransferases), or *SAM4* (encoding an enzyme involved in S-adenosyl-methionine biosynthesis). These data imply the possibility of a methyl modification that is specific to an H2B isotype and/or H2A.Z.

To identify chemicals that relate to functional differences between the two H2B protein isotypes rather than expression differences due to the hemizygous mutations, the Giaever lab rescreened the top hit chemicals using integrated strains that we constructed to express only Htb1 or Htb2 (figure 4.11a). These strains eliminate inconsistencies due to plasmid-based expression. Our integrated strains and the original *htb1Δ* /*HTB1* and *htb2Δ* /*HTB2* heterozygous diploid cells were grown in a plate reader assay to determine the cellular fitness (table 4.3 and table 4.4) (*34*). Surprisingly, for all chemicals tested, the sensitivities of the integrated *htb1-* and *htb2-* strains were approximately equal to wild type as monitored by growth in liquid culture (table 4.3) or a halo assay (figure 4.11b). Therefore, the phenotypes of the hemizygous strains published in their chemical-genomic screen were likely due to changes in *HTB* expression rather than protein function.

4.4 Discussion

Although our results showed a preference for the Htb2 isotype in H2A.Z-H2B dimers, it does not represent an enrichment based on the absolute levels of Htb1 and Htb2 in chromatin (figure 4.2a,b and 4.3c). Consistent with this interpretation, we were unable to define a functional relationship between H2A.Z and Htb2. H2A.Z expression, chromatin incorporation, and modification status was Htb2-independent, and likewise, Htb2 expression, chromatin incorporation, and modification status was H2A.Z-

independent (figures 4.3 and 4.4). Therefore, if H2A.Z does preferentially associate with Htb2, the functional significance must be subtle. For example, the Htb2 isotype might act with H2A.Z at silent chromatin boundaries. This hypothesis predicts that Htb2 would be preferentially enriched with H2A.Z at boundary regions and that *htb2*- strains would have defects in boundary maintenance. Alternatively, Htb2 might preferentially associate with H2A.Z in the nucleosomes that flank the transcription start site of active genes and facilitate transcription initiation. Our inability to connect Htb2 to H2A.Z function suggests that the two fold enrichment of Htb2 observed in H2A.Z-H2B dimers was likely a reflection of the two-fold increase in Htb2 expression compared to Htb1 (figure 4.3c).

We discovered three new H2B modifications: K3ac, K37me$_{2,3}$, and R102me$_2$ (figure 4.5) all of which were H2A.Z-independent. Acetylation on histone tails, like K3ac, can direct transcriptional programs. For example, within the H4 tail, acetylation on K5, 8, and 12 have non-specific cumulative affects on transcription whereas K16ac dictates a unique transcriptional program (*37*). Therefore, Htb1-K3ac may act cumulatively with other acetyl groups on the H2B tail to promote active transcription. Alternatively, because Htb1-K3ac represents an isotype-specific modification, it may confer a unique transcription response. Although mutating H2B-K3, -K37, and -R102 to alanine did not affect cellular fitness under the conditions we tested (figure 4.6), it is likely that future studies will discover environmental or genetic backgrounds where the modifications exert a fitness effect. H2B-K37me$_{2,3}$ was observed on H2B peptides in multiple biological replicates, however H2B-K3ac and -R102me$_2$ were each only observed in one replicate. Therefore, these modifications may be in low abundance or a mis-assigment of the mass spectra. Defining the roles of these modifications will likely require a more global analysis of these alanine point mutant strains, such as transcription profiling and E-MAPs (epistatic miniarray profile).

Surprisingly, the single striking difference between Htb1 and Htb2 was the significantly smaller fraction of unmodified Htb2 protein compared to Htb1 (figure 4.4b,c). Although in principle, this difference could result from increased Htb2 incorporation into chromatin, where it then becomes modified, chromatin association assays suggested that this was not the case (figure 4.3b and 4.4c). Acetylation neutralizes lysine's positive charge and therefore has the potential to reduce histone-DNA contacts and generate a more open chromatin conformation (*38*). Therefore, Htb2 might be preferentially enriched at actively transcribed regions that undergo increased nuclesome turnover. This enrichment would be consistent with the preferential association of Htb2 with H2A.Z. Additionally, this difference in acetylation levels may influence histone chaperone recognition in an isotype-specific manner. Alternatively, the two-fold increase in *HTB2* expression compared to *HTB1* may account for the unique modification profiles (figure 4.3c). A promoter-swap experiment would determine whether the isotype-specific acetylation pattern resulted from changes in H2B expression or protein sequence.

Using competitive growth experiments, we established under several growth conditions that strains that expressed only the Htb1 or Htb2 isotype were, to a first

approximation, equally fit. The ability of strains with either isotype to win a competitive growth experiment was likely due to a chance mutation in one strain or the other that enhanced its fitness under the experimental conditions independent of the H2B isotype. Although chemicals were indentified that produced fitness differences between *htb1Δ/HTB1* and *htb2Δ/HTB2* heterozygotes (figure 4.10), these sensitivities were likely due to differences in isotype expression rather than protein function (table 4.4 and figure 4.11b). E-MAPs or transcriptional profiling using integrated strains that express only Htb1 or Htb2 could be leveraged to identify unique H2B isotype-specific functions (figure 4.10b). Changes in gene expression may reflect differential localization of the Htb1 and Htb2 isotypes in chromatin. Because differentially tagging each H2B isotype within the same stain affects *HTB* expression and cellular fitness (data not shown), chromatin immunoprecipiation (ChIP) experiments will compare strains with either Htb1 or Htb2 tagged, using the same epitope, in parallel cultures.

Although evolution has preserved the sequence changes between Htb1 and Htb2, it is unclear whether these changes have functional impacts in common laboratory contexts. Although we were not able to identify a relationship between H2A.Z and Htb1 or Htb2, we expect that the interplay between histone isotypes, variants, and modifications has the potential to provide an additional layer of transcriptional control. Mass spectrometry analyses coupled with chemical-genomic profiling represents a promising strategy for discovering these relationships and defining their functional impact.

4.5 Tables

Table 4.1. Yeast strains used in chapter 4.

Strain	Parent	Genotype	Source
JRY3009	W303	*MATα ade2-1 his3-11 leu2-3,112 trp1-1 ura3-52 can1-100*	R. Rothstein
JRY7971	W303	*MATa HTZ1-3xFLAG::KanMX*	J. Babiarz
JBY037	W303	*MATa HTA1-3xFLAG::KanMX*	J. Babiarz
JRY7972	W303	*MATα HTZ1-3xFLAG::KanMX*	J. Babiarz
RZY088	W303	*MATα (hta1-htb1)Δ::LEU2MX (hta2-htb2)Δ::TRP1MX HTZ1-3xFLAG::KanMX [pRZ001 HIS3 HTA1-HTB1]*	This study
RZY090	W303	*MATα (hta1-htb1)Δ::LEU2MX (hta2-htb2)Δ::TRP1MX HTZ1-3xFLAG::KanMX [pRZ018 HIS3 HTA1-HTB2*]*	This study
RZY101	W303	*MATa HTB1-3xFLAG::KanMX*	This study
JBY039	W303	*MATa HTB2-3xFLAG::KanMX*	J. Babiarz
RZY108	W303	*MATa HTB1-3xFLAG::KanMX htz1Δ::HIS3MX*	This study
RZY110	W303	*MATa HTB2-3xFLAG::KanMX htz1Δ::HIS3MX*	This study
JRY7754	W303	*MATα htz1Δ::HIS3MX*	M. Kobor
RZY014	W303	*MATα (hta1-htb1)Δ::LEU2MX (hta2-htb2)Δ::TRP1MX [pRZ001 HIS3 HTA1-HTB1]*	This study
RZY015	W303	*MATα (hta1-htb1)Δ::LEU2MX (hta2-htb2)Δ::TRP1MX htz1Δ::HIS3MX [pRZ001 HIS3 HTA1-HTB1]*	This study
RZY069	W303	*MATα (hta1-htb1)Δ::LEU2MX (hta2-htb2)Δ::TRP1MX [pRZ002 HIS3 HTA1-htb1K37A]*	This study
RZY026	W303	*MATα (hta1-htb1)Δ::LEU2MX (hta2-htb2)Δ::TRP1MX [pRZ040 HIS3 HTA1-htb1K3A]*	This study
RZY030	W303	*MATα (hta1-htb1)Δ::LEU2MX (hta2-htb2)Δ::TRP1MX [pRZ005 HIS3 HTA1-htb1R102A]*	This study
RZY041	W303	*MATa (hta1-htb1)Δ::LEU2MX (hta2-htb2)Δ::TRP1MX [pRZ015 URA3 HTA1-HTB1]*	This study
RZY078	W303	*MATa (hta1-htb1)Δ::LEU2MX (hta2-htb2)Δ::TRP1MX [pRZ018 HIS3 HTA1-HTB2*]*	This study
RZY093	W303	*MATa (hta1-htb1)Δ::LEU2MX (hta2-htb2)Δ::TRP1MX [pRZ001 HIS3 HTA1-HTB1]*	This study
RZY084	W303	*MATa (hta1-htb1)Δ::LEU2MX (hta2-htb2)Δ::TRP1MX [pRZ027 URA3 HTA1-HTB2*]*	This study
BY4743	S288c	*MATa/α his3Δ1/his3Δ1 leu2Δ0 /leu2Δ0 lys2Δ0/LYS2 MET15/met15Δ0 ura3Δ0 /ura3Δ0*	R. Rothstein
23583	S288c	*MATa/α htb1Δ::KanMX4/HTB1*	Knock-out collection
23026	S288c	*MATa/α htb2Δ::KanMX4/HTB2*	Knock-out collection
RZY344	W303	*MATα htb2::HTB1* (htb2- integrated strain isolate 1)*	This study
RZY346	W303	*MATα htb2::HTB1* (htb2- integrated strain isolate 2)*	This study
RZY186	W303	*MATα htb1::HTB2* (htb1- integrated strain isolate 1)*	This study
RZY619	W303	*MATα htb1::HTB2* (htb1- integrated strain isolate 2)*	This study

Table 4.2. Plasmids used in chapter 4.

Plasmid	Backbone	Yeast Selection	Bacterial Resistance	Insert	Source
pRZ001	pRS313	*HIS3*	*AMP*	*HTA1-HTB1*	This study
pRZ002	pRS313	*HIS3*	*AMP*	*HTA1-htb1K37A*	This study
pRZ040	pRS313	*HIS3*	*AMP*	*HTA1-htb1K3A*	This study
pRZ005	pRS313	*HIS3*	*AMP*	*HTA1-htb1R102A*	This study
pRZ015	pRS316	*URA3*	*AMP*	*HTA1-HTB1*	This study
pRZ018	pRS313	*HIS3*	*AMP*	*HTA1-HTB2* (htb1A2S, K3A, T27V, A35*	This study
pRZ027	pRS316	*URA3*	*AMP*	*HTA1-HTB2* (htb1A2S, K3A, T27V, A35*	This study
pRZ008	pRS313	*HIS3*	*AMP*	*HTA2-HTB2*	This study
pRZ092	pRS313	*HIS3*	*AMP*	*HTA2-HTB1* (htb2S2A A3K V27T V35A)*	This study
pRZ062	pRS406	*URA3*	*AMP*	*HTB2* (htb1A2S, K3A, T27V, A35V)*	This study
pRZ088	pRS406	*URA3*	*AMP*	*HTB1* (htb2S2A A3K V27T V35A)*	This study

Table 4.3. Re-screening the top hit chemicals from Hillenmeyer *et al*. 2008 in *htb1Δ/HTB1* and *htb2Δ/HTB2* heterozygotes.

Plate reader growth assays were performed with liquid cultures containing the indicated titrated chemicals and strains (growth assay and analysis were performed by the Giaever lab as described in materials and methods). Percent fitness values for each strain were based on the doubling time in media +/- the indicated chemical for one biological replicate. Percent fitness for each mutant strain was normalized to wild type. NSC 693632, cloxiquin, acriflavinium hydrochloride, sanguinarine sulfate, and FK506 were among the top hits for *htb1Δ/HTB1* heterozygotes in the original screen. Distamycin A, streptovitacin, phloretin, and NSC 604586 were among the top hits for *htb2Δ/HTB2* heterozygotes.

Drug	Conc. (uM)	Strain	% Fitness
NSC 693632	50	Wild Type Diploid	1.00
		htb1Δ/HTB1	0.53
		htb2Δ/HTB2	0.84
Cloxiquin	15.6	Wild Type Diploid	1.00
		htb1Δ/HTB1	0.88
		htb2Δ/HTB2	0.90
Acriflavinium hydrochloride	100	Wild Type Diploid	1.00
		htb1Δ/HTB1	0.99
		htb2Δ/HTB2	1.07
Sanguinarine sulfate	25	Wild Type Diploid	1.00
		htb1Δ/HTB1	0.95
		htb2Δ/HTB2	0.81
FK506	100	Wild Type Diploid	1.00
		htb1Δ/HTB1	1.02
		htb2Δ/HTB2	1.13
Distamycin	100	Wild Type Diploid	1.00
		htb1Δ/HTB1	0.98
		htb2Δ/HTB2	0.88
Streptovitacin	50	Wild Type Diploid	1.00
		htb1Δ/HTB1	0.68
		htb2Δ/HTB2	0.35
Phloretin	1000	Wild Type Diploid	1.00
		htb1Δ/HTB1	1.11
		htb2Δ/HTB2	0.98
NSC 604586	100	Wild Type Diploid	1.00
		htb1Δ/HTB1	3.69
		htb2Δ/HTB2	7.23

Table 4.4. Re-screening the top hit chemicals from Hillenmeyer *et al*. 2008 in *htb1-* and *htb2-* integrated mutant strains.
Plate reader growth assays were performed and percent fitness was calculated as in table 4.3. Two biological replicates were performed for each mutant background (indicated as (1) or (2)).

Drug	Conc. (uM)	Strain	% Fitness
NSC 693632		Wild Type	1.00
		htb1- (1)	0.96
		htb1- (2)	1.02
		htb2- (1)	1.01
	5	htb2- (2)	1.01
		Wild Type	1.00
		htb1- (1)	0.96
		htb1- (2)	1.02
		htb2- (1)	1.01
	10	htb2- (2)	1.01
		Wild Type	1.00
		htb1- (1)	1.00
		htb1- (2)	1.01
		htb2- (1)	1.03
	20	htb2- (2)	0.96
		Wild Type	1.00
		htb1- (1)	1.05
		htb1- (2)	1.02
		htb2- (1)	1.02
	30	htb2- (2)	1.02
		Wild Type	1.00
		htb1- (1)	1.05
		htb1- (2)	1.04
		htb2- (1)	1.12
	40	htb2- (2)	1.01
		Wild Type	1.00
		htb1- (1)	1.29
		htb1- (2)	1.29
		htb2- (1)	1.37
	50	htb2- (2)	0.87

Drug	Conc. (uM)	Strain	% Fitness
Cloxiquin		Wild Type	1.00
		htb1- (1)	0.99
		htb1- (2)	1.02
		htb2- (1)	1.03
	5	htb2- (2)	1.00
		Wild Type	1.00
		htb1- (1)	0.99
		htb1- (2)	1.00
		htb2- (1)	1.04
	10	htb2- (2)	1.00
		Wild Type	1.00
		htb1- (1)	1.06
		htb1- (2)	1.07
		htb2- (1)	1.02
	15	htb2- (2)	0.94
		Wild Type	1.00
		htb1- (1)	1.12
		htb1- (2)	0.87
		htb2- (1)	2.68
	20	htb2- (2)	1.06
		Wild Type	1.00
		htb1- (1)	0.96
		htb1- (2)	1.23
		htb2- (1)	0.93
	25	htb2- (2)	0.99
		Wild Type	1.00
		htb1- (1)	1.03
		htb1- (2)	1.21
		htb2- (1)	1.10
	30	htb2- (2)	1.09

Table 4.3. (cont.).

Drug	Conc. (uM)	Strain	% Fitness
Acriflavinium Hydrochloride		Wild Type	1.00
		htb1- (1)	0.96
		htb1- (2)	0.99
		htb2- (1)	0.96
	50	htb2- (2)	1.02
		Wild Type	1.00
		htb1- (1)	0.98
		htb1- (2)	0.95
		htb2- (1)	0.98
	100	htb2- (2)	0.99
		Wild Type	1.00
		htb1- (1)	1.00
		htb1- (2)	0.89
		htb2- (1)	0.88
	150	htb2- (2)	0.97
		Wild Type	1.00
		htb1- (1)	1.17
		htb1- (2)	1.02
		htb2- (1)	0.83
	200	htb2- (2)	0.95
		Wild Type	1.00
		htb1- (1)	0.91
		htb1- (2)	1.16
		htb2- (1)	0.90
	250	htb2- (2)	1.03
Sanguinarine Sulfate		Wild Type	1.00
		htb1- (1)	0.82
		htb1- (2)	1.01
		htb2- (1)	0.82
	5	htb2- (2)	1.00
		Wild Type	1.00
		htb1- (1)	1.01
		htb1- (2)	1.01
		htb2- (1)	0.99
	10	htb2- (2)	1.00
		Wild Type	1.00
		htb1- (1)	1.03
		htb1- (2)	0.97
	20	htb2- (1)	0.92
		htb2- (2)	0.96
		Wild Type	1.00
		htb1- (1)	1.07
		htb1- (2)	0.98
		htb2- (1)	0.70
	30	htb2- (2)	0.58

Drug	Conc. (uM)	Strain	% Fitness
FK506		Wild Type	1.00
		htb1- (1)	1.00
		htb1- (2)	1.00
		htb2- (1)	1.00
	5	htb2- (2)	0.96
		Wild Type	1.00
		htb1- (1)	1.00
		htb1- (2)	1.00
		htb2- (1)	0.98
	10	htb2- (2)	0.99
		Wild Type	1.00
		htb1- (1)	1.01
		htb1- (2)	0.99
		htb2- (1)	1.02
	20	htb2- (2)	1.01
		Wild Type	1.00
		htb1- (1)	1.00
		htb1- (2)	1.00
		htb2- (1)	0.99
	30	htb2- (2)	0.98
		Wild Type	1.00
		htb1- (1)	0.98
		htb1- (2)	1.05
		htb2- (1)	0.95
	40	htb2- (2)	1.01
		Wild Type	1.00
		htb1- (1)	1.08
		htb1- (2)	0.99
		htb2- (1)	0.98
	50	htb2- (2)	0.99

Table 4.3 (cont.)

Drug	Conc. (uM)	Strain	% Fitness
Distamycin A		Wild Type	1.00
		htb1- (1)	1.06
		htb1- (2)	1.05
		htb2- (1)	1.04
	50	htb2- (2)	1.04
		Wild Type	1.00
		htb1- (1)	0.98
		htb1- (2)	0.94
		htb2- (1)	0.97
	100	htb2- (2)	0.91
		Wild Type	1.00
		htb1- (1)	0.94
		htb1- (2)	0.94
		htb2- (1)	0.95
	150	htb2- (2)	0.95
		Wild Type	1.00
		htb1- (1)	0.99
		htb1- (2)	0.93
		htb2- (1)	0.92
	200	htb2- (2)	0.88
		Wild Type	1.00
		htb1- (1)	1.04
		htb1- (2)	1.04
		htb2- (1)	1.05
	250	htb2- (2)	1.04
		Wild Type	1.00
		htb1- (1)	0.88
		htb1- (2)	2.11
		htb2- (1)	0.83
	300	htb2- (2)	1.12
		Wild Type	1.00
		htb1- (1)	0.90
		htb1- (2)	0.99
		htb2- (1)	0.85
	400	htb2- (2)	1.10

Drug	Conc. (uM)	Strain	% Fitness
Streptovitacin		Wild Type	1.00
		htb1- (1)	0.94
		htb1- (2)	0.94
		htb2- (1)	0.97
	5	htb2- (2)	0.97
		Wild Type	1.00
		htb1- (1)	0.96
		htb1- (2)	0.96
		htb2- (1)	0.98
	10	htb2- (2)	0.97
		Wild Type	1.00
		htb1- (1)	0.94
		htb1- (2)	0.92
		htb2- (1)	0.98
	20	htb2- (2)	0.92
		Wild Type	1.00
		htb1- (1)	0.98
		htb1- (2)	0.96
		htb2- (1)	0.98
	30	htb2- (2)	0.96
		Wild Type	1.00
		htb1- (1)	0.97
		htb1- (2)	0.96
		htb2- (1)	1.00
	40	htb2- (2)	0.98
		Wild Type	1.00
		htb1- (1)	1.01
		htb1- (2)	0.98
		htb2- (1)	0.97
	50	htb2- (2)	0.93

Table 4.3. (cont.).

Drug	Conc. (uM)	Strain	% Fitness
Phloretin		Wild Type	1.00
		htb1- (1)	1.03
		htb1- (2)	1.01
		htb2- (1)	1.04
	0.5	htb2- (2)	0.97
		Wild Type	1.00
		htb1- (1)	1.01
		htb1- (2)	0.94
		htb2- (1)	0.98
	1	htb2- (2)	0.94
		Wild Type	1.00
		htb1- (1)	1.08
		htb1- (2)	0.97
		htb2- (1)	0.84
	1.5	htb2- (2)	0.79
		Wild Type	1.00
		htb1- (1)	1.08
		htb1- (2)	1.06
		htb2- (1)	1.07
	2	htb2- (2)	1.01
		Wild Type	1.00
		htb1- (1)	1.12
		htb1- (2)	1.11
		htb2- (1)	1.01
	2.5	htb2- (2)	1.41
		Wild Type	1.00
		htb1- (1)	1.12
		htb1- (2)	1.09
		htb2- (1)	1.97
	3	htb2- (2)	1.92
		Wild Type	1.00
		htb1- (1)	1.30
		htb1- (2)	1.57
		htb2- (1)	1.15
	4	htb2- (2)	1.16

Drug	Conc. (uM)	Strain	% Fitness
NSC 604586		Wild Type	1.00
		htb1- (1)	1.18
		htb1- (2)	1.11
		htb2- (1)	1.04
	50	htb2- (2)	1.05
		Wild Type	1.00
		htb1- (1)	1.07
		htb1- (2)	1.07
		htb2- (1)	1.00
	100	htb2- (2)	1.08
		Wild Type	1.00
		htb1- (1)	1.15
		htb1- (2)	1.03
		htb2- (1)	1.01
	150	htb2- (2)	0.97
		Wild Type	1.00
		htb1- (1)	1.13
		htb1- (2)	1.05
		htb2- (1)	0.98
	200	htb2- (2)	1.00
		Wild Type	1.00
		htb1- (1)	1.17
		htb1- (2)	1.05
		htb2- (1)	1.00
	250	htb2- (2)	1.02
		Wild Type	1.00
		htb1- (1)	1.15
		htb1- (2)	1.08
		htb2- (1)	1.00
	300	htb2- (2)	0.97
		Wild Type	1.00
		htb1- (1)	0.99
		htb1- (2)	0.95
		htb2- (1)	0.89
	400	htb2- (2)	0.88

4.6 Figures

Figure 4.1. The differences between Htb1 and Htb2 are conserved across the *Saccharomyces sensu stricto* clade.
(A) The *S. cerevisiae* canonical histone genes are expressed in gene pairs with divergent promoters. Htb1 is highlighted in blue and Htb2 is highlighted in yellow. (B) Htb1 and Htb2 differ at four amino acids. Shown is a pair-wise alignment of the Htb1 and Htb2 N-terminal tails. Arrows indicate divergent residues. (C) H2B A2S and K3A substitutions are conserved. Shown is a multiple sequence alignment of Htb1 and Htb2 from the *Saccharomyces sensu stricto* species. Arrows indicate divergent residues.

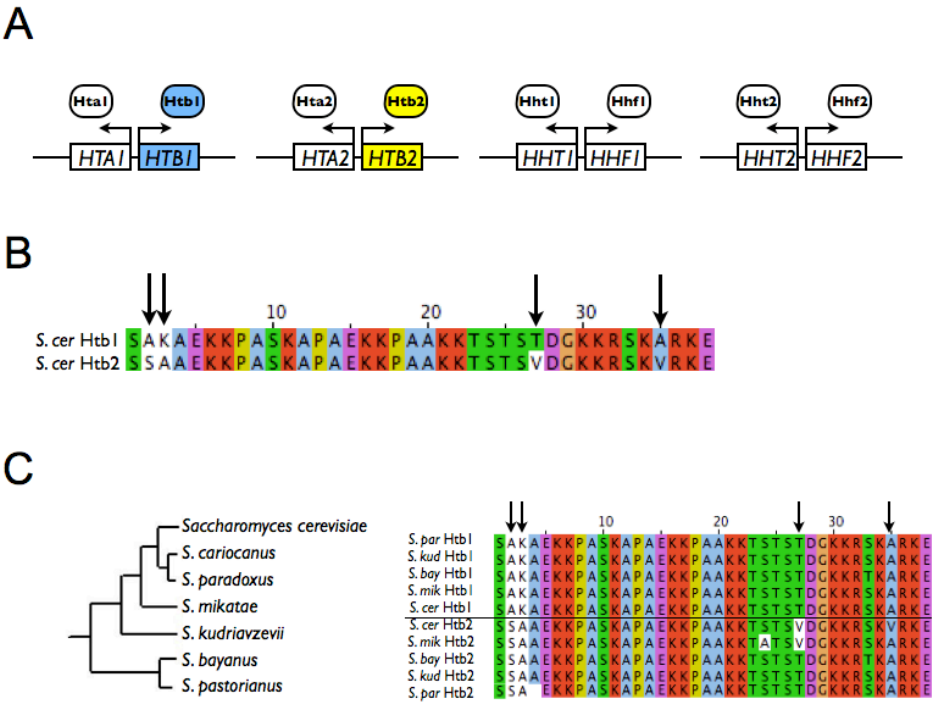

Figure 4.2. H2A.Z preferentially associated with the Htb2 isotype.
(A) A previous analysis showed a 10-fold preference for Htb2 in H2A.Z-H2B dimers. H2A.Z-H2B dimers were purified from *S. cerevisiae* and analyzed by LC-MS. Shown is the chromatogram and peak identities. (B) Current experiments found a smaller ratio of Htb2 to Htb1 in H2A.Z-H2B dimers. H2A.Z-H2B (B) and H2A-H2B (C) dimers were purified from *S. cerevisiae* and analyzed by LC-MS. Shown is the chromatogram and peak identities.

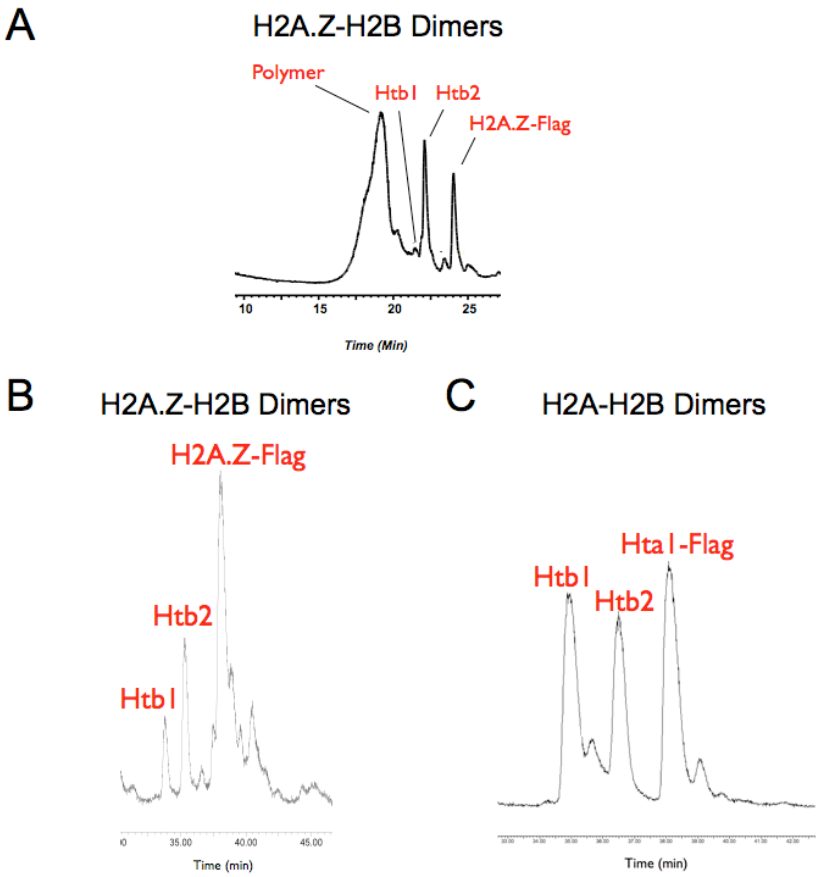

Figure 4.3. H2A.Z and Htb2 did not affect each other's expression or chromatin association.

(A) H2A.Z expression and chromatin association was not H2B isotype-dependent. H2A.Z chromatin association was analyzed in *htb1*- and *htb2*- strains (strains described in materials and methods). Shown is an anti-FLAG immunoblot of soluble (Free Histone) and insoluble (Chromatin) cellular fractions. (B) The expression and chromatin association of Htb1 and Htb2 were not H2A.Z-dependent. Shown are anti-FLAG immunoblots of chromatin association assays as described in (A). (C) The cellular ratio of Htb1 to Htb2 was not H2A.Z-dependent. Bulk histones were purified from *S. cerevisiae* and analyzed by LC-MS. Shown is the chromatogram and peak identities.

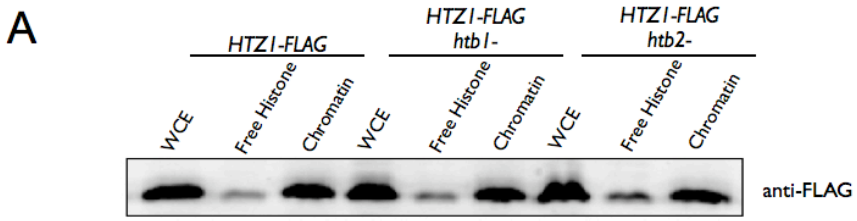

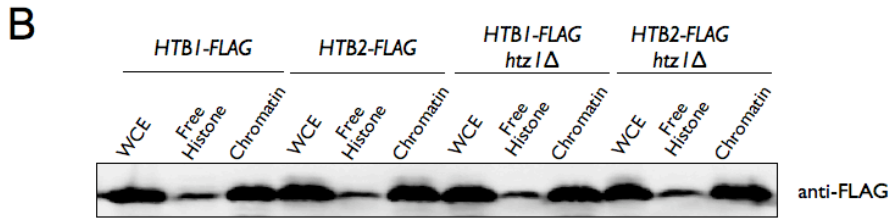

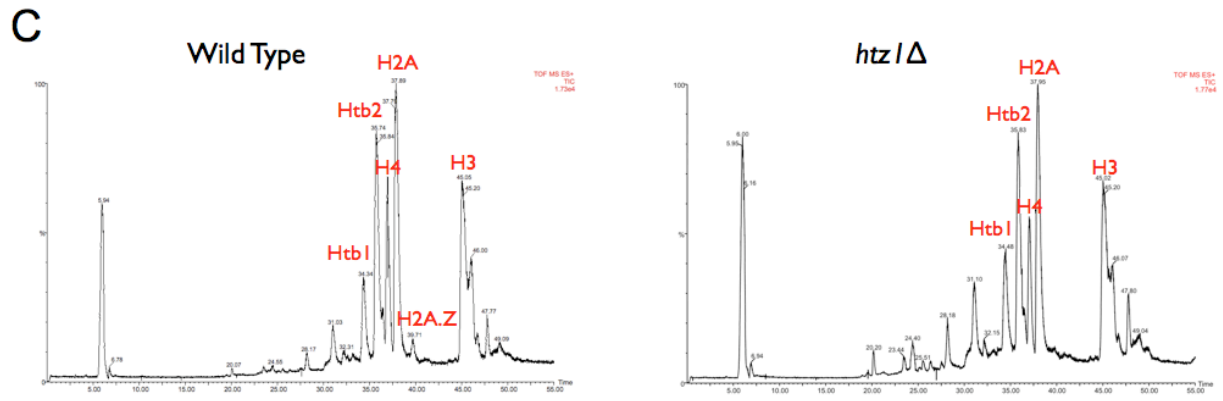

Figure 4.4. H2A.Z and Htb2 did not affect each other's modification profile.
(A) The modification profile of H2B was similar in H2A-H2B and H2A.Z-H2B dimers. H2A-H2B (left) and H2A.Z-H2B (right) dimers were purified from *S. cerevisiae* and resolved on an acetic acid urea (AU) gel. Shown are images of the Coomassie Brilliant Blue stained AU gel. (B) The modification profile of Htb1, Htb2, and H2A.Z were not changed in *htz1Δ* or H2B isotype mutant backgrounds, respectively. Htb1 (left), Htb2 (center), and H2A.Z (right) were purified from *S. cerevisiae*, separated on an AU gel, and visualized by anti-FLAG immunoblotting. (C) Htb1 contained a larger fraction of unmodified protein compared to Htb2. Chromatin associated assays were performed as described in figure 4.3a. Fractionated samples were immunopurified with anti-FLAG resin, resolved on AU gels, and visualized by anti-FLAG immunoblotting.

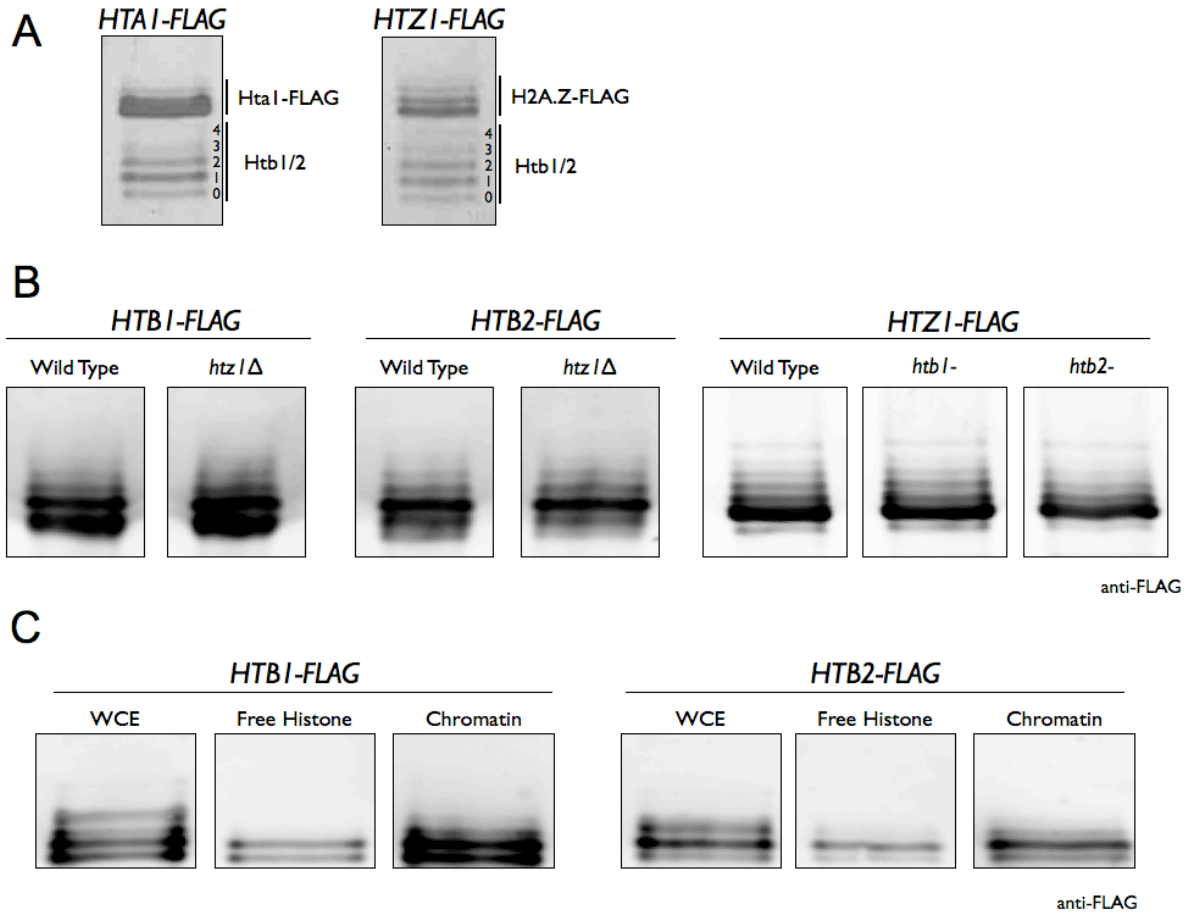

Figure 4.5. Identification of three new H2B modifications.
(A) H2A-H2B dimers were purified from *S. cerevisiae* for LC-MS/MS analysis. Shown is purified H2B on a Coomassie stained gel. (B) H2B-K3ac was exclusive to the Htb1 isotype. (top) A pair-wise alignment of the Htb1 and Htb2 tails. For columns: "*" indicates amino acids are identical, ":" indicates a conserved substitution, "." indicates a semi-conserved substitution. Htb1-K3 is indicated by a red arrow. (bottom) Shown are the tandem mass spectra of b and y Htb1 peptides acetylated at K3. (C) H2B was methylated at K37 and R102. Shown are the tandem mass spectra of b and y H2B peptides methylated at K37 (left) and R102 (right). (D) H2B-K37 and -R102 and the adjacent residues are conserved. A multiple sequence alignment of H2B between yeast and mammals. Columns are labeled as described in (B). K37 and R102 are indicated by red arrows. (E) The nucleosomal placement of H2B-K37 and R102. The x-ray crystal structure of an *S. cerevisiae* H2A, H2B, H3, H4 tetramer wrapped in DNA is shown in cartoon representation: H4 in blue, H3 in red, H2A in cyan, and H2B in green. H2B-K37 is shown in dark pink space filling spheres. H2B-R102 is shown in light pink space filling spheres (PDB 1ID3).

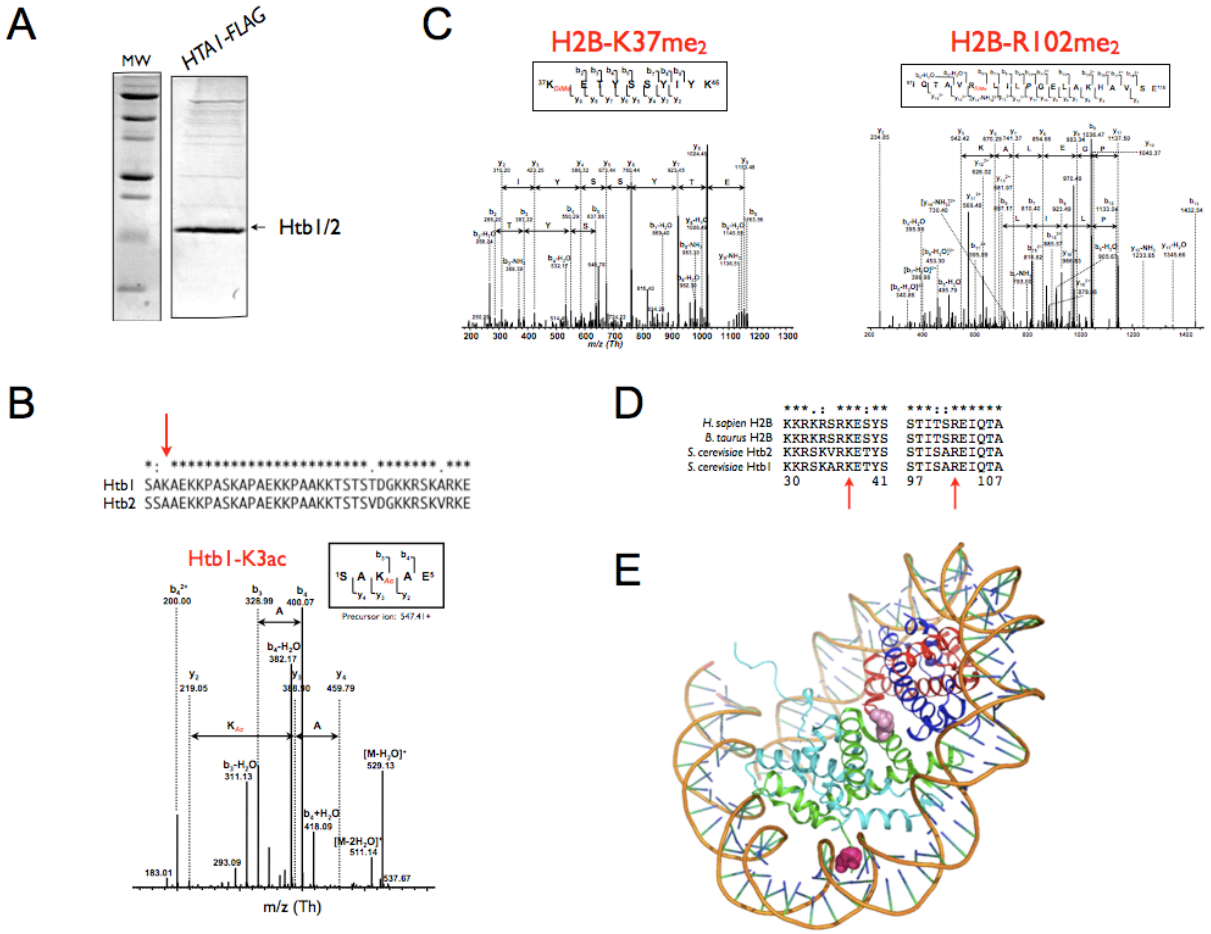

Figure 4.6. H2B-K3, -K37, or -R102 alanine point mutants did not have chemical sensitivities.

(A) 10- and (B) 5-fold serial dilutions of yeast culture were spotted onto media containing the indicated growth conditions. Strains had both endogenous copies of *H2A-H2B* knocked-out and wild type or mutant *HTA1-HTB1* on a plasmid (described in materials and methods). CSM-HIS media maintained selection of *HTA1-HTB1* plasmids. Mutants were spotted onto media containing caffeine [3 mM], formamide [1.5%], KCl [1.5 M], benomyl [34.4 μM], hydroxyurea (HU) [110 mM], camptothecin (CPT) [0.017 μM], methyl-methanesulfonate [0.006%], or UV [7mJ].

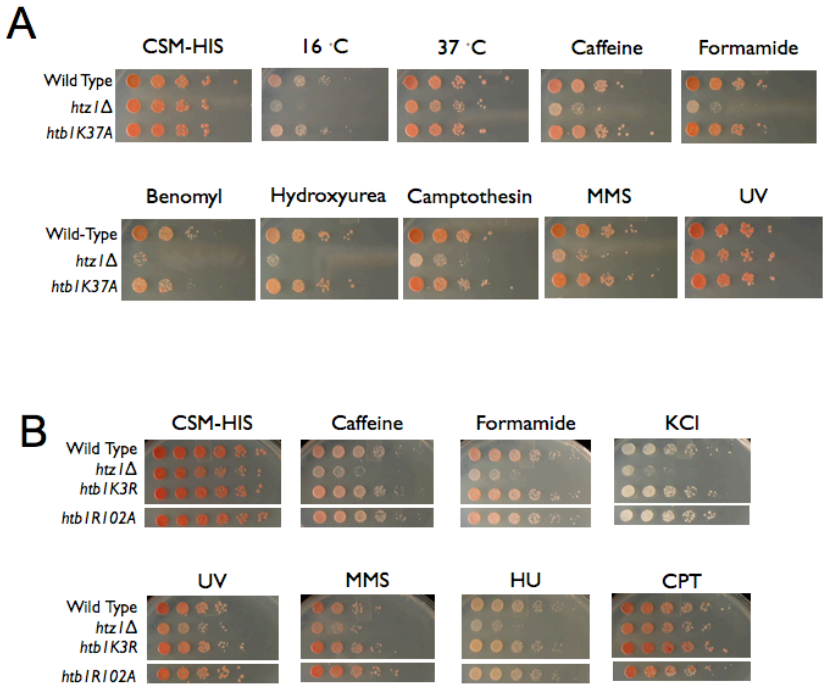

Figure 4.7. Competitive growth experiments.
(A) Strains engineered to express only the Htb1 (*htb2*-) or Htb2 (*htb1*-) isotype have the same amount of H2B. Whole cell extracts were immunoblotted with an anti-H2B antibody and an anti-actin loading control. *htb1*- and *htb2*- strains are depicted in (B) and are described in the text and the materials and methods. (B) *htb1*- and *htb2*- strains were co-cultured for 10 days (see materials and methods for more details). Every 24 hours, a portion of the culture was removed and analyzed by restriction fragment length polymorphism (RFLP) analysis (described in figure 4.8c) and auxotrophic selection by plating on non-selective media, CSM-URA, and CSM-HIS.

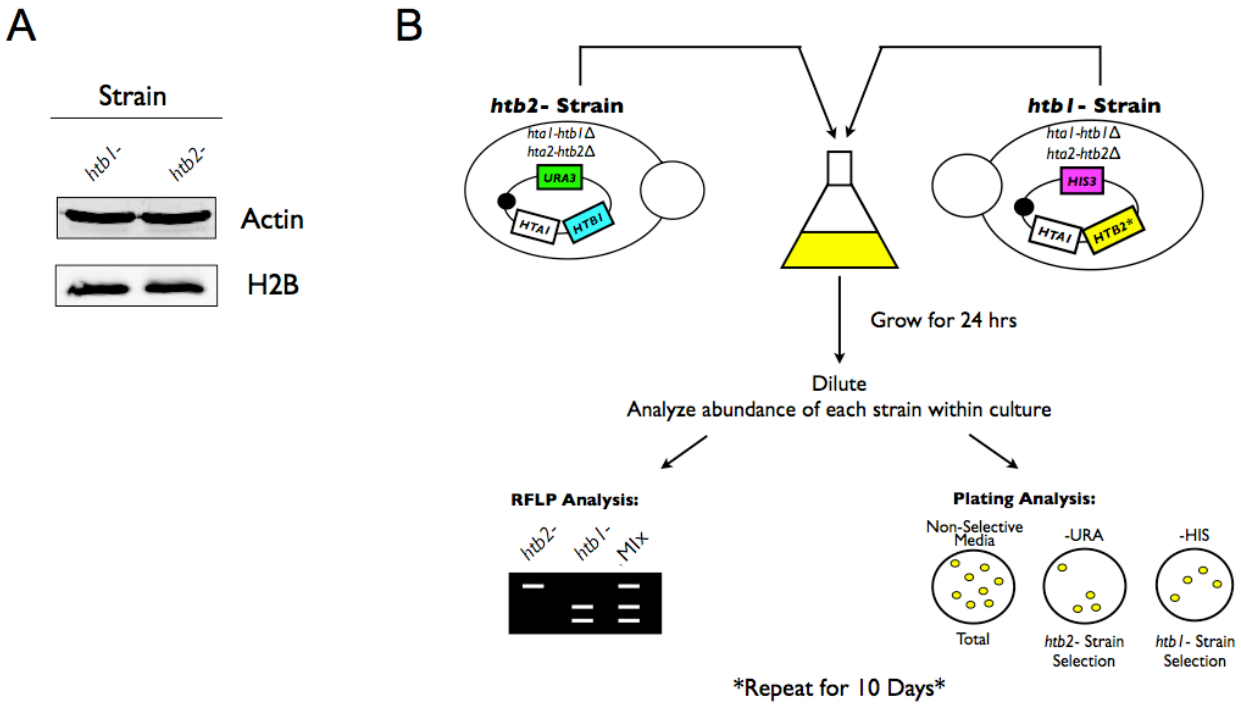

Figure 4.8. *htb1*- versus *htb2*- competitive fitness.
(A) Competing strains expressed either Htb1 or Htb2 as the only source of H2B. The *htb2*- strain (left) expressed *HTA1-HTB1* off a *Ura*$^{+}$ plasmid. The *htb1*- strain (right) expressed *HTA1-HTB2** off a *His*$^{+}$ plasmid. *HTB2** is the *HTB1* gene with the Htb1-specific residues mutated to the Htb2-specific residues, resulting in Htb2 protein. (B) Auxotrophic selection showed *htb1*- strains (highlighted in yellow) out-competing *htb2*- strains (highlighted in blue) in ~7 days. Every 24-hours, auxotrophic selection determined the percent abundance of each strain within the liquid culture as described in figure 4.7b. Shown are the ratios of the number of colonies that grew on CSM-HIS (*htb1*- strain) vs. CSM-URA (*htb2*- strain) compared to non-selective media for five biological replicates (Trials A-E). (C) RFLP analysis distinguished competing *htb1*- from *htb2*- strains in liquid culture. Following 24-hours of growth, total genomic DNA was extracted from a portion of the culture and the *HTB* ORF was PCR amplified with primers that target sequence common to both *HTB1* and *HTB2**. The amplified DNA was digested with the PstI restriction endonuclease and resolved on an agarose gel. Shown are EtBr stained agarose gels for five biological replicates. (D) DNA bands from (C) were quantified using ImageJ software and represented as percent abundance as in (B).

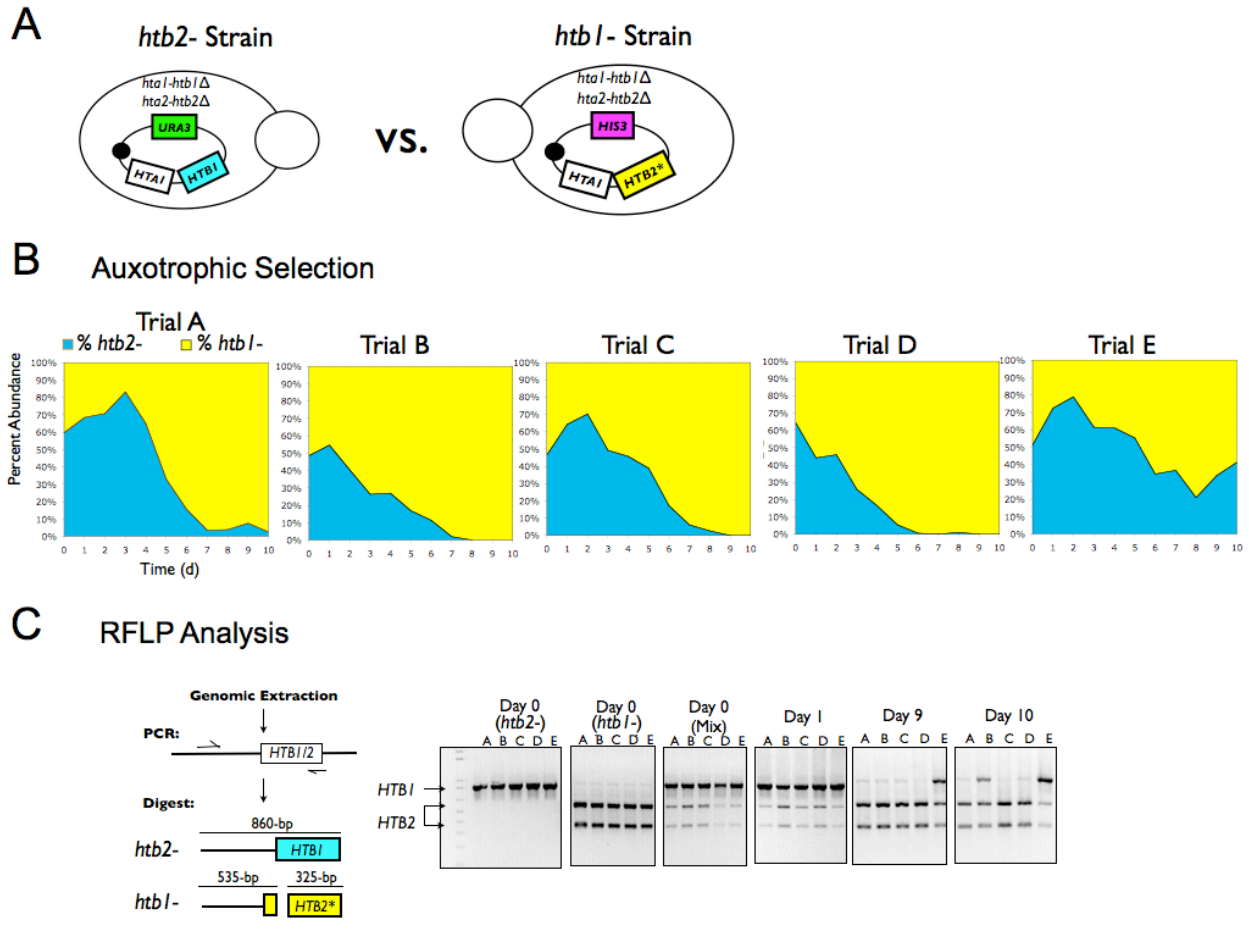

D

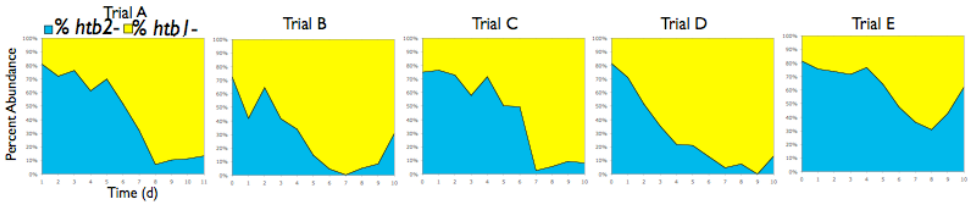
Trial A
% htb2-
% htb1-
Trial B
Trial C
Trial D
Trial E
Percent Abundance
Time (d)

Figure 4.9. Auxotrophic markers affected competitive fitness.
(A) Competitive growth experiments were performed with one biological replicate as described in figure 4.7b. Strains used in the left panel were as described in figure 4.8a. Strains used in the right panel contained the reciprocal auxotrophies. Shown are the percent abundances of the *htb1*- and *htb2*- strains within liquid culture as measured by auxotrophic selection. (B) RFLP analysis determined the ratio *htb1*- to *htb2*- strains, which contained identical auxotrophies, in liquid culture. Strains expressed *HTB1* or *HTB2** off *His*+ (top panel) or *Ura*+ (bottom panel) plasmids. RFLP analysis was performed as described in figure 4.7b.

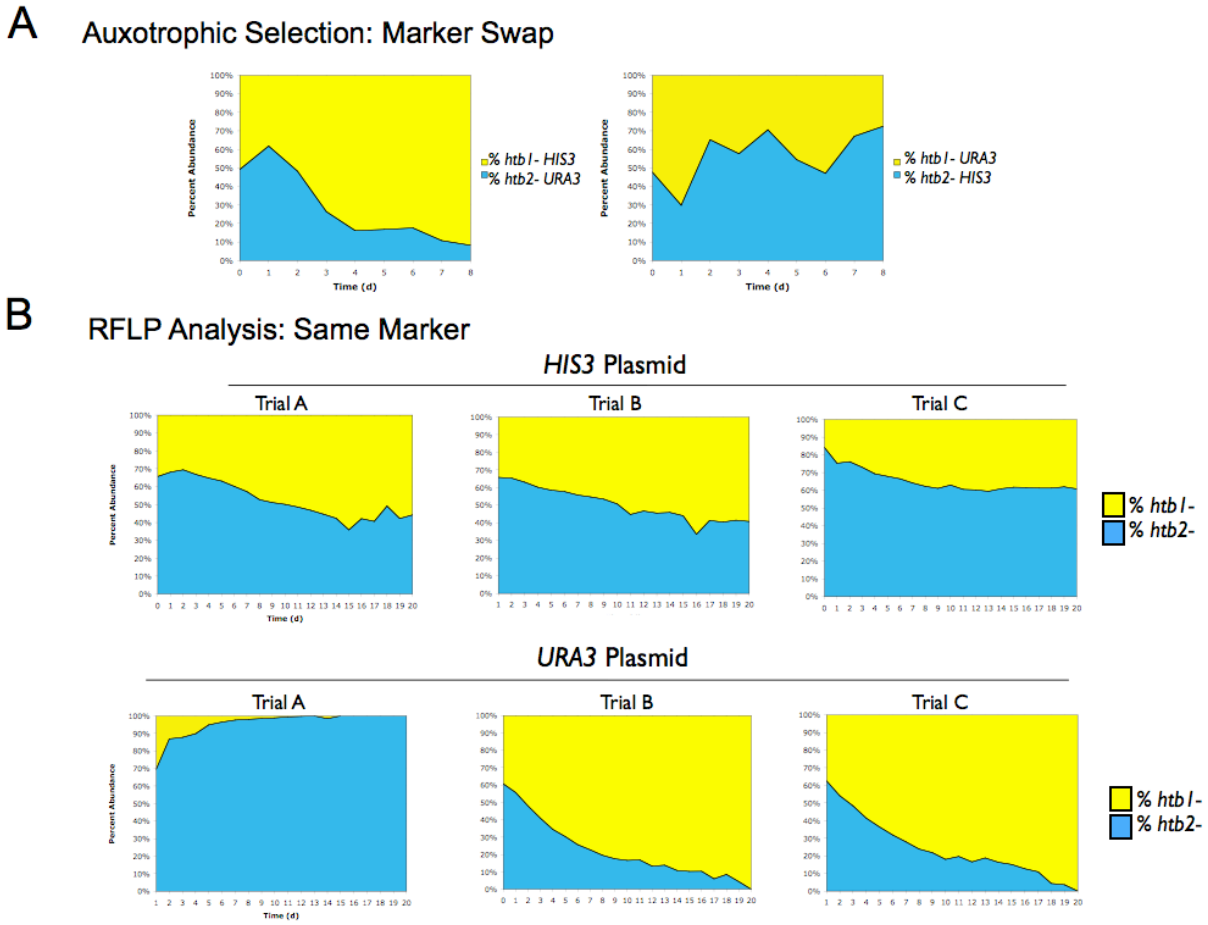

Figure 4.10. *htb1Δ/HTB1* and *htb2Δ/HTB2* heterozygous diploids have distinct chemical-genomic profiles.

Analysis of chemical-genomic data from Hillenmeyer *et al*. 2008. Bar graph illustrates chemicals significant (-log(P>2)) for either H2B heterozygote sorted by decreasing significance of *htb1Δ/HTB1* phenotype and increasing significance of *htb2Δ/HTB2* phenotype. *htb1Δ/HTB1* (blue) and *htb2Δ/HTB2* (yellow) heterozygous strains do not share chemicals with significant (p<0.01) phenotypes.

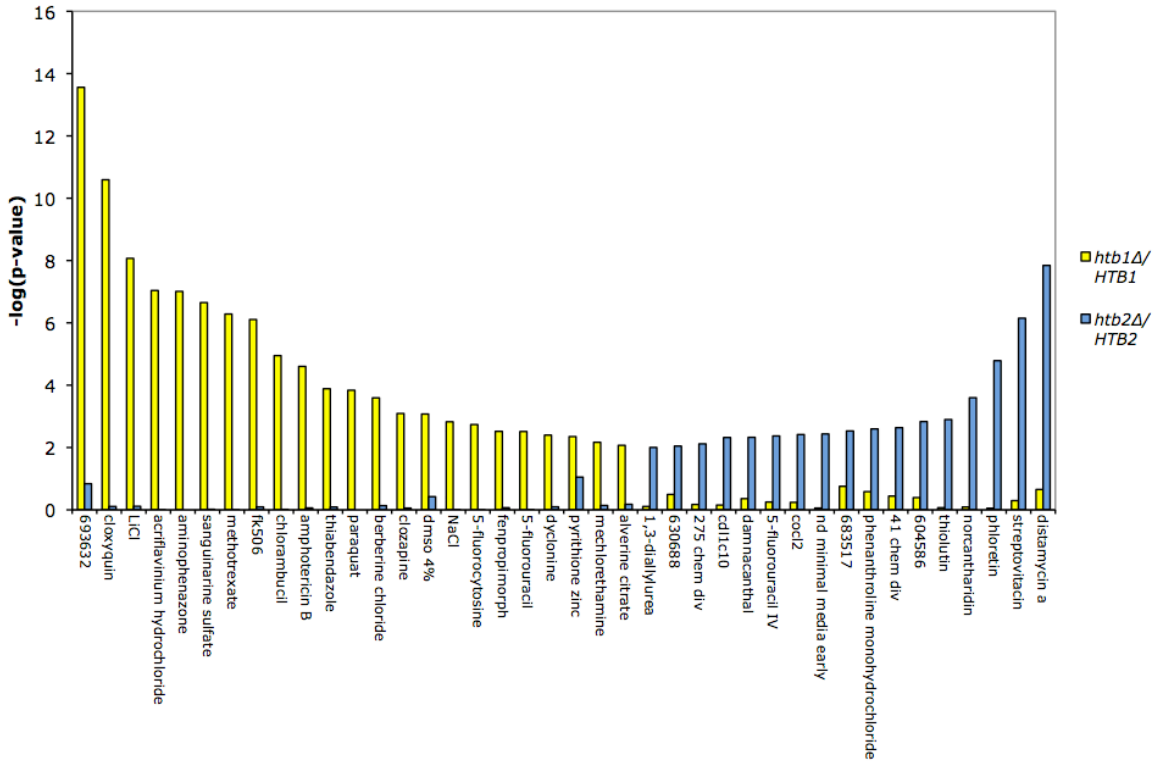

Figure 4.11. Chemical-sensitivities of H2B heterozygotes were due to changes in *HTB* expression.

(A) Integrated strains that expressed only Htb1 or Htb2 were constructed to control for plasmid-based phenotypes. (top) In wild type cells *HTB1* and *HTB2* are expressed as H2A-H2B pairs. (bottom left) The *htb2-* integrated strain mutated the Htb2-specific residues within the *HTB2* locus to the Htb1-specific residues (referred to as *HTB1**). (bottom right) the *htb1-* integrated strain mutated the Htb1-specific residues within the *HTB1* locus to the Htb2-specific residues (referred to as *HTB2**). (B) Halo assay showed no difference in fitness between wild type, *htb1-*, and *htb2-* strains. Halo size was measured using Keynote software.

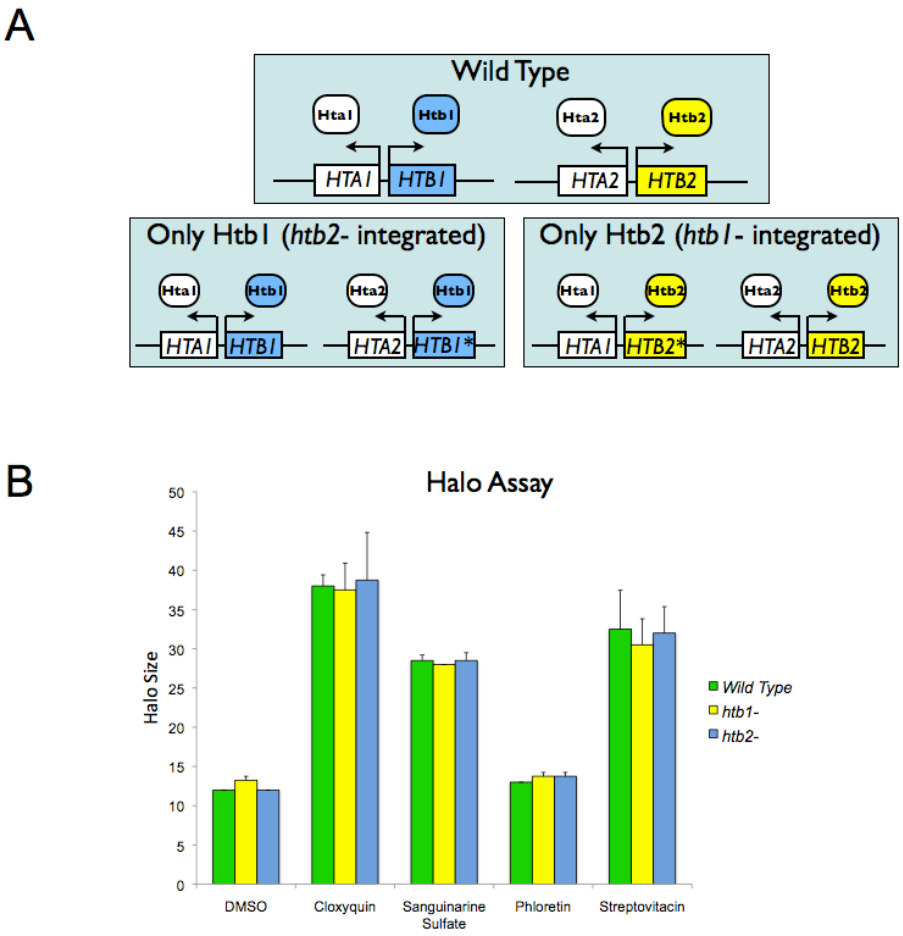

4.7 References

1. Luger, K., Mader, A. W., Richmond, R. K., Sargent, D. F., and Richmond, T. J. (1997) Crystal structure of the nucleosome core particle at 2.8 A resolution, *Nature 389*, 251-260.
2. Cliften, P., Sudarsanam, P., Desikan, A., Fulton, L., Fulton, B., Majors, J., Waterston, R., Cohen, B. A., and Johnston, M. (2003) Finding functional features in Saccharomyces genomes by phylogenetic footprinting, *Science (New York, N.Y 301*, 71-76.
3. Kellis, M., Patterson, N., Endrizzi, M., Birren, B., and Lander, E. S. (2003) Sequencing and comparison of yeast species to identify genes and regulatory elements, *Nature 423*, 241-254.
4. Franklin, S. G., and Zweidler, A. (1977) Non-allelic variants of histones 2a, 2b and 3 in mammals, *Nature 266*, 273-275.
5. Ahmad, K., and Henikoff, S. (2002) The histone variant H3.3 marks active chromatin by replication-independent nucleosome assembly, *Molecular cell 9*, 1191-1200.
6. Ray-Gallet, D., Quivy, J. P., Scamps, C., Martini, E. M., Lipinski, M., and Almouzni, G. (2002) HIRA is critical for a nucleosome assembly pathway independent of DNA synthesis, *Molecular cell 9*, 1091-1100.
7. McKittrick, E., Gafken, P. R., Ahmad, K., and Henikoff, S. (2004) Histone H3.3 is enriched in covalent modifications associated with active chromatin, *Proceedings of the National Academy of Sciences of the United States of America 101*, 1525-1530.
8. Jin, C., Zang, C., Wei, G., Cui, K., Peng, W., Zhao, K., and Felsenfeld, G. (2009) H3.3/H2A.Z double variant-containing nucleosomes mark 'nucleosome-free regions' of active promoters and other regulatory regions, *Nature genetics 41*, 941-945.
9. Gunjan, A., Paik, J., and Verreault, A. (2005) Regulation of histone synthesis and nucleosome assembly, *Biochimie 87*, 625-635.
10. Sherwood, P. W., Tsang, S. V., and Osley, M. A. (1993) Characterization of HIR1 and HIR2, two genes required for regulation of histone gene transcription in Saccharomyces cerevisiae, *Mol Cell Biol 13*, 28-38.
11. Spector, M. S., Raff, A., DeSilva, H., Lee, K., and Osley, M. A. (1997) Hir1p and Hir2p function as transcriptional corepressors to regulate histone gene transcription in the Saccharomyces cerevisiae cell cycle, *Mol Cell Biol 17*, 545-552.
12. Fillingham, J., Kainth, P., Lambert, J. P., van Bakel, H., Tsui, K., Pena-Castillo, L., Nislow, C., Figeys, D., Hughes, T. R., Greenblatt, J., and Andrews, B. J. (2009) Two-color cell array screen reveals interdependent roles for histone chaperones and a chromatin boundary regulator in histone gene repression, *Molecular cell 35*, 340-351.
13. Moran, L., Norris, D., and Osley, M. A. (1990) A yeast H2A-H2B promoter can be regulated by changes in histone gene copy number, *Genes & development 4*, 752-763.

14. Sun, Z. W., and Allis, C. D. (2002) Ubiquitination of histone H2B regulates H3 methylation and gene silencing in yeast, *Nature 418*, 104-108.
15. Kurdistani, S. K., Tavazoie, S., and Grunstein, M. (2004) Mapping global histone acetylation patterns to gene expression, *Cell 117*, 721-733.
16. Ahn, S. H., Cheung, W. L., Hsu, J. Y., Diaz, R. L., Smith, M. M., and Allis, C. D. (2005) Sterile 20 kinase phosphorylates histone H2B at serine 10 during hydrogen peroxide-induced apoptosis in S. cerevisiae, *Cell 120*, 25-36.
17. Meneghini, M. D., Wu, M., and Madhani, H. D. (2003) Conserved histone variant H2A.Z protects euchromatin from the ectopic spread of silent heterochromatin, *Cell 112*, 725-736.
18. Raisner, R. M., Hartley, P. D., Meneghini, M. D., Bao, M. Z., Liu, C. L., Schreiber, S. L., Rando, O. J., and Madhani, H. D. (2005) Histone variant H2A.Z marks the 5' ends of both active and inactive genes in euchromatin, *Cell 123*, 233-248.
19. Zhang, H., Roberts, D. N., and Cairns, B. R. (2005) Genome-wide dynamics of Htz1, a histone H2A variant that poises repressed/basal promoters for activation through histone loss, *Cell 123*, 219-231.
20. Hillenmeyer, M. E., Fung, E., Wildenhain, J., Pierce, S. E., Hoon, S., Lee, W., Proctor, M., St Onge, R. P., Tyers, M., Koller, D., Altman, R. B., Davis, R. W., Nislow, C., and Giaever, G. (2008) The chemical genomic portrait of yeast: uncovering a phenotype for all genes, *Science 320*, 362-365.
21. Goldstein, A. L., and McCusker, J. H. (1999) Three new dominant drug resistance cassettes for gene disruption in Saccharomyces cerevisiae, *Yeast (Chichester, England) 15*, 1541-1553.
22. Longtine, M. S., McKenzie, A., 3rd, Demarini, D. J., Shah, N. G., Wach, A., Brachat, A., Philippsen, P., and Pringle, J. R. (1998) Additional modules for versatile and economical PCR-based gene deletion and modification in Saccharomyces cerevisiae, *Yeast (Chichester, England) 14*, 953-961.
23. Gelbart, M. E., Rechsteiner, T., Richmond, T. J., and Tsukiyama, T. (2001) Interactions of Isw2 chromatin remodeling complex with nucleosomal arrays: analyses using recombinant yeast histones and immobilized templates, *Molecular and cellular biology 21*, 2098-2106.
24. Sikorski, R. S., and Hieter, P. (1989) A system of shuttle vectors and yeast host strains designed for efficient manipulation of DNA in Saccharomyces cerevisiae, *Genetics 122*, 19-27.
25. Gietz, R. D., and Woods, R. A. (2002) Transformation of yeast by lithium acetate/single-stranded carrier DNA/polyethylene glycol method, *Methods in enzymology 350*, 87-96.
26. Makarova, O., Kamberov, E., and Margolis, B. (2000) Generation of deletion and point mutations with one primer in a single cloning step, *BioTechniques 29*, 970-972.
27. Babiarz, J. E., Halley, J. E., and Rine, J. (2006) Telomeric heterochromatin boundaries require NuA4-dependent acetylation of histone variant H2A.Z in Saccharomyces cerevisiae, *Genes & development 20*, 700-710.
28. Zill, O. A., Scannell, D., Teytelman, L., and Rine, J. (2010) Co-evolution of transcriptional silencing proteins and the DNA elements specifying their assembly, *PLoS biology 8*, e1000550.

29. VanDemark, A. P., Blanksma, M., Ferris, E., Heroux, A., Hill, C. P., and Formosa, T. (2006) The structure of the yFACT Pob3-M domain, its interaction with the DNA replication factor RPA, and a potential role in nucleosome deposition, *Molecular cell 22*, 363-374.
30. Kobor, M. S., Venkatasubrahmanyam, S., Meneghini, M. D., Gin, J. W., Jennings, J. L., Link, A. J., Madhani, H. D., and Rine, J. (2004) A protein complex containing the conserved Swi2/Snf2-related ATPase Swr1p deposits histone variant H2A.Z into euchromatin, *PLoS biology 2*, E131.
31. Su, X., Jacob, N. K., Amunugama, R., Lucas, D. M., Knapp, A. R., Ren, C., Davis, M. E., Marcucci, G., Parthun, M. R., Byrd, J. C., Fishel, R., and Freitas, M. A. (2007) Liquid chromatography mass spectrometry profiling of histones, *Journal of chromatography 850*, 440-454.
32. Lo, W. S., Henry, K. W., Schwartz, M. F., and Berger, S. L. (2004) Histone modification patterns during gene activation, *Methods in enzymology 377*, 130-153.
33. Hoffman, C. S., and Winston, F. (1987) A ten-minute DNA preparation from yeast efficiently releases autonomous plasmids for transformation of Escherichia coli, *Gene 57*, 267-272.
34. Ericson, E., Hoon, S., St Onge, R. P., Giaever, G., and Nislow, C. (2010) Exploring gene function and drug action using chemogenomic dosage assays, *Methods in enzymology 470*, 233-255.
35. Lennox, R. W., and Cohen, L. H. (1989) Analysis of histone subtypes and their modified forms by polyacrylamide gel electrophoresis, *Methods in enzymology 170*, 532-549.
36. White, C. L., Suto, R. K., and Luger, K. (2001) Structure of the yeast nucleosome core particle reveals fundamental changes in internucleosome interactions, *The EMBO journal 20*, 5207-5218.
37. Dion, M. F., Altschuler, S. J., Wu, L. F., and Rando, O. J. (2005) Genomic characterization reveals a simple histone H4 acetylation code, *Proceedings of the National Academy of Sciences of the United States of America 102*, 5501-5506.
38. Shogren-Knaak, M., Ishii, H., Sun, J. M., Pazin, M. J., Davie, J. R., and Peterson, C. L. (2006) Histone H4-K16 acetylation controls chromatin structure and protein interactions, *Science (New York, N.Y 311*, 844-847.